Doctoral Dissertation
Doctoral Program in Energy Engineering (30th Cycle)

Implantable medical devices for drug and cell release

By

Marco Farina

* * * * * *

Supervisors

Prof. D. Demarchi, Supervisor
Prof. A. Grattoni, Co- Supervisor

Doctoral Examination Committee:

Prof. Jason Sakamoto, Referee, Houston Methodist Hospital Research Institute
Prof. Marco Mazza, Referee, University of Applied Sciences Western Switzerland
Prof. Gabriella Olmo, Politecnico di Torino
Prof. Gianluca Piccinini, Politecnico di Torino
Prof. Paolo Motto Ros, Istituto Italiano di Tecnologia

Politecnico di Torino
2018

Declaration

I hereby declare that, the contents and organization of this dissertation constitute my own original work and does not compromise in any way the rights of third parties, including those relating to the security of personal data.

Marco Farina
2018

* This dissertation is presented in partial fulfillment of the requirements for Ph.D. degree in the Graduate School of Politecnico di Torino (ScuDo).

This thesis, these years of research, are dedicated to my parents,
Esmeralda and Prof. Civera

Acknowledgements

This thesis represents not only my work at the bench of a laboratory, it is the achievement of a milestone after years of training at Houston Methodist Hospital Research Institute (HMRI) and Politecnico di Torino. My experience at HMRI has been nothing short of amazing. Since my first day, I felt that I was in an environment where I was encouraged to contribute. Here, I have been given unique opportunities that have made my experience special and pushed my career forward. These experiences include working at the Department of Nanomedicine starting as a Masters student and continuing as PhD candidate of Politecnico di Torino. The completion of this thesis is the result of the lessons I learned during my training and I wish to show all of my gratitude for having received the opportunity to work on the NICHE (Neovascularized Implantable Cell Homing and Encapsulation) project. NICHE is the result of work by many people coming from different scientific backgrounds, cultures and languages. All of them contributed to enriching my life as engineer and as man of the world, thank you all.

First and foremost, I wish to thank my advisors, Professor Alessandro Grattoni, chairman of the Nanomedicine Department at HMRI, Danilo Demarchi, Associate Professor at Politecnico di Torino, Department of Electronics and Telecommunications and Professor Mauro Ferrari, CEO and president of HMRI. They each fulfilled different roles as mentors and without them I would not have a Ph.D., I would not know how science looks like from a clinical point of view, I would not know how to translate a clinical need into an engineering product, and I would not know how much I could enjoy Tex-Mex food.

Prof. Grattoni has been supportive since the days I began working on a project in which I didn't have previous experience; I remember him calling me into the lab asking me to perform some experiments and my answer would always be the same "ok, I will manage it. I don't know how right now but I will manage it". What I really want to acknowledge is that he really

invested on me in terms of time, mentorship and of course, economically. He corrected me when I was wrong and he celebrated me when I got things right. In these years, I really believe that I was able to work on a project with a big and concrete clinical impact and that allowed me to develop many interdisciplinary skills. Among the several opportunities that Prof. Grattoni gave me, the one that shacked me the most was receiving access to the glorious Kennedy Space Center in Orlando, Florida, to witness the launch of the SpaceX Rocket CRS-13 used to ship one of the devices developed in his lab. I don't even have words to communicate how happy this made me even though the agreement was that upon my return to Houston, I had to finish writing one of the longest papers you can find in literature. He definitely knows how to motivate people! Thank you for everything Ale.

In Prof. Demarchi, I found a strong and reliable supporter of the NICHE project which gave me the opportunity to invest all these years in a project that was very important to me. As a professor, he taught me the theory behind micro and nano systems for electronics and biomedical applications and, as mentor, he guided me in the selection of the PhD exams that would have been more important to my field of application. Moreover, I am very thankful for what he did for me in a very delicate situation of my life. After deciding to pursue my PhD under the mentorship of Prof. Civera, a tragic event suddenly made my path more insecure. Prof. Demarchi, without any hesitation decided to support me and allowed me to achieve the results presented in this thesis. Thank you.

I have been blessed for what Prof. Ferrari did when he received my first email, in early 2013, where I asked him for the possibility to do an internship at HMRI for my master thesis. I was a simple student without relevant lab experience and 3 days after receiving my email, he gave me the contact of Prof. Grattoni and in a matter of few months I was already in Houston. Even as the CEO and President of a very important institution, he always finds the time to welcome and listen to people like me. He believed in my willingness to learn and thanks to his good example, I can really say that I know what I want to achieve in my future. Thank you.

During these years I applied the knowledge I learned at Politecnico di Torino and at HMRI I had the chance to translate it in a biological field that was really new to me. Dozens of people have helped and taught me immensely. First of all, my colleagues: Dr. Corrine Chua, Jessica Rhudy, Dr. Usha Thekkedath, Dr. Andrea Ballerini, Dr. Carly Figueira, Dr. Giacomo Bruno, Giovanni Scorrano, Dr. Fernanda Pons, Maria Luisa Lotito, Nicola di Trani, Nicola di Marzio, Veronica Vighetto, Celeste Marcato, Elena Riscaldina, Dino Barile, Gianluca Torchio, Dr. Thomas Geninatti, Dr. Eugenia Nicolov, Dr. Silvia Ferrati, Dr. Antons Sizovs, Nicola Di Trani, Anthonia Susnjar and Antonia Silvestri.

Dr. Chua, Jessica, Dr. Ballerini and Dr. Thekkedath dedicated a lot of time and effort in the NICHE project teaching me how to perform cell culture, *in vivo* studies and most importantly I always found in them a lot of scientific and moral support, fundamental to achieve the results reported in this thesis. Thank you.

A special thank goes to Giovanni that has been my colleague for over 4 years and was my last deskmate over the last year. We supported each other during the difficult moments and thanks to him the thesis and paper writing process was more enjoyable and sustainable.

Among all the scientific collaborators that supported me over throughout these years, I praise for the mentorship of Daniel Fraga, Dr. Omaima Sabek and Dr. Osama A. Gaber from the Department of Transplantation of the Houston Methodist Hospital.

I thank Prof. Acharya Ghanashyam, Dr. Crystal Shin, Dr. Ravi Pathak, Dr. Andrew Sikora from Baylor College of Medicine for their important contribution as collaborators in the development and testing of the NICHE.

I would also like to thank the contribution of Dr. David Tinkey, HMRI, for his teachings in animal handling and surgery; Dr. Jianhua Gu, HMRI, director of the SEM and AFM microscopy core and Dr. Enrica De Rosa, HMRI, for instrument and device training and teaching.

Crystal, Fabiola, Nitin and Jackie of the Nanomedicine Department, thanks for helping me navigating through all the burocracy and administrative aspects and allowing me to always have a good time at HMRI.

Lastly, I would like to thank my family, Esmeralda and all my friends for all their love and encouragement. Even though I was far away from them, they always been very supportive and proud of what I wanted to achieve. Thank you.

Dear Gigi, thank you for showing me how science can be exciting and enjoyable. I will never forget the impact you had on me. Thank you.

Marco

Abstract

Cell therapy is an emerging treatment strategy for a wide range of diseases. Blood cells, pancreatic islets, hepatocytes and stem cells are only a few of the vast array of cell types explored for this purpose. Appropriate cell delivery and encapsulation systems are needed for immune-sequestration and protection of the cells and to enable them to function as an artificial organ. Current research is focused on developing an ideal strategy to provide a protected and vascularized environment for the subcutaneous transplantation of cells for their long-term function. Thus, the encapsulating material or device should permit the cells to function as an artificial organ. In this case, by compartmentalizing the therapeutic cells within a semi-permeable membrane, and protecting its viability and function from being impaired by the host immune system, complement proteins and antibodies and permit bi-directional transport of oxygen and the release of therapeutic agents such as hormones. Physical parameters such as porosity, rigidity and tortuosity, chemical composition and surface functionalization of the materials, and the ability to refill and or retrieve the device play an important role in engineering the encapsulating material and device ensuring the long-term functioning of the graft.

To meet these needs, in this thesis is presented the design, fabrication and In Vivo validation of an adaptable, scalable and refillable cell encapsulation system (NICHE, Neovascularized Implantable Cell Homing and Encapsulation) for subcutaneous transplantation of autologous endocrine cells.

The innovative aspects of this technology are multiple: 1) 3D printing technology permits adjustment of structure design in accordance to implantation site and cell volume in a time and costly manner; 2) Minimally invasive surgery to implant in the subcutaneous tissue; 3) Allows vascularization and tissue formation within the device prior to cell transplantation; 4) Allows for cell refilling via minimally invasive

transcutaneous injection; 5) Easy removal in case of an adverse body reaction.

Over the course of the PhD, my contribution has been focused on NICHE structure design, and its validation in vitro and in vivo.

First, NICHE was tested in murine, swine and in nonhuman primate animal models to evaluate the formation of a highly vascularized environment within the device. Next, to validate NICHE as a technological platform for cell encapsulation, human pancreatic islets and Leydig cells were transplanted using murine animal models.

The results of the in vivo experiments confirm insulin and testosterone release for up to 22 and 11 weeks, respectively. Therefore, demonstrating the possibility within NICHE to become an optimal environment for transplanted cells.

It is important to realize that the here presented NICHE does not include immune protection strategies to avoid graft rejection. Correspondingly, it is designed for autologous cell transplantation only.

However, in order to perform heterologous cell transplantations, Grattoni's Team is currently developing a second version of the NICHE with immunosuppressant properties. This device implements a nanochannel membrane for the sustained release of immunosuppressant drugs with the objective of achieving local immunosuppression while minimizing systemic drug exposure and associated adverse effects.

In the light of the promising results, NICHE has the potential means to provide a valuable and universally applicable cell transplantation encapsulation system for a wide spectrum of endocrine diseases. The aforementioned approach could also be explored for cell therapy delivery in other pathologies, such as cardiovascular and neurodegenerative diseases.

Contents

List of Figures

List of Tables

Chapter 1

Introduction About This Thesis

Goal and Thesis Scope

The objective of the thesis was to develop and assess in vitro and in vivo a 3D printed implantable encapsulation system for cell transplantation. This thesis is divided in four main chapters. In Chapter 2 the history and impact of recent cell encapsulation technologies that are currently under clinical investigation is presented. Chapter 3 describes the development and mechanical properties of the 3D printed NICHE. Chapter 4 describes as approach for addressing the limitation in cell availability by differentiation of human mesenchymal stem cells into islet-like insulin-producing cells. Chapter 5 presents the in vivo validation of the 3D printed device in small and large animal models. An ore detail outline of each chapter is presented here below:

Chapter 2

Cell-based therapy is emerging as a promising strategy for treating a wide range of human diseases, such as diabetes, blood disorders, acute liver failure, spinal cord injury, and several types of cancer. Pancreatic islets, blood cells, hepatocytes, and stem cells are among the many cell types currently used for this strategy. The encapsulation of these “therapeutic” cells is under intense investigation to not only prevent immune rejection but also provide a controlled and supportive environment so that their function is preserved long-term. In this chapter, various encapsulation strategies developed in academic and industrial settings are reviewed, including the state-of-the-art technologies in advanced preclinical phase as well as those undergoing clinical trials. Advantages and challenges are indicated for each technology.

This chapter contains reedited parts of the review manuscript submitted for consideration for publication in Advanced Drug Delivery titled “Cell

Encapsulation: Overcoming Barriers in Cell Transplantation in Diabetes and Beyond" and authored by ***Marco Farina****, Jenolyn F. Alexander, Usha Thekkedath, Mauro Ferrari, Alessandro Grattoni. The manuscript is currently under peer-review.*

Chapter 3

Cell transplantation in bioengineered scaffolds and encapsulation systems has shown great promise in regenerative medicine. Depending on the site of implantation, type of cells and their expected function, these systems are designed to provide cells with a physiological-like environment while providing mechanical support and promoting long-term viability and function of the graft. In this chapter, we describe the development of a minimally invasive 3D printed system termed neovascularized implantable cell homing and encapsulation (NICHE) for subcutaneous transplantation of endocrine cells, including pancreatic islets and Leydig cells. The suitability of the NICHE for long term in vivo deployment is investigated by assessing mechanical behavior of both fresh devices under simulated subcutaneous conditions and NICHE retrieved from subcutaneous implantation in pigs. Both experimental and numerical studies were performed with a focus on validating the constitutive material model used in the numerical analysis for accuracy and reliability. Notably, homogeneous isotropic constitutive material model calibrated by means of uniaxial testing well suited experimental results. The results highlight the long-term durability for in vivo applications and the potential applicability of the model to predict the mechanical behavior of similar devices in various physiological settings.

Part of the results described in this chapter have been published in the manuscript titled "Mechanical characterization and numerical simulation of a subcutaneous implantable 3D printed cell encapsulation system", authored by Federica Adamo,* ***Marco Farina*****, Usha Thekkedath, Alessandro Grattoni and Raffaella Sesana, (*equal contribution, co-first*

authorship) in Journal of the Mechanical Behavior of Biomedical Materials, https://doi.org/10.1016/j.jmbbm.2018.03.023.

Chapter 4

Diabetes is one of the most prevalent, costly, and debilitating diseases in the world. Pancreas and islet transplants have shown success in re-establishing glucose control and reversing diabetic complications. However, both are limited by donor availability, need for continuous immunosuppression, loss of transplanted tissue due to dispersion, and lack of vascularization. To overcome the limitations of poor islet availability, in this chapter we investigate the potential of bone marrow–derived mesenchymal stem cells differentiated into islet-like insulin-producing aggregates (ILIPAs). Islet-like insulin-producing aggregates, characterized by gene expression, are shown to be similar to pancreatic islets and display positive immunostaining for insulin and glucagon. Moreover, in order to ensure the biocompatibility of the PLA (Polylactic acid) adopted for fabricating the NICHE, we encapsulated ILIPAs (Insulin like in the 3D device and tested in vitro showing that encapsulated islet-like insulin-producing aggregates maintained viability and function, producing steady levels of insulin for at least 4 weeks. NICHE—islet-like insulin-producing aggregate technology investigated in this chapter as a proof of concept holds potential as an effective and innovative approach for diabetes cell therapy.

Part of the results described in this chapter have been published in the manuscript titled "Three-dimensional printed polymeric system to encapsulate human mesenchymal stem cells differentiated into islet-like insulin-producing aggregates for diabetes treatment", authored by Omaima M. Sabek, **Marco Farina***, Daniel W. Fraga, Solmaz Afshar, Andrea Ballerini, Carly S. Filgueira, Usha R. Thekkedath, Alessandro Grattoni and A. Osama Gaber, (*equal contribution, co-first authorship), Journal of Tissue Engineering, 2016, 7: 1–13, DOI: 10.1177/2041731416638198*

Chapter 5

In this chapter, we present the in vivo validation of the NICHE as technological platform for the transplantation of multiple cell types. Specifically, we transplanted human pancreatic islets or Leydig cells in in Nu/Nu female mice or *Rag1-/-* castrated mice, respectively. For both cell lines, we evaluated the vascularization and tissue formation within the NICHE prior to cell transplantation. The NICHEs protected the encapsulated cells from acute hypoxia and kept them functional over 22 weeks (human pancreatic islets) and 14 weeks (Leydig cells). The adaptability of the encapsulation system was demonstrated by refilling some of the experimental groups transcutaneously with additional islets.

The results described in this chapter have been published in the following paper ***Marco Farina****, Andrea Ballerini, Daniel W. Fraga, Eugenia Nicolov, Matthew Hogan, Danilo Demarchi, Francesco Scaglione, Omaima M. Sabek, Philip Horner, Usha Thekkedath, Osama A. Gaber, Alessandro Grattoni, 3D Printed Vascularized Device for Subcutaneous Transplantation of Human Islets, Biotechnology Journal, 2017, 12, 1700169, DOI: 10.1002/biot.201700169. Other results presented are included in the following manuscript currently under peer-review:* ***Marco Farina****, Corrine Ying Xuan Chua, Andrea Ballerini, Usha Thekkedath, Jenolyn F. Alexander, Jessica R. Rhudy, Gianluca Torchio, Daniel Fraga, Ravi R. Pathak, Mariana Villanueva, Crystal S. Shin, Jean A. Niles, Raffaella Sesana, Danilo Demarchi, Andrew G. Sikora, Ghanashyam S. Acharya, A. Osama Gaber, Joan E. Nichols and Alessandro Grattoni, Transcutaneously refillable, 3D-printed biopolymeric encapsulation system for the transplantation of endocrine cells, Biomaterials.*

Chapter 2

Cell encapsulation: overcoming barriers in cell transplantation in diabetes and beyond

2.1 Cell-Based Therapy

Cell-based therapy consists of implanting or delivering living cells or, sustaining their development in a patient for treating a certain disease or condition [1]. In contrast to small molecule drugs and biologics such as engineered proteins and antibodies, which are the predominant treatment modalities for most diseases, cell-based therapy delivers complex living entities that are capable of sensing, modulating their function and responding to the environment. The migratory and proliferative capacity, production and delivery of therapeutics and intercellular interactions are some of the characteristics of cells that can be manipulated to address unmet needs of various pathologies including diabetes, cancer, spinal cord injuries, autoimmune and neurodegenerative diseases [2]. For example, in the treatment of osteoarthritis, conventional treatment using opioids and non-steroidal anti-inflammatory drugs aids in pain relief but does not restore damaged tissue. In contrast, cell therapies utilizing induced pluripotent stem cells or autologous chondrocytes repair the damaged cartilage as well as renovate the injured tissue [3]. Transplantation of these cells may thus become a standard treatment option and in certain cases, as in the treatment of diabetes and liver failure, is predicted to replace whole organ transplant [4,5].

The practice of adopting cells for therapeutic purposes has dramatically evolved over the years. Blood transfusions practiced in the 1600s [6], renal transplantation in animal models by Dr. Emerich Ulmannn in 1902 [7,8], blood vessel and organ transplantation by Drs. Alexis Carrel and Charles Guthrie in the early 1900s [9], injections of ox parathyroid cells to human patients in 1931 and lyophilized cells in 1949 by Dr. Paul Niehans [10], and transplantation of islets encapsulated in semipermeable microcapsules by Dr. Thomas M.S. Chang in 1964 [11] represent early pioneering developments in the field of cell transplantation. Today, cell

types from different sources are being evaluated to treat a number of diseases, as a personalized approach.

Currently, one of the most researched areas in cell transplantation is diabetes, which continues increasing in prevalence. Type 1 diabetes mellitus (T1DM) is elicited by severe inhibition of pancreatic β cell function which leads to complete lack of insulin production. As a result, exogenous insulin is required to be administered to the patients for survival. Despite significant advances in the treatment of T1DM, the management of the disease is still suboptimal and link to chronic complications, comorbidity and mortality even in individuals at a relatively young age. Whole-pancreas transplantation has shown to prevent chronic complications and result in adequate glycemic control. However, the invasiveness of the intervention, post-surgical morbidity and high mortality are still of concern [12–14]. To address the continuous treatment need for “brittle T1DM” patients, a severe form of diabetes, intravascular cell infusion transplanting allogenic pancreatic islets was developed as a better alternative [15].

Pancreatic islet transplantation was first attempted in 1893 [16]. It took eighty years to demonstrate acceptable rate of success, even in the absence of an immune barrier [17,18] (i.e. using autografts). In the 1980s, several autotransplant trials were performed extracting islets from patient’s own pancreas and infusing them into liver via the portal vein. Unfortunately, these early trials achieved insulin independence for only 10% of patients [19,20]. Success of this approach was significantly improved with the development of the Edmonton protocol at the University of Alberta in 2000. In the NCT00706420 trial, all treated patients with T1DM (7) gained insulin independence and retained it for 12 months post-transplant [21]. Since then, human pancreatic islet transplantation has transitioned from a rare, experimental protocol to a routine and safe clinical procedure with over 1,500 interventions performed worldwide (1,011 allogeneic transplants and 660 autologous transplants according to the Collaborative Islet Transplant Registry (CITR). Recently, a 12-year

follow-up of seven patients from the 2000 study reported continuous function of the transplanted islets over a decade since the procedure [22]. Since their first transplant procedure, one patient maintained insulin independence without supplemental diabetic medication or transplants, while another patient maintained insulin independence for 10.9 years and three patients received subsequent islet transplants. At the end of the study, five patients were being administered insulin while two patients were insulin independent. Long term safety of the islet transplantation was demonstrated since no adverse infections, hypoglycemia or lymphoma were observed in the patients.

The establishment of the Edmonton protocol for islet autotransplantation represents an outstanding advance in the field. However, its success over the years has been challenged by islets dispersion post injection in the portal vein, and the limited number of viable islets that could be retrieved from the patient. While addressing the first issue is topic of research, the need for additional cell sources has prompted the use of allogenic or xenogenic cells from donors. This requires combating transplant immune rejection and the ensuing need for lifelong immunosuppressive treatments, which significantly reduce patient's quality of life [23]. One of the first attempts to solve the problem of immune rejection was done by Drs. Prehn, Weaver and Algire in 1954. Using immunized mice, they demonstrated that transplanted homologous (allogeneic) cells did not trigger immune response when administered to the peritoneal cavity and encapsulated by a porous membrane [24]. Encouraged by this result, physical means to provide immunoisolation of the transplant graft and abrogate immune rejection via semipermeable membranes have been extensively investigated by several research groups. More recently, biological approaches involving genetic manipulation of transplant cells to avoid systemic immune suppression regimens are topic of research [25–30].

The general objective of encapsulation materials or devices is to enable the transplanted cells to function as an artificial organ, by

compartmentalizing the therapeutic cells within a protected environment, and promoting viability and function long term. These systems need to allow for bi-directional transport of oxygen, metabolic products and real time and unobstructed release of therapeutic agents such as hormones or enzymes in response to external biological stimuli [31–33]. These functional requirements mean that physical parameters such as porosity, rigidity and tortuosity, chemical composition, and surface functionalization of membranes, device refillability and replaceability, all need to be considered when engineering an effective encapsulation technology [23,34]. The breadth of requirements has led to a surge in synthetic and bio-based materials being tested as means of encapsulating a wide variety of cells. Present day strategies comprise of implantable, personalized, and multifunctional living cell factories that are capable of providing immune protection and allow for controlled and continuous delivery of therapeutics. These structures are capable of housing a vast array of cell types such as patient's own cells, animal derived and engineered cells, by synergistically leveraging genetic and bioengineering, material science, and nanotechnology [35–37].

Cell-based therapy is making paradigm changes in the treatment of many diseases including some that were considered incurable, such as diabetes. It is already established as a standard-of-care treatment and reimbursable by insurance companies or covered by national health systems in several countries. Given the increasing rates of diabetes worldwide, the approval of islet-based therapy provides an opportunity for cell therapeutics to exit the investigative, niche arena and become a globally recognized standard-of-care [4]. Beyond diabetes, the strategy of transplanting cells is used or explored for the treatment of other pathologies (Fig. 2.1). A plethora of cells from autologous, allogeneic or xenogeneic sources – stem cells (neural, mesenchymal, induced pluripotent), pancreatic islets, fibroblasts and renal proximal tubule cells are being tested for treating different diseases such as neurodegenerative and chronic eye diseases, cancer, diabetes, cardiovascular diseases, wound regeneration and renal failure [38,38–42,36,43,3,4]. Ideally, these

cells upon encapsulation and implantation at a specific site in the body would function as the native organ.

In this review, we describe various encapsulation strategies including the state-of-the-art technologies in advanced preclinical phase, as well as those undergoing clinical trials for diabetes and other diseases. First, we introduce the types of cells used in cell transplantation highlighting the various sources and applications. Second, we present current strategies of cell microencapsulation and macroencapsulation in diabetes. We describe each encapsulation approach, and assess their advantages and challenges. We also highlight the importance of “smart” - stimuli-responsive and “live” - encapsulated cell systems in overcoming obstacles in cell transplantation and delivering them for patient use. Third, we describe the applications of encapsulated cell therapies in other pathologies, such as chronic eye diseases - age-related macular degeneration (ARMD) and diabetic retinopathy, neurodegenerative diseases - Alzheimer’s and Parkinson’s, several types of cancer, chronic wounds - venous leg ulcers (VLU) and diabetic foot ulcers (DFU), cardiovascular diseases - myocardial infarction (MI) as well as renal diseases - acute kidney injury (AKI) and end stage renal disease (ESRD).

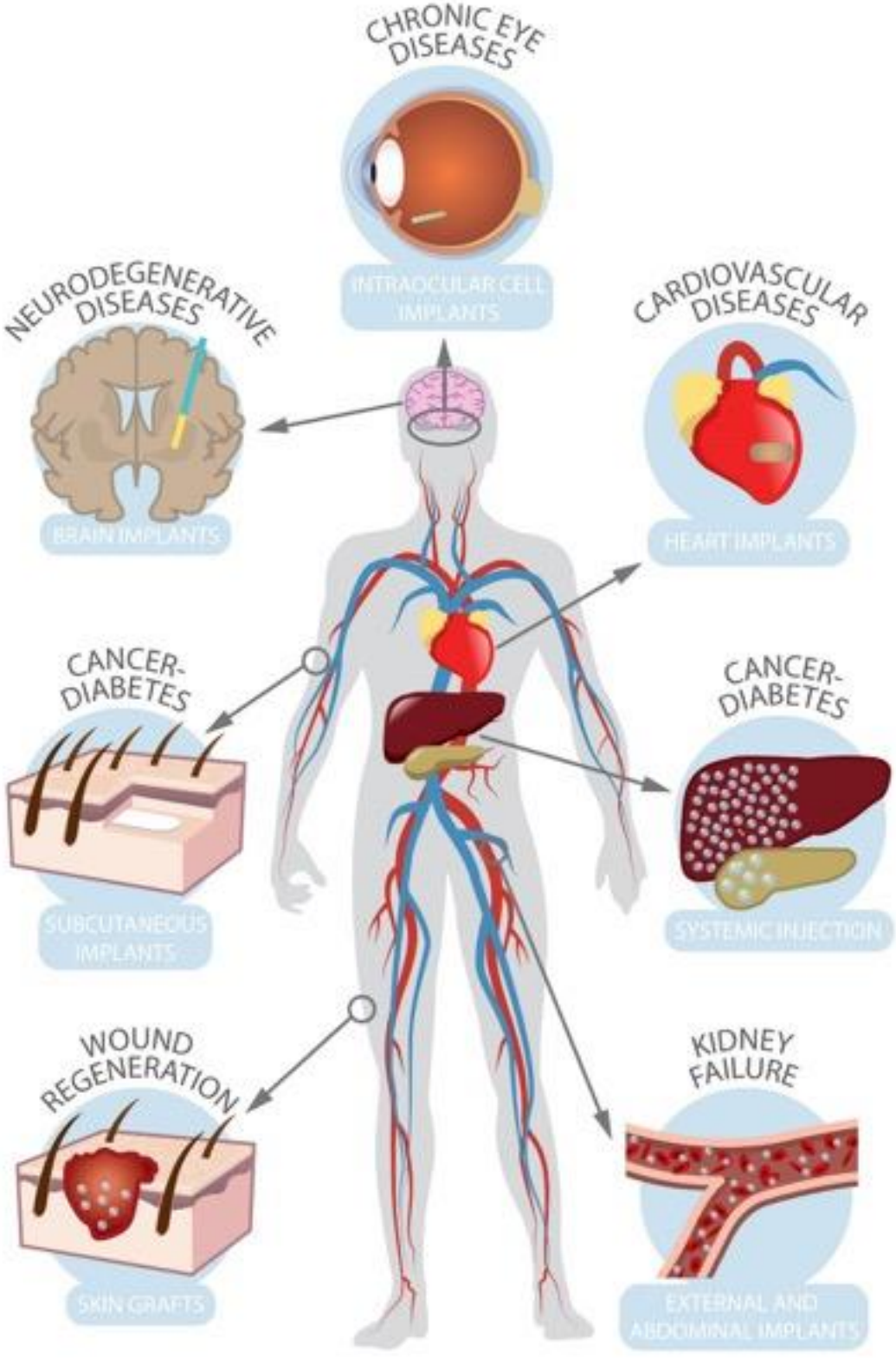

***Figure 2.1**: Schematic diagram of various representative strategies and cell types under advanced pre-clinical and clinical development, where cells, upon encapsulation and implantation, are used to restore or mimic and replace the function of the diseased organs.*

2.2 Cell Types

The choice of cells for transplantation mainly depends on the pathology treated and target organ. Cells secreting therapeutic antibodies, hormones and aiding in regeneration of damaged or defective tissues are often selected for therapeutic transplantation. Cell viability and controlled release of therapeutic factors from cells are essential parameters in establishing long-term function and efficient therapy. The cell source could be autologous, allogeneic or xenogeneic. The therapeutic potential of cell transplantation for many chronic conditions has led to a greater demand for high quality cells, resulting in the development of innovative tissue engineering strategies for stem cell derived therapeutic cells and evaluation of animal derived cells. Even though non-human primates (NHP) are the most closely related species to humans and the NHP xenografts would be more physiologically and immunogenically compatible, apes being endangered, the use of NHP cells raises ethical concerns. Pigs have been the next alternative species of choice [42]. In addition to primary and genetically engineered cells, artificial cell-like structures such as polymersomes have also been investigated for therapeutic use [27,28]. Some of the most widely tested cell types for transplantation are summarized below (Fig. 2.2).

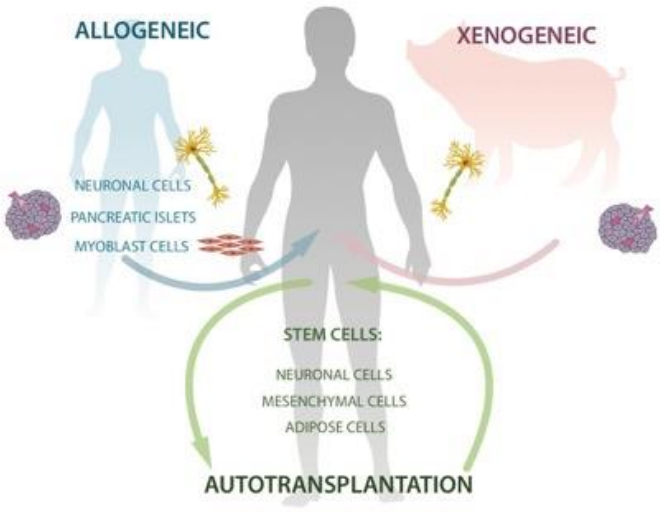

Figure 2.2: *Cell sources for cell therapy applications*

2.2.1 Cells for Allogeneic or Xenogeneic Transplantation

A variety of human and animal cell types are evaluated for therapeutic transplantation into humans. While their detailed descriptions are beyond the scope of this review, various cell types that are being investigated in advanced preclinical or clinical studies are described below.

Pancreatic Islets

Pancreatic islets or islets of Langerhans are clusters of endocrine cells in the pancreas including beta cells, which sense blood glucose levels and release necessary amount of insulin to maintain normal blood sugar levels. Pancreatic islets harvested from human cadaveric donors and transplanted via portal vein injection have been shown to be a valuable alternative to frequent administration of insulin injections to treat type 1 diabetes. However, due to the poor yield of harvesting protocols, islets from multiple (2 to 4) donors are required to achieve insulin independence. Further, challenges associated with immune suppression, and loss of viability and function over time remain significant hurdles to improve transplantation outcomes [44]. For this, immune segregation for islet transplants has been widely studied with materials such as alginate, chitosan, agarose, gelatin and other polymeric materials as wells macro scale devices [45]. Detailed descriptions of these encapsulation systems are provided in subsequent sections of this review. Several clinical trials for assessing the safety, metabolic and immune responses have been performed or are ongoing for alginate encapsulated human beta cells (NCT00790257, NCT00790257), and macroencapsulated human islets (NCT02064309). In an attempt to improve islet availability other sources have been explored. Porcine insulin differs from human insulin by just a single amino acid, and pigs are considered a suitable choice for harvesting islets from a xenogeneic source [42,46]. In light of this, porcine islets encapsulated in agarose are being investigated for clinical use [43].

Myoblasts

Encapsulation of muscle cells (myoblasts) is being researched pre-clinically for therapeutic protein delivery for skeletal muscle regeneration. Puicher *et al.* showed that genetically engineered murine myoblasts could be used in the treatment of Hurler's syndrome – also known as mucopolysaccharidosis type I (MPS I). C2C12 cells, transfected to secrete high levels of lysosomal enzyme α-l-iduronidase (IDUA) [47], were encapsulated in alginate microcapsules and implanted intraperitoneally in mice. Increase in enzyme activity and drop in glycosaminoglycan activity were observed up to a period of 3 months. In another study by Lathuilière A. et al, C2C12 murine myoblast cells were infected with lentiviral vectors subcloned with firefly luciferase cDNA [48]. These genetically engineered cells expressing luciferase were then encapsulated in polymeric flat sheet macrodevices and implanted subcutaneously in the dorsum of mice. The density of injected cells, porosity of the permeable membrane and stiffness of the hydrogel used for encapsulation were tuned to achieve prolonged viability of cells and delivery of recombinant proteins in vivo [48]. The same research group showed that myoblasts genetically engineered to express anti-amyloid-β antibodies and encapsulated in the flat sheet device, could be used for treatment of Alzheimer's disease [49]. 3D-bioprinted constructs comprising of myoblast cells have shown to mimic skeletal muscle tissue in vitro and in vivo. The implantation of these bioartificial constructs in mice showed promise for muscle tissue regeneration and reconstruction [50]. These studies served as pioneering proof-of-concept for the allogenic implantation of myoblast cells for a prolonged therapeutic delivery and cost-effective alternative to recombinant protein therapy as well as tissue regeneration [48–51].

Choroid Plexus

The highly active and vascularized cluster of epithelial cells, situated in the blood - cerebrospinal fluid barrier - choroid plexus is responsible for a number of functions including maintenance of brain homeostasis,

production of cerebrospinal fluid, detection and transmission of immune signals [52,53] and clearance of toxic agents from the brain [54]. Encapsulation of the choroid plexus is under study for the treatment of conditions including aging disorders, cochlear [55,56] and neuro - degenerative diseases [57], chronic wounds [58] and Huntington's disease [59]. Further, it is clinically tested for Parkinson 's disease (NCT01734733) [60,61] owing to its abundance of trophic and regenerative components and ability to adapt and function in different microenvironments [58]. Borlongan *et al.* demonstrated that alginate encapsulated choroid plexus cells, when transplanted into a rodent model of Huntington's disease, were able to release neurotrophic factors and protect the striatal neurons from damage [59]. Later the same group showed that alginate encapsulated porcine xenografts could provide structural and functional neuroprotection in a rodent model of stroke [62]. Luo *et al.* demonstrated the neuroprotective efficacy of alginate encapsulated porcine choroid plexus cells in a non-human primate model of Parkinson's disease, without the need for immunosuppressant drugs [63]. These notable examples demonstrate the great clinical potential of encapsulated choroid plexus cells in delivering multiple neurotrophic agents to offer structural and functional protection for various neurodegenerative and traumatic conditions.

2.2.2 Cells for Autologous Transplantation

Patient derived cells for transplantation are either cells harvested from native organ as in the case trauma or surgical removal (eg. for pancreatectomy) or are differentiated from stem cells, using specific protocols. Below, various autologous cell types are presented, with particular emphasis given to stem cells, due to their largely untapped potential for the management of various diseases.

Pancreatic Islets

Transplantation of autologous pancreatic islets is usually performed when a patient with chronic pancreatitis undergoes total pancreatectomy for intractable pain not controllable via medical treatment. Cells are isolated from patient's own pancreas and transplanted back through portal vein. Since its first clinical application by the researchers at the University of Minnesota School of Medicine in 1977, advances in cell isolation and purification have improved islet autotransplant outcomes, and expanded its clinical use [64]. However, only a handful of clinical centers in the United States are performing this procedure and there is no available information on its worldwide use. While the clinical outcome depends on the yield of islets and about 70% of patients require insulin therapy long term after surgery, most still benefit from functioning islets, and a simpler management of diabetes.

Stem Cells

Stem cell therapy has advanced as the treatment option for a number of diseases including cardiovascular, neurological, degenerative and autoimmune diseases, blood and bone marrow cancers, burns, corneal damage and organ failure. Stem cells have the potential to serve as an unlimited source for the development of various therapeutic cell types [65]. With the promise of islet transplantation in reversing diabetes and to address insufficient supply of islets from donors, increasing efforts have been focused on generating functional insulin-producing beta-like cells from stem cells. Several protocols have been developed to systematically guide the differentiation of human embryonic stem cells (hESCs), and more recently, induced pluripotent stem cells (iPSCs), into pancreatic endoderm (PE). PE cells have been shown to mature in vivo and function similarly to beta cells for prolonged periods following transplantation. In other cases, cells were transplanted after being fully differentiated into beta cells in vitro. While the results have been encouraging, recent efforts are directed towards improving differentiation conditions, cell expansion at specific progenitor stages, and purification

of target cell populations to obtain sufficient quantities of functional pancreatic beta-like cells. About 6000 clinical studies utilizing stem cells are currently registered and some of them utilize encapsulated stem cells. Some of the macroencapsulated stem cell derived beta cells (ViaCyte PEC-01) have reached the clinical trial stage now. However, challenges related to graft vascularization and viability and uncertainty about their long term fate in the host body, including teratoma formation, are to be addressed before their routine clinical use. Various strategies to address these challenges by many research groups are discussed in detail in the subsequent sections of this review.

Human Embryonic Stem-Cell Derived Beta Cells: In a preclinical study, human embryonic stem cell – derived mature beta cells that are glucose responsive, when encapsulated in alginate derivatives and implanted in the mice intraperitoneal cavity, were shown to induce glycemic correction and survival even at 174 days post-delivery without being accompanied by immunosuppressive treatment [66]. In case of ViaCyte product, a rapidly developing one to treat type 1 and type 2 diabetic patients, human embryonic stem cells are being differentiated into beta cell precursors (PEC-01^{TM}) and encapsulated in the Encaptra® drug delivery system. After subcutaneous implantation, the beta cell precursors further differentiate into mature insulin secreting cells, controlling blood glucose levels.

Pluripotent Stem Cells: Pluripotent stem cells (PSCs) have the ability to self-renew and differentiate into three germ layers including ectoderm, endoderm and mesoderm. Because of this ability they have the potential to play an important role in regenerative medicine and cell therapy. Through cellular reprogramming, it is possible to modify adult somatic cells using a cocktail of factors and reprogram them into embryonic state producing induced pluripotent stem cells, iPSC. Similar procedure can be used to reprogram somatic cells via factors present in the oocyte. Dr. *Shinya Yamanaka* shared the Nobel Prize for Medicine in 2012 for iPSC technology and several research groups are actively pursuing this

for diabetes treatment, regenerative medicine and drug delivery as well as for disease modeling purposes. Melton *et al.* at Harvard University have demonstrated the preclinical development of glucose responsive beta cells from human PSCs for the treatment of T1D [67].

Mesenchymal Stem Cells: Mesenchymal stem cells (MSCs) are studied by many research groups for diabetes treatment, to generate insulin-producing cells [68], counteract autoimmunity [69,70], enhance islet engraftment and survival [71,72], and to treat diabetic ulcers and limb ischemia [73]. MSCs have also shown improved metabolic control in experimental models of type 2 diabetes (T2D) [74]. In a preclinical study, Gaber, Grattoni *et al.* have demonstrated that human bone marrow – derived mesenchymal stem cells, differentiated into islet like insulin producing cell aggregates (ILIPAs), encapsulated in a platelet lysate based gel matrix and housed in a 3D-printed polymeric device remained viable and secreted insulin for several weeks, proving potential as an autologous transplantable system for treating diabetes [36].

In another preclinical study by Kauer *et al.* bone marrow - derived human mesenchymal stem cells were encapsulated in a synthetic extracellular matrix, along with murine neural stem cells, and administered into tumor cavity site of mouse models of human glioblastoma multiforme post tumor resection. This resulted in tumor size reduction, increase in survival rate, prolonged retention of encapsulated cells, tumor targeted migration and release of therapeutics. This study holds promise that patients' own stem cells can be manipulated to deliver anticancer agents to improve survival [75].

Adipose-Derived Cells: Adipose derived stem cells are easy to isolate, secrete several angiogenic factors and have great promise in the regeneration of ischemic tissue. However, they present limitations primarily due to poor survival, after transplantation. In a study, Cheng *et al.* encapsulated adipose derived stem cells in thermosensitive chitosan/gelatin hydrogel and demonstrated their sustained release, increasing the viability and promise for the treatment of ischemic diseases

[76]. In another study Xu *et al.* used a high density three-dimensional (3D) micromass model system to improve early chondrogenesis with adipose derived cells [77].

Adipose derived regenerative cells (ADRC) are a blend of adult stem cells, endothelial progenitor cells, leucocytes and smooth muscle cells. They can differentiate into several tissue types, such as bone, cartilage, fat, skeletal muscle, smooth muscle and cardiac muscle and hence show great promise in regenerative medicine. Cytori Therapeutics Inc. is conducting a safety and feasibility clinical trial (NCT01556022) to evaluate ADRCs derived from patients' own adipose tissue and specifically formulated for the treatment of chronic myocardial ischemia.

Fibroblasts: are another cell type, widely being investigated for encapsulated transplantation. In an in vitro study, mouse NIH 3T3 fibroblasts encapsulated in calcium alginate remained viable for up to 150 days and released vascular endothelial growth factor for several weeks, suggesting that they may be able to induce angiogenesis and maintain cardiac function post myocardial infarction [41]. Microencapsulated fibroblasts, genetically engineered to secrete human basic fibroblast growth factor for treatment of retinal dystrophies, were shown to survive for 90 days in vitro and upon xenogeneic transplantation in rats [38,39]. Encapsulation of genetically engineered fibroblasts is also being evaluated for treatment of spinal cord injury [40].

In majority of cases, encapsulation has shown to improve the in vivo viability of transplanted cells and enhance their functional ability for the intended therapeutic use, by providing a protected environment. Different strategies and a variety of natural and synthetic materials and their combinations have been investigated for this purpose, and are presented in the following sections of this review.

2.3 Strategies of Encapsulated Cell Transplantation in Diabetes

Based on the geometry of the encapsulation system, the encapsulation strategies can be classified as microencapsulation, wherein individual cells are enveloped in a micron scale immunoisolating membrane, or macroencapsulation in which groups of cells are encased in a suitable membrane which could further be housed in a device. In this section, we describe the different types of microencapsulation materials, their clinical applications in diabetes treatment, the various macroencapsulation systems, their clinical status in diabetes followed by the clinical advancements of encapsulated cell transplantation for treating various disease conditions including chronic eye and neurodegenerative diseases, cancer, chronic wounds, cardiovascular diseases and kidney dysfunction.

2.3.1 Encapsulation Materials

Cell coating and microencapsulation are two strategies that are being extensively explored in order to address the challenges of immune rejection of transplanted cells. While cell coating refers to the deposition of a suitable polymeric membrane onto the cell surface, microencapsulation involves encasement of single cells or clusters in a polymeric matrix or membrane of micron range thickness. Both cell coating and microencapsulating materials allow for immunoisolation of the transplanted cells by preventing entry and interaction with the host immune cells, antibodies and complements several kDaltons in size. Thus, they provide permselective protection to the encapsulated cells while allowing diffusion of essential small molecules from the host into the graft and the simultaneous release of hormones, metabolites and waste produced by the encapsulated cells. The size of microcapsules is often reported to influence the determination of the transplant site and immunogenicity of

the microcapsule system. Adverse effects have been associated with increase in volume of the encapsulated graft while, thickness of the capsule membrane influences the permeability for substance exchange and the diffusion rate of the therapeutic agents [34,78]. The diffusive properties and mechanical stability of the microcapsules were significantly enhanced in vitro, when capsule size was reduced from 1000 μm to 400 μm. This resulted in the improved functioning of the encapsulated rat islets and murine hepatocytes [25,79,80]. The first microcapsules were designed to be 600-800 μm in diameter and now with conformal coating, it is possible to achieve close to 200 μm diameter capsules, rendering the system to be implanted in retrievable sites in the body [81–83]. Microencapsulation strategies utilizing different types of natural as well as synthetic materials are being evaluated based on the biochemical properties of the materials and the functional requirements of the transplanted cells. Here, we introduce the various microencapsulation techniques.

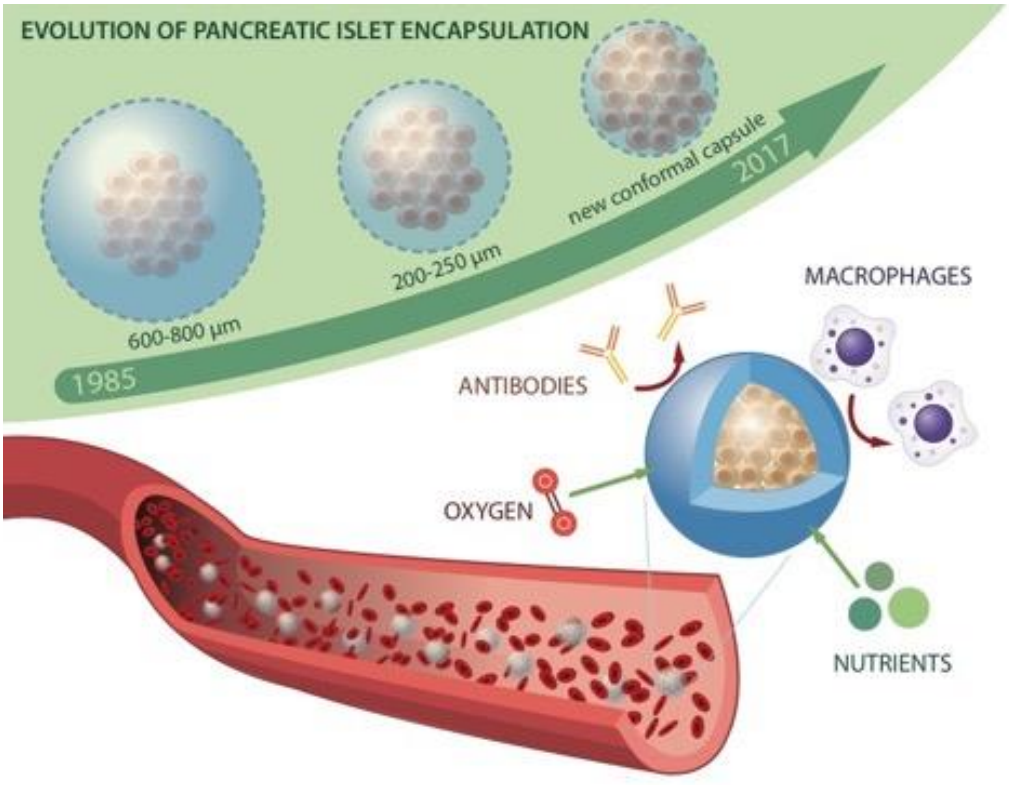

Figure 2.3: *Schematic of conformal coating and microencapsulation in pancreatic islet transplantation.* ***(A)*** *Over the years, significant efforts were spent in minimizing the ratio between encapsulation volume and surface area.* ***(B)*** *The semi-permeable membrane protects the encapsulated cells from the immune*

system of the recipient while permitting the diffusion of molecules such as nutrients, oxygen, glucose, oxygen and insulin.

Alginate Microcapsules: Alginate has been a widely explored encapsulating material due to the ease of generating microspheres, its rapid cross-linking potential to form gels, and the flexibility of incorporating other functional polymers [26]. Alginate does not present significant permselectivity against immune cells and factors that can destroy the encapsulated cells [84]. As such, polycations including poly-L-lysine (PLL) [85], poly(vinylamine) [86] and poly(allylamine) [87], poly-L-ornithine (PLO) [23], and chitosan [88] have been used as coating materials in alginate microcapsules to optimize the porosity, and enhance the efficacy and the biocompatibility of the microcapsule system. A typical alginate microcapsule comprises of an alginate core and an alginate outer shell, sandwiching a semi-permeable polycationic layer. Microencapsulation of islets using alginate has been promising in that it has proven to protect the encapsulated graft from host immune attack and prolong islet survival and is extensively evaluated in several preclinical and clinical trials. Graft xenosis and fibrosis were also shown to be prevented [89]. One of the main factors leading to necrosis of alginate microencapsulated cells is the host immune response [90]. Derived from seaweeds and algae via harsh chemical regimens, the polysaccharide alginate contains protein residues and toxins, including pathogen associated molecular patterns' (PAMPs), which trigger inflammation, cell protrusion and complete fibrosis of the microcapsules [90,91]. A high concentration of mannuronic acid in the alginate copolymer is also known to elicit fibrosis. The stability of the outer alginate layer is important since it contributes to masking the inflammatory response stimulated by the PLL layer. Physical (surface roughness and charge) and mechanical (elasticity) properties of the alginate microcapsules play a role in determining the survival of the encapsulated cells [92–94]. However, the optimal values of these parameters, corresponding to the recipient and the site of transplantation are yet to be established from clinical studies.

PEG Coating: With the objective of overcoming the in vivo cytotoxicity and instability of PLL and other polycations, polyethylene glycol (PEG) and various polymers (e.g. chitosan, xanthan, agarose and cellulose) are used as coating materials [26]. The low immunogenic potential of PEG, its stability in physiological conditions, tunable biomechanical properties, and controllable protein adsorption, thickness, and porosity make it highly suitable for cell microencapsulation [95,96]. A variety of shapes of PEG-based microencapsulation systems have been designed. When subject to glucose challenges, PEG encapsulated islets have shown to release insulin and also restored immunocompromised diabetic mice to normoglycemia for 110 days [97]. PEG encapsulated islets were also clinically assessed [98] and currently evaluated in advanced preclinical studies, as conformal coatings, in combination with matrigel. The main drawback of the PEG coating is that it creates an unfavorable cell microenvironment which can be overcome by incorporating collagen and laminin [99].

Agarose Microcapsules: Agarose, another naturally occurring polysaccharide obtained from red algae, exhibits several properties of a suitable microencapsulating material. As a responsive polymer, the aqueous solutions of agarose go through a sol–gel transition with change in temperature [100,101]. While the conformation of a random coil is maintained over the sol-gel temperature, when cooled it is transformed to a double helix. By leveraging this sol–gel transformation at approximately 37°C, agarose formulations can be employed for encapsulating cells. Agarose is a naturally occurring polysaccharide. It is less likely to trigger fibrosis and host inflammatory response and is also not biodegradable which makes it suitable for long term implants [102].

Cellulose Microcapsules: Cell-in-a-Box® microencapsulation system, developed by PharmaCyte Biotech in partnership with Austrianova, utilizes cellulose sulfate and polymers such as polydiallydimethyl ammonium chloride to encapsulate genetically modified cells or beta cells by droplet formation. A combination of biocompatible

natural and encapsulating polymers are passed through a microfluidic device to form microdroplets of a semipermeable membrane housing the therapeutic cells. The 0.7 to 0.8 mm sized microdroplets housing insulin producing cells referred to as the artificial pancreas is used for the treatment of type 1 and insulin-dependent type 2 diabetes. Preclinical studies in diabetic rats showed that transplantation of porcine insulin-producing islet cells restored normal blood glucose levels and maintained for six months. Similar microdroplets encasing about 10,000 genetically modified liver cells, referred to as the artificial liver activates the chemodrug ifosfamide at the tumor site and kills the tumor. Clinical trial of the artificial liver is being initiated for the treatment of locally advanced inoperable pancreatic cancer (LAPC) [103–108].

Although the different encapsulating materials demonstrate different advantages in providing immunoisolation of the graft there are several hurdles left to overcome for their successful clinical deployment, starting from the choice of a suitable site for transplantation. Subcutaneous transplantation is potentially of interest to minimize the invasiveness of the procedure. Even though the subcutaneous tissue is known to deliver sufficient oxygen tension of 20 to 40 mmHg, transplantation of cells, as an example pancreatic islets, into an unaltered subcutaneous site has never been known to reverse diabetes in humans or in animal models [109–112]. This may be due to the inhospitable microenvironment owing to inadequate vascularization. Thus, angiogenesis stimulation is crucial for successful islet transplantation at the subcutaneous site. For this reason, oxygen generators [113], polymers [114,115], meshes [116], encapsulation devices [117,118], matrices [119], growth factors such as fibroblast growth factor, vascular endothelial growth factor and hepatocyte growth factor [119] as well as co-transplantation with mesenchymal stem cells have all been explored with some success [120,121]. Another critical issue is adverse tissue responses against the encapsulating capsules. Some of the reactions may be linked to the material or its components in the encapsulation. It has been shown that ‘pathogen associated molecular

patterns' (PAMPs), which strongly trigger inflammatory responses are present in alginate.

Cell protrusion, which has been associated with most encapsulation systems represents another challenge [91]. Over a certain limit, protrusion is known to generate high inflammatory responses which result in fibrosis of the transplanted microcapsules and necrosis of the transplanted cells. The different elasticities and mechanical robustness of the capsules [97], which determine the optimal conditions for cell survival and functioning are yet to be established. Along with these properties, factors such as roughness and charge of the microcapsule surface [85,122] and adsorption of protein [123,124], are vital to the success of the transplant.

One of the main limitation of all microencapsulation approaches is that the transplanted cells cannot be retrieved in case of adverse reactions. This represents a safety concern, particularly in the case of stem cells, whose long term fate are unclear and that have the potential to differentiate into tumors [125,126]. An unmet need in cell encapsulation is the ability to monitor the delivered cells. Once microcapsules are transplanted, the only way to assess their functional state is through invasive recovery surgery. An unmet need in cell encapsulation is the possibility of monitoring the delivered cells. Invasive recovery surgery is the only mean to retrieve the transplanted microcapsules and examine the functional state of the encapsulated cells. Barnett et al. have designed an interesting method to overcome this issue by using alginate-based radiopaque microcapsules, comprising of barium sulfate or bismuth sulfate, which could be observed by X-ray [127]. Although, the radiopaque agents did not affect cell viability and capsule permeability, the other materials employed in this work require more extensive examination.

2.3.2 Microencapsulation in Diabetes

In this section, we describe recent developments and deployment of microencapsulation systems in the field of diabetes treatment. Table 2.1 shows the relevant microencapsulation materials, cell sources and sites of

implantation of these systems. Their applications in other disease treatments are discussed in a later section.

Table 2.1: *Clinical studies of microencapsulation systems for different application fields.*

Company - Institution	Material	Cell source	Graft site	Phase	Ref.
DRI	PEG-MG	Xeno-allo pancreatic islets	Epididymal fat pad	Preclinical	[140]
LCT	PLO-Alginate	Porcine Insulin cell	Peritoneal cavity	I/IIa	[144]
Encapsulife	Organic polymers	Xeno-allo pancreatic islets	Peritoneal cavity	Preclinical	[134-135]
Vicapsys	Alginate	Porcine islet cell graft	Intraperitoneal cavity	Preclinical	[145-146]

Agarose encapsulated grafts were first shown to reverse diabetes in mice by Iwata in 1988, with the non-obese diabetic allografts surviving for 80 days while isografts survived indefinitely [128]. In a more recent syngeneic islet transplant study without immunosuppression, mice implanted with the agarose microencapsulated islets were functional for more than 100 days. Encapsulated islets survived autoimmune destruction in contrast to the non-encapsulated islet grafts that lost their function in 2 weeks and shown to be destroyed by complete infiltration by mononuclear cells and destroyed [129].

Alginate microencapsulation of human pancreatic islets demonstrated partial success clinically with limited survival period post-transplantation n 1994 [130]. Interestingly, alginate microencapsulated neonatal porcine islets were functional and survived over 9.5 years when first implanted intraperitoneally (15,000 IEQs/kg) in a type 1 diabetic patient in 1996 [131–133]. In addition to the 30% insulin reduction, there were no signs of xenosis or fibrosis of the graft.

An interesting approach to avoid the use of immunosuppressive drugs and achieve immunoisolation of the transplanted pancreatic beta cells was designed by Encapsulife. Islet cells microencapsulated in a five-component, triple layered polymeric system, were simply anchored without attachment to the peritoneal cavity by means of a 15-minute laparoscopic

procedure. This method of implantation enabled optimum nutrient and fluid exchange for the transplanted islets as well as stimulated insulin production. When canine pancreatic islets, encapsulated using this approach were transplanted to the pancreatectomized canines' peritoneal cavity, the fasting blood glucose of all the nine experimental subjects, were normalized for 214 days without the use of any immunosuppressive or anti-inflammatory drugs [134,135].

Alginate encapsulated beta cell grafts with systemic immunosuppressive regimen such as basiliximab, anti-thymocyte globulin, tacrolimus and sirolimus were tested by Keymeulen group at AZ-VUB and University Hospital Brussels, Belgium demonstrated better outcome with encapsulated grafts than non-encapsulated controls in an immunodeficient mouse model [136,137]. An on-going phase II clinical trial, NCT01379729, involving non-uremic type 1 diabetic patients is currently assessing survival and function of the allografts of microencapsulated beta cells implanted in the peritoneal cavity. The microencapsulated grafts showed glucose secretory response in both mouse and human studies. Dr. Riccardo Calafiore and team at University of Perugia, Italy are developing microencapsules of human islets in a sodium alginate and PLO microbead based system [138,139]. Clinical evaluations have shown that the intraperitoneal transplantation of the microcapsules in non-immunosuppressed type 1 diabetic patients elicited no immune response even with subsequent implants. However, the metabolic efficacy was limited due to poor oxygen and nutrient supply, affecting insulin secretion [83].

Islets are non-uniform in size and range from 50 to 350 μm. Typical microcapsules are uniform in size and range from 500 to 1500 μm. Encapsulated grafts of such volume can suffer from islet aggregation and poor oxygen and nutrient distribution potentially leading to necrosis. Microencapsulation methods involving a thin coating to maintain volume comparable to the naked islet grafts, are being assessed to overcome this drawback [93]. Alice Tomei and team at the Diabetes Research Institute of

Miami are developing a system where islets are conformally coated (shrink wrapped) with a PEG hydrogel layer and matrigel (MG) extracellular matrix [140]. This system is characterized by enhanced immunoisolation and islet function owing to its permselectivity and minimal immunogenicity [140]. The aim of this process is to facilitate implantation in favorable sites and minimize core hypoxia and delayed insulin release [82]. This method did not negatively affect islet function in vitro and in vivo [141]. When the conformally coated PEG MG islets from Balb/c mice were transplanted into the epididymal fat sites of diabetic C57BL/6 mice, at a dose of 750-1000 IEQ/mouse, the islets survived over 100 days without the administration of immunosuppressive drugs [140].

Another tri-layered encapsulation technology of significance is IMMUPEL™, developed by a New Zealand based company, Living Cell Technologies Limited (LCT Ltd). Diabecell™ and NTCELL®, both adopt the IMMUPEL™ technology – intermediate PLO layer sandwiched by alginate layers - eliminating the need for immunosuppressive regimens post-transplantation [125,142]. Xenogeneic transplant of DIABECELL® has shown to lower the daily insulin requirement in diabetic rats as well as non-human primates [143]. It was also shown to have a favorable safety profile in mice, rabbits and dogs. In human trials, conducted in Argentina, New Zealand and Russia, DIABECELL® was safely implanted in the peritoneal cavity of type 1 diabetic patients. HbA1c, insulin dose and unaware hypoglycaemic events were significantly lowered with increased dosage [144]. With no signs of adverse reactions to up to 3 implants per patient, 6 patients demonstrating long term blood glucose control and the remaining 2 were completely insulin independent for up to 8 months, DIABECELL® was clinically approved in Russia in 2010.

An advancing microencapsulation technology aimed at encapsulating and protecting the islet graft is VICAPSYS's VICAPSYN™eluting alginate system. This 200-600 μm system is designed to comprise 1-2 human or porcine islets microencapsulated by biocompatible polymers which gradually release VICAPSYN™ over time. VICAPSYN™ provides immunoisolation by repelling T-cells and prevents fibrosis and graft

rejection. The angiogenic properties of VICAPSYN™ is proposed to enhance perfusion of the islets and enhance vascularization at the transplant site. Transplants of the CXCL12 incorporating alginate microcapsules, in the intraperitoneal cavity of healthy NHPs demonstrated the absence of inflammatory cells when adjacent to the mesentery while capsules devoid of CXCL12 were marked with significant inflammation and fibrosis. Two autologous transplants of the encapsulated islets were found to be functional when retrieved 30 days post-transplant. Allogeneic islet transplant studies are ongoing [145,146].

2.3.3 Macroencapsulation Systems

Microencapsulation and cell coating strategies have achieved important milestones in particular by limiting the access of host's immune system to the transplanted cells [45]. However, achieving long term cell survival is still a major challenge for the many reasons previously described including dispersion, suboptimal oxygenation and engraftment [26,147,148].

Macroencapsulation systems have been developed to overcome these challenges using larger devices with a planar or cylindrical geometry, to provide a suitable hosting microenvironment for cells. The reservoir of these implantable devices often designed to avoid cell clustering while protecting cells from mechanical stress. Importantly, cells are isolated from direct contact with the host tissues via permeable flat sheet membranes or the lumen of semipermeable hollow fiber. This represents a significant advantage of macroencapsulation as it offers the option of full cell retrieval, in case of loss of function, adverse effects, or malignant transformation of the transplanted tissue [149,150].

Macrocapsules are classified in two main categories: *i) Intravascular systems,* which connect the graft as a shunt to the systemic circulation. *ii) Extravascular devices*, which rely on the formation of new blood vessels at interface between the host tissue and the device interface [93,147,151].

In some of the intravascular devices, cells are encapsulated within a semi-permeable membrane containing polymeric capillaries. After cells

transplantation within the membranes, these devices are directly connected to the host systemic circulation by vascular anastomoses creating an intravascular shunt. The close proximity with the recipient's blood stream constitutes an important advantage in terms of ideal oxygen and nutrient supply, thereby enhancing graft survival [147]. This feature is also of paramount importance for cells whose therapeutic function is to secrete molecules in response to biological stimuli, in real time, as is the case for pancreatic islets. However, intravascular systems generate the risk of thromboembolic events, which require intense anticoagulation therapy and associated adverse effects (e.g bleeding and gangrene, among others). This has rendered intravascular devices are no longer suitable for routine clinical application. Extravascular devices are usually associated with lower risk to the recipient. These systems are designed in the form of either tubular or planar diffusion chambers. Common sites of implantation are the peritoneal cavity, an omental pocket, or subcutaneous tissues, which make their implantation simpler, less invasive, and mostly free of major surgical complications. Despite the advances in cell engineering, it is unlikely that transplanted cells would survive and function indefinitely. Pragmatically, strategies for the substitution, or replenishment of cells have to be considered in the context of clinical deployment these systems. In this context, extravascular macroencapsulation devices, especially those designed for subcutaneous implantation, offer a solution via device retrieval or transcutaneous cell loading and replacement.

Diabetes is the medical field for which macroencapsulation strategies have been most widely explored for decades. In the following sections, we present early developments of macroencapsulation devices in diabetes, followed by current approaches in advanced preclinical clinical study as well as under clinical trials.

2.3.4 Early Macroencapsulation in Diabetes

One of the earliest pioneering studies attempting the implantation insulinoma tissues in a perm-selective membrane is the one by Dr. Bisceglie in 1933. The study focused on determining the effect of the absence of vasculature on the survival of implanted tissues. However, the

credit for originally developing an extravascular diffusion device based on a flat membrane system should go to Dr. Algire and his colleagues Drs. Prehn and Weaver. They studied both the cellular mechanisms of tissue rejection and tumor growth, the results of which were reported in a series of publications from 1948–1959 [147–155]. Notably, they found that while host cell exclusion achieved allograft survival, by itself it was not sufficient to protect xenograft transplants long term. This work led to the strategy of artificially creating an immune-privileged site for cell implantation and opened the door to pancreatic islet encapsulation studies that followed.

In the 1970s, following Algire's approach, Millipore Corporation produced an extravascular transplantation chamber for allotransplants. The device featured membranes with pore sizes in the order of 450 nm, with the objective of preventing direct cell–cell contact between the graft and the host [156]. In vivo assessments showed that cells remained viable only for a few weeks. Fibroblast overgrowth around the device was observed, which raised concerns about device biocompatibility. In an attempt to reduce the fibroblastic response, attempts were made to oat the outer surface of membranes with collagenase [157]. This approach helped eliminating the fibrous capsule directly in contact with the membrane. However, a fibrotic encapsulation formed at a short distance from the membrane, still limiting the inward and outward diffusion of molecules and nutrients [158].

Additional factors challenging the success of these permselective systems were ascribed to the lack of mechanical robustness and chemical stability of membranes *in vivo*. The development of silicon nanofluidic systems based on microfabrication and sacrificial layer techniques [159]fostered new approaches to cell encapsulation systems. In fact, peculiar properties of transport in nanochannels [160,161] can be leveraged to achieve better control of molecule permeation and diffusion via physical and electrostatic confinement [162–164]. Starting in the early 1990s, Ferrari, Desai *et al.* generated microfabricated capsules with regular patterns of slit-nanochannels in size smaller than 100 nm [165] for molecular sieving [166] and cell immune isolation [167,168]. They showed that islets and insulinoma cells encapsulated in these systems within a

supportive matrix, were viable and glucose responsive in vitro and in vivo in mice models [169]. These ceramic-based systems offered enhanced mechanical robustness and biocompatibility [170] showing minimal fibrotic encapsulation surrounding the device. However, long term graft survival was still elusive likely due to the lack of proper cell oxygenation.

In the late 1990s, Baxter Healthcare that subsequently became Theracyte™, provided an important contribution in the field of macroencapsulation systems by designing a planar device employing a double membrane approach for immune protection and vascularization of the cells [171]. An outer Teflon membrane offered mechanical strength and promoted capillary ingrowth, while an inner hydrogel semipermeable membrane was used for allograft immune protection. High level of vascularization was achieved subcutaneously in rats and cell function was shown [115,172]. Despite these promising results, a fibrotic capsule overgrowth still challenged cell retrieval. Baxter's technology is still used by various research groups and important players in the cell encapsulation field such as Living Cell Technologies (LCT), Betalogics of Janssen Pharmaceuticals, and Viacyte.

Other macroencapsulation strategies based on alginate were developed, in late 1990s, to achieve immune protection and to support cell viability and function. Suzuki *et al.* implanted encapsulated islets into the epididymal fat pad(s) in streptozotocin-treated diabetic mice and demonstrated their in vivo viability and function for 12 weeks [173]. Islet Sheet Medical conceived alginate based islet sheets (250 μm) and tested them with allogenic islets sutured on to the omentum of dogs, demonstrating euglycemia for 84 days [174]. More recently, human islets were encapsulated within the islet sheets and tested both in vitro and in rats demonstrating islet survival [175].

Recently, various other companies developed a number of approaches, without reaching clinical evaluation. Among them, *Encelle* transplanted intramuscularly porcine islets encapsulated in a hydrogel matrix and supported by a polyester net; *BetaGene* in partnership with *Gore Hybrid Technologies* designed a subcutaneously

implantable flexible tube containing islets. However, most of these technologies failed to reach clinical evaluation.

3.3.5 Current Macroencapsulation in Diabetes

More recently, external oxygen supplementation, vascularization of the devices prior to cell transplantation and the use of autologous cell sources have been adopted as strategies for achieving long term cell survival. Despite the difficulties in achieving suitable vascularization, subcutaneous implantation is now considered as one of the target implantation sites. Advantages include reduced invasiveness of surgical procedure and the potential for transcutaneous loading, replenishment and retrieval of cells. Table 2.2 lists recent macroencapsulation technologies are under advanced preclinical and clinical investigation and that are discussed in greater details below.

Table 2.2. *Current macroencapsulation systems under advanced stage of development for diabetes treatment.*

Company - Institution	Material	Cell source	Graft site	Phase	Ref.
TheraCyte	PTFE membrane	Islet ESC derived	Subcutaneous	I	[171]
Beta-O_2 Technologies	Teflon/Alginate	Human pancreatic islets	Subcutaneous	I/II	[178]
Viacyte	PTFE membrane	Human embryonic stem cells	Subcutaneous	I/II	[180-182]
Houston Methodist Hospital	Medical grade polymer/Silicon	Human pancreatic islets/beta cells	Subcutaneous	Preclinical	[35,36]
Monolayer Cellular Device	Alginate	Pig islets	Subcutaneous	I	[197]
Defymed	Medical grade polymers	Insulin secreting cell	Subcutaneous	Preclinical	[192]
DRI	Plasma-thrombin biologic scaffold	Human islets	Omentum	I/II	[202]
Sernova	Medical grade polymers	Human Islets	Subcutaneous	I/II	[191]

βAir. To improve cell oxygenation within the device, an implantable bioreactor was developed by the Israel based company Beta-O_2 Technologies Ltd. This device, named βAir (Fig. 2.4A) is a subcutaneous system that comprises a reservoir containing islets encapsulated in an alginate hydrogel slab, and a gas chamber that allows oxygen supplementation through a tubing system, to improve cell oxygenation within the device. A porous membrane protects islets from immune

rejection and a silicon membrane allows the passage of oxygen contained in the gas reservoir. Preliminary studies in rats and pigs showed that daily oxygen supplementation via injection preserved islets function for up to 90 days [176]. In 2012, ßAir was implanted in a 63-year-old patient in Germany. The case report indicated that islets retained function for the 10-month study duration, achieving persistent graft function, regulated insulin secretion and preservation of islet morphology and function without any immunosuppressive therapy [177]. A phase I/II clinical trial (NCT02064309) [178] with 4 patients is ongoing (expected to end in 2018) with the primary objective to investigate the safety of implantation βAir containing human islets in type 1 diabetic subjects [179]. The secondary objective of the trial is to evaluate the efficacy of the βAir device in improving glycemic control, and the incidence of hypoglycemic episodes. Other key developments proposed by Beta-O_2 are a market ready version-2 device that holds enough beta cells to replace insulin altogether, instead of being an add-on to insulin therapy and to advance from cadaver cells to stem cells in the coming years.

PEC-Encap and PEC-Direct. Over the past decade, ViaCyte, Inc. (San Diego, CA) has developed two subcutaneously implantable devices for the encapsulation of stem cell derived pancreatic progenitor cells (PEC-01™) for diabetes treatment. Both promote vascularization prior to cell transplantation in order to avoid graft hypoxia events [94]. **PEC-Encap**™ device (Fig. 2.4B) consists of an immunoprotective membrane (Encaptra®) that allows oxygen and nutrients permeation from the vasculature generated on its outside, while limiting access to immune cells. **PEC-Direct**™, instead, consists of a polymeric membrane that allows direct vascularization of the encapsulated cells within the device. In this case immunosuppressive regimens are required to protect the graft from host's immunerejection. PEC-Encap™ approach was shown to retain robust graft function for at least 6 months following transplantation. In late 2014 Viacyte started a phase I/II clinical trial (NCT02239354) [180] with the purpose to test safety and efficacy of PEC-Encap™ implanted subcutaneously in type 1 diabetes patients, over two years. In 2016 a 3-

year follow up safety study (NCT02939118) [181] was started in subjects previously implanted with PEC-Encap™. The expected recruitment is 200 patients. An open-label clinical trial is ongoing to evaluate the safety and efficacy of PEC-Direct. In the first Cohort, T1D patients were implanted with the devices loaded with specific cells called sentinels. These cells, after the retrieval of the implant, will be examined histologically to evaluate the engraftment and maturation of the insulin-producing cells. On August 1, 2017, ViaCyte announced that the PEC-Direct™ implantation in the first patient took place in collaboration between University of Alberta Hospital in Edmonton, Alberta, and the UC San Diego Altman Clinical Trials Research Institute (NCT03162926) [178]. In the second Cohort up to 40 patients will be evaluate the ability of PEC-Direct™ to release a clinically relevant level of insulin [182]. On Jan. 5, 2018 in the first patient of the Cohort 2 was implanted a potentially efficacious dose of PEC-01™. In the coming months, the company proposes to expand the trial to additional centers in Canada and in the US, including the University of Minnesota. Efficacy results from this trial are expected by the first half of 2019.

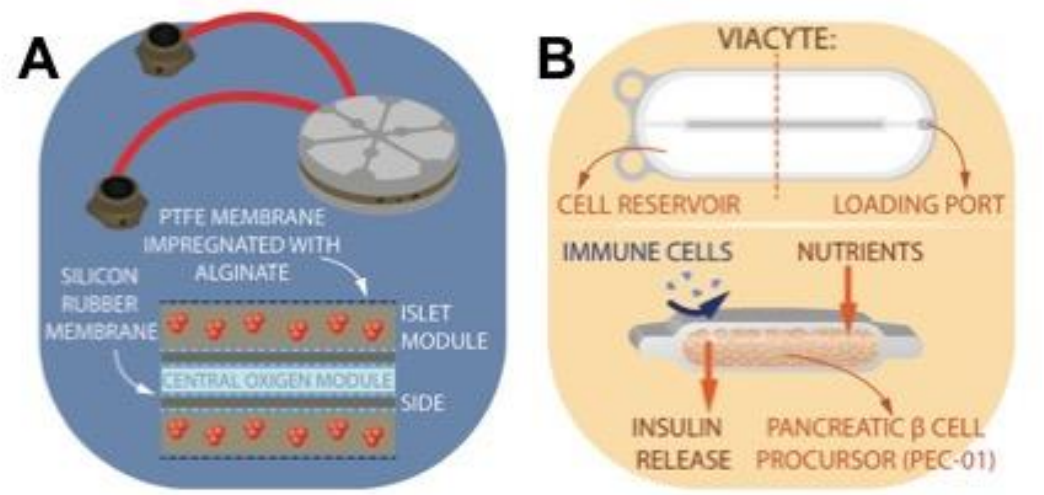

Figure 2.4: *(A) Schematic view of the ßAir device showing the central gas module connected to the two access ports for exogenous oxygen refueling. The core of the device can be charged with oxygen to diffuse outwards to the two compartments surround the central gas cavity where alginate-immobilized pancreatic islets are housed. The central module is covered by hydrophylized PTFE porous membranes. (B) Schematic of the PEC-Encap™ device, which is composed by an immunoprotective membrane (Encaptra ®) that allows the transport of nutrients from the exterior of the device and hormones from the*

encapsulated cells.

Cell Pouch. A different approach developed by Sernova Corporation (Canada) [183] allows to pre-vascularize a subcutaneous site before the administration of the cells, through a port. The discoidal device named Cell Pouch™ (Figure 2.5A) is implanted and maintained subcutaneously for 4 to 5 weeks. At the end of this period, islets are injected within the device. The Cell Pouch™ device does not protect transplanted cells from immune rejection and so immunosuppressant drug administration is required. To avoid immune rejection, immunesuppressant drug Transplanted cells in this vascularized space were proven to be functional, enabling diabetes reversal in a murine model [183,184]. Sernova's islet cell replacement therapy is currently in phase I/II development stage for Type-1 diabetes at University of Alberta [185]. In order to protect insulin producing islets from immune system attack locally within the Cell Pouch™, Sernova developed the Sertolin™ technology. Preclinical studies are ongoing.

MAILPAN. With the purpose of developing an non-biodegradable, biocompatible material, Defymed [186], a spin-off of CeeD (European Center for Diabetes Studies) is developing an implantable device known as MAILPAN® (Macroencapsulation of pancreatic Islets) (Fig. 2.5B), with a first focus on type 1 diabetes and applicable to several other diseases. MAILPAN® is a semi-permeable device, designed to be implanted into a patient's abdomen that aims to work as a bio-artificial pancreas. Similarly, to other systems, MAILPAN encapsulates insulin-secreting cells within the cell chamber made of impermeable membranes to the immune system, but permeable to oxygen, nutrients, glucose and insulin. Thanks to the presence of input and output ports, cells within the MAILPAN® can be replaced without the need for surgery. In 2016 Defymed signed a strategic collaboration with Semma Therapeutics in order to use the MAILPAN technology to encapsulate Semma stem cell-derived insulin-secreting cells. Pre-clinical studies are ongoing.

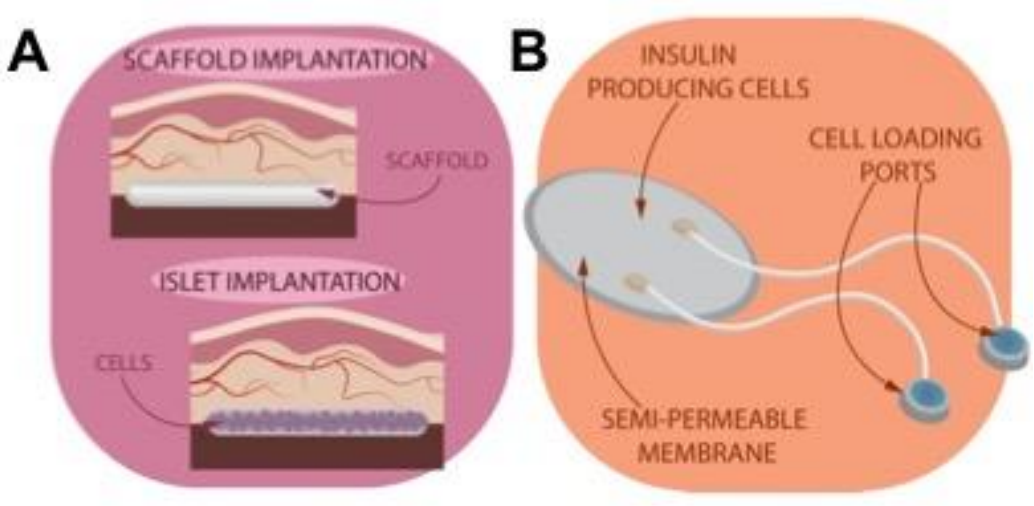

Figure 2.5: *(A) Cell Punch System where a polymeric scaffold is subcutaneously implanted and then removed leaving leaving a void vascularized space where the islets are transplanted. (B) Graphic representation of MAILPAN system composed by cell chamber and two ports for the external cell loading.*

In the macrodevices described above, the transplanted cells are housed between flat-sheet double membranes made with water-insoluble polymers [187] such as PTFE, PLA and Teflon. Other research groups adopt a "monolayer" configuration where cells are seeded as a monolayer within water-soluble polymers such as acellular collagen matrix and hyaluronic acid to provide a more natural and potentially less immunogenic environment to the encapsulated cells [188].

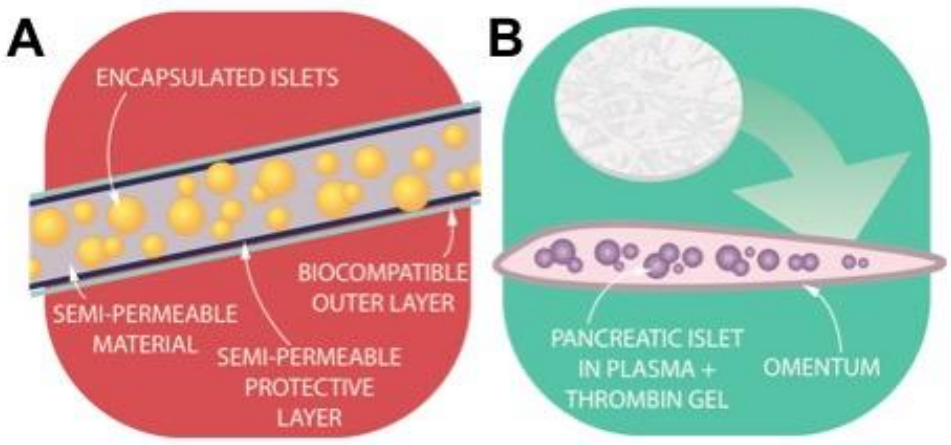

Figure 2.6: *(A) Scheme of Monolayer Cellular device planar consisting on a flat sheet made of acellular collagen matrix containing porcine islets encapsulated as alginate macrocapsules. (B) BioHub technology where the*

donor islet cells are combined within a biodegradable scaffold made with patient's own plasma, thrombin and a clinical-grade enzyme. The area of the omentum is then folded over around the scaffold.

Monolayer Cellular Device (MCM), developed by Dufrane et al. [189] at University Clinical Hospital Saint-Luc, Brussels, consists of a planar flat sheet made of acellular collagen matrix where porcine islets are seeded and encapsulated as alginate macrocapsules [190] (Figure 2.6A). Designated for subcutaneous implantation, it successfully controlled diabetes for 6 months in diabetic cynomolgus macaques, without the need of immunosuppression. Moreover, after transplantation of new monolayer cellular devices, diabetes was controlled for up to 1 year. [188]

The implantation of a Monolayer Cellular Device in a 74-years old T1DM patient showed no inflammation and no immunization against donor cells for 361 days. Diabetes control and graft function was achieved during 11 months post-transplantation. A 61% reduction of hypoglycaemic episodes was obtained. After 11 months, the device was easily removed showing the macroscopical integrity of the graft without sign of inflammation [191]. In 2016, a Phase I clinical trial involving 15 type 1 diabetes patients was completed at the Université Catholique de Louvain (NCT00790257) [192]. As an additional effort to improve vascularization of the device, adult pig islets were co-transplanted with either bone marrow or adipose mesenchymal stem cells (BM-MSCs or AMSCs, respectively) [193]. However, despite the improved oxygenation and neoangiogenesis, MSCs only slightly improved the long term function of the device in an NHP model [193].

BioHub. Another technology based on the encapsulation of pancreatic islets within a biological material has been developed at the Diabetes Research institute (DRI) of Miami [194]. This scaffold system, known as BioHub, is composed of a gel-like substance made with the patient's own plasma combined with thrombin. The scaffold containing pancreatic islets is then implanted onto patient’s omentum (Fig. 2.6B). Over time, the gel degrades leaving the islets intact, while new blood vessels are formed to support their survival and function. The omentum was chosen for relatively

easy access and its dense vasculature. Studies conducted in small animal model demonstrated an improved metabolic function and cytoarchitecture preservation of the encapsulated cells within the highly vascularized BioHub scaffold. Long-term nonfasting normoglycemia and adequate glucose levels were achieved [195]. BioHub is being evaluated in an ongoing clinical trial (NCT02213003) [196]. In May 2017, Baidal *et al.* published part of the results of the ongoing study (NCT02213003), where the patient, a 43-year-old woman with a 25-year history of type 1 diabetes, received a total of 602,395 islet equivalents from one deceased donor encapsulated within the autologous engineered-tissue and implanted onto the omentum [197]. BioHub restored euglycemia and insulin independence for 12 months. Although this strategy still requires the administration of immunosuppressive regimens, it demonstrates that the omentum could be considered as a good site for islet transplantation adopting the BioHub technique. The ongoing study aims to test the safety and long-term feasibility of the approach for islet transplantation.

2.4 Cell transplantation beyond Diabetes

Many other medical conditions have been targeted with cell therapies and encapsulation strategies, especially those involving a protein deficiency (Table 2.3). Here we present the most successful micro or macro encapsulation approaches and applications that are currently under investigation or already approved for clinical use.

Table 2.3: Clinical studies of macro encapsulation systems for different application fields.

Application	Company - Institution	Material	Cell source	Graft site	Phase	Ref.
Chronic eye disease	Neurotech	Implantable polymer	Human retiunal pigment epithelial cells	Eye	II/III	[210]
Neurodegenerative diseases	NsGene	Implantable polymer	GDNF secreting cells	Intracranical	II	[230,231]
Neurodegenerative diseases	NsGene	Implantable polymer	NGF secreting cells	Intracranical	I	[237,238]
Cancer	MaxiVax	Implantable polymer	GM-CSF secreting cells	Subcutaneous	II	[246]
Wound healing	Organogenesis	Extracellular matrix	Fibroblasts/epidermal keratinocytes	Cutaneous	FDA approved	[254]
Wound healing	Organogenesis	Polyglactin scaffold	Fibroblasts	Cutaneous	FDA approved	[255,256]
Kidney failure	CytoPherx	Polycarbonate/EPDM/niobium coated carbon	Renal epithelial cells	External	IIb	[265,265]
Kidney failure	Sentien Biotechnologies	Biocompatible polymers	Mesenchymal stem cell	External	I/II	[266,267]
Kidney failure	UCSF	Silicon	Human kidney tubule cells	Abdomen	Preclinical	[268-270]

2.4.1 Chronic Eye Diseases

Stem cell therapies are under development for several ophthalmic conditions including age-related macular degeneration (ARMD) and diabetic retinopathy as well as to provide trophic factors to protect compromised retinal neurons and to restore neural circuits.

Utilizing its technological platform, Neurotech Pharmaceuticals, Inc. (Cumberland, RI) [198] has created intraocular implants for the treatment

of a broad array of eye diseases that can deliver therapeutic proteins directly to the back of the eye for up to two years. These implants contain human retinal pigment epithelium cells (NTC-201) that have been engineered to produce and release a desired therapeutic agent and that are encapsulated in a semi-permeable hollow fiber membrane protected by a permeable exterior capsule (Fig. 2.7A). The implant is surgically inserted in the vitreous allowing oxygen and nutrients to freely diffuse inside the device, and therapeutic to freely diffuse outward. The implant termed Renexus® (NT-501) developed by Neurotech Pharmaceuticals [199] (Fig. 2.7A), is an implantable polymeric device containing NCT-201 cells secreting ciliary neurotrophic factor (CNTF), and going through phase II and III clinical trials for the potential treatment of retinitis pigmentosa (RP), [200,201] age-related macular degeneration (AMD), [202] glaucoma neuroprotection [203], vision restoration [204] and macular telangiectasia (MacTel). In June 2017 Neurotech announced the results of the phase II trial on MacTel (NCT03071965) [205] showing achieving a significant reduction in the progressive loss of photoreceptors in the treated patients as compared to untreated individuals, at 24 months. Neurotech plans to initiate a phase III trial for the therapy by the end of 2017 and this therapy has the potential to become the first treatment available for macular telangiectasia. Neurotech is currently developing more advanced versions of this platform including NT-503 device secreting VEGF-antagonists to treat wet AMD [206] and NT-506 for the treatment of wet AMD by secreting a PDGF (platelet-derived growth factor) antagonist. With this system, the company expects to improve efficacy and reduce scarring of the retina.

2.4.1 Neurodegenerative diseases:

Chronic, degenerative central nervous system (CNS) diseases is currently the fourth leading cause of death affecting over 37 million people worldwide [207]. Despite extensive research efforts, most of these diseases lack of a cure. To date, the most promising approaches for their management consist on the delivering of neurotrophic or angiogenic

factors from engineered cells to slow, or even reverse the ongoing degeneration and its related neurological deficits [208,209]. Encapsulated cell therapy is developed as a means to overcome the challenges of sustained, controlled delivery of these factors across the blood brain barrier (BBB) [210]. Macro devices encapsulating cells in semipermeable hollow fiber membranes have been investigated for CNS pathologies such as Alzheimer's disease (AD), Parkinson's disease (PD), and Huntington's disease (HD) [152,211–213]. Early studies in guinea pigs or NHP brains using xenografts showed that un-encapsulated cells were rapidly rejected, while cells in intact capsules remained viable, confirming the promise of encapsulation [214,215].

Parkinson's disease (PD) is a degenerative disorder of the CNS characterized by the development of progressive and debilitating motor impairments due to the dysfunction of dopamine-secreting neurons in the substantia nigra.

Initial validation of the possibility to use encapsulated PC12 cells implanted into the striatum for the treatment of PD came from studies in both rodents and NHPs [40,215,216].

Several studies have demonstrated the benefits of glial cell line-derived neurotrophic factor (GDNF) in preventing the loss of nigral neurons and abnormal motor function and enhancing dopaminergic function [217,218]. Unfortunately, the main limitation is that GDNF cannot be effectively delivered to the brain via systemic administration. To overcome this, encapsulated cells were implanted, in a small animal model, immediately rostral to the substantia nigra achieving a release approximately to 5 ng of GDNF/day. The results of these studies shown an attenuation of lost neurons but without having a significant effect on dopamine within the striatum [219–221]. Despite the potential role that encapsulated cells may have in the treatment of PD, the levels of GDNF and neurturin delivered were clinically not sufficient to register any beneficial effects. New technologies able to release with levels of GDNF are under investigation.

NsGene A/S (Ballerup, Denmark) has developed a tubular device (Fig. 2.7B) composed by polysulfone hollow fiber membrane for the

encapsulation of genetically engineered human cell line secreting GDNF [222–224], which, when implanted bilaterally into the putamen of the brain, have shown long-term stability (>1 year) in animal models and clinical trials [225,226]. Beyond GDNF, this product has potential for delivering various cell-derived substance, alone or in combination, to the CNS. In the first half of 2015, an IND has been filed to support a Phase Ib trial in approximately 12 patients with PD to demonstrate its safety and feasibility.

Alzheimer's disease (AD) is an irreversible and progressive brain disorder that mostly affects older population. AD is the most prevalent form of adult onset dementia and is expected to affect 115 million patients by 2050 [227].

AD is characterized by a progressive deterioration of cognitive and mnemonic ability, which is at least partially related to the degeneration of basal forebrain cholinergic neurons. Current therapies cannot prevent the loss of cholinergic neurons or the associated memory deficits. Encapsulated nerve growth factor (NGF) secreting BHK implants were shown to be efficacious in rats and NHPs in inducing a robust development of cholinergic fibers close to the implant site [226,228,229]. More recently, understanding the role of Aβ aggregates and neurofibrillary tangles in AD pathology, anti-Aβ therapies have been tested to prevent or delay development of AD [230,231]. Macroencapsulation devices composed by hollow fibers were used to transplant myoblasts genetically engineered able to release a single-chain variable antibody fragment (scFv) directed against the N-terminus of the Aβ peptide.

This treatment reduced Aβ production and deposition and improved behavioral deficits associated with the amyloid pathology. However, the invasiveness of the procedure is a major obstacle to clinical development in presymptomatic AD patients [211].

In order to increase the volume of the transplanted cells and reducing the invasiveness of the implant, novel flat sheet devices were developed for subcutaneous implantation [211]. These devices are composed of two porous polymer membranes enclosed in two mesh sheets, for mechanical stability and neovascularization. The inner chamber can contain up to several millions of myoblast cells, loaded into the device via a dedicated

port. Studies in mice have demonstrated that subcutaneously implanted Encapsulated Cell Therapy (ECT) devices achieved a release of 50 µg/ml of anti-Aβ IgG antibody for 19 weeks [49]. Ongoing investigations shown that similar levels of mAb can be achieved for more than 10 [211]. These results seem to validate the ECT technology combined with myogenic cells for the long-term delivery of anti-Aβ mAbs leading to a significant reduction of the amyloid brain pathology in Alzheimer's mouse models. Another encapsulation device for Alzheimer treatment developed by NsGene (NsG0202), showed, in clinical studies (NCT01163825) [232], that a sustained delivery of NGF at low doses to the basal forebrain cholinergic neurons could have clinical benefits on the progression and even prevention of AD [233,234].

2.4.3 Cancer

Immunotherapy refers to the modulation of the natural immune response in order to treat or prevent diseases including cancer. Studies have reported that endostatin-expressing cells in an immunoisolation device are effective in inhibiting the growth of melanoma and Ehrlich tumors [235]. As an example, mice fibroblasts engineered for the secretion of endostatin were encapsulated in Theracyte™ devices and subcutaneously implanted in mice at a site distant from the tumors [235]. A 42.4% reduction in melanoma growth was obtained [236,237]. These reports in the literature prove that macroencapsulation could provide a promising platform for innovative therapeutic strategies in cancer treatment [235].

Recently, MaxiVax SA (Switzerland) [238], a Swiss biotechnology company, conceived a flat macroencapsulation device specifically designed for subcutaneous implantation of cells capable of localized release of granulocyte-macrophage colony-stimulating factor (GM-CSF) for the treatment of solid tumors [211]. The assembled device is composed of two permeable membranes presenting a length, width, and thickness of 27, 12 and 1.2 mm, respectively (Fig. 2.7C). A loading port is integrated into the device to allow the injection of cells into the device.

Clinical trials were performed in patients with various types of cancer, such as renal cell carcinoma , melanoma, prostate, lung and pancreas cancer [238]. The clinical results highlighted the ability of GM-CSF to induce an effective anti-tumor immune response when secreted locally at the site of cancer cell injection [239]. A new system from MaxiVax named MVX-ONCO-1 is designed to allow for the local delivery of GM-CSF combined with irradiated tumor cells from the patient [240]. The objective is to deliver tumor antigens and cytokines at the same site as tumor cell injection, to produce a local adjuvant vaccine effect [241]. The first phase I clinical study (NCT02193503)[242] targeted patients with a variety of solid tumors, including pancreas, colon, head and neck, chordoma, prostate and ovarian, with failed standard therapies. The 8- week study, with 6 vaccine injections and 6 subcutaneous implantations of the immune booster demonstrated that MVX-ONCO-1 was safe and well tolerated, with no occurrence of any serious adverse events [242]. No clinically significant local or systemic reactions were reported. The company is initiating a Phase II clinical trial for head and neck cancer and other solid tumors. MVX-ONCO-1 the first in men cell encapsulation system developed for cancer immunotherapy. Numerous preclinical studies following similar immunotherapy approaches are ongoing. These are beyond the scope of this work, but are extensively reviewed in the literature (refs).

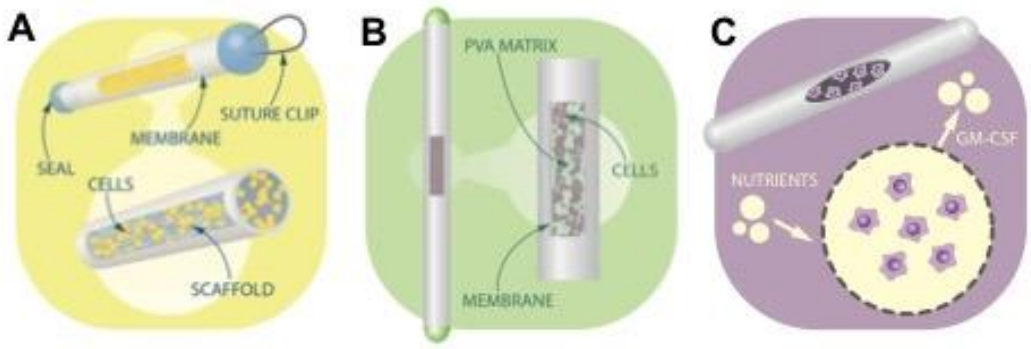

Figure 2.7: *(A) NTC-501 technology for chronic eye diseases, consisting of a semi-permeable exterior capsule and internal scaffolding, which allows for controlled cell growth and continuous protein release. (B) NsGene straw-like device implanted in the brain of patients, contains living cells which are genetically modified to produce a therapeutic factor. (C) MVX-ONCO-1 encapsulation device containing allogenic cells for the release of GM-CSF.*

2.4.4 Wound Healing and Regeneration

Chronic wounds affect about 2% of the world population corresponding to 6.5 million patients, with a cost of $ 25 billion annually in the United States alone [243]. Venous leg ulcers (VLU), diabetic foot ulcers (DFU) and pressure ulcers are the most prevalent of chronic and non-healing wounds. Among several new treatment modalities for tissue regeneration, stem cell-based therapies have gained interest as a promising approach and demonstrated to enhance wound healing, and increase blood vessel and granular tissue formation [244].

Various delivery systems have been developed to protect and improve the regenerative potential of stem cells within a wound environment. Of these, bioscaffolds, composed of collagen, hyaluronic acid, or other naturally derived or synthetic materials, have become popular to encapsulate stem cells [245–247]. Rustard *et al* showed that seeding stem cells onto a pullulan-collagen preserves cell expression of stemness-related genes and significantly accelerates wound healing [248].

By the geometrical and chemical alteration of porous scaffolds, a wide range of progenitor cell therapeutics has been valuated. Moreover, in order to modulate stem cell activity and wound healing capability, scaffolds have been supplemented with growth factors, small molecules, anti-inflammatory and/or antioxidant substances [249]. These advanced materials play an important role in enhancing survival and functionality of the encapsulated cells, beyond their normal physiological capacity.

Apligraf® (Organogenesis Inc.) is an FDA approved product for treatment of venous and diabetic leg ulcers, consisting of an extracellular matrix, allogenic dermal fibroblasts and epidermal keratinocytes to provide growth factores and wound closure, and a stratum corneum for mechanical strength and as a barrier to infections [250].

In 2012, the same company received FDA approval for GINTUIT™ (allogeneic cultured keratinocytes and fibroblasts in bovine collagen) an allogeneic cellularized scaffold (Fig. 2.8A). This was shown to predictably generate new and aesthetically appealing oral soft tissue for the treatment of mucogingival conditions in adults. Shire Pharmaceuticals (United

Kingdom) developed Dermagraft®, a technology acquired by Organogenesis in 2014. Dermagraft® is another tissue engineered and FDA approved product, consisting of fibroblast–derived dermal substitute generated by the culture of neonatal dermal fibroblasts onto a bioabsorbable polyglactin mesh scaffold [251]. Dermagraft was validated in an extensive Phase 3 clinical study (NCT01181440) [252] where it was demonstrated to have faster and complete wound closure as compared to the control group.

2.4.5 Kidney Failure

Every year more than 200,000 people in the United States are affected by acute kidney injury (AKI) and end stage renal disease (ESRD) with a mortality rate of about 50% [253]. Despite decades of efforts for the development of novel renal replacement therapies, the morbidity and mortality associated with these disease states have remained unaltered [254]. While conventional treatment is mainly focused on organ removal, newer strategies such as cell therapy and cell processing aim to reduce the need for dialysis and transplantation.

Some of the current applications involve the seeding of cells within implantable or external devices such as hollow-fiber bioreactors or encapsulating membranes [255,256].

The strategy adopted by Humes and colleagues at the University of Michigan, is to administer cell therapy from an extracorporeal circuit, allowing for immunoisolation and enabling the use of allogeneic cells [257].

The developed device, called renal tubule assist device (RAD), is an external encapsulation system, composed of polysulfone hollow fibers coated with collagen IV containing living renal proximal tubule cells. RAD in canine and porcine models reached an improved regulation of plasma cytokine levels, cardiovascular performances, leading to an increase of survival times [258–260]. Phase I/II clinical trial on 10 patients showed that RAD therapy was safe over 24 hours and cells viability and functionality throughout therapy was demonstrated. Results also indicated a 50%

reduction in the mortality rates. In a Phase II randomized, open-label trial, involving 58 patients with AKI at 12 clinical sites, RAD treatment increased survival rate by day 28 from 61% (patients treated with conventional CVVH) to 33% of those patients treated with RAD [253,261,261]. Despite the achieved results, a follow-up Phase IIb study was suspended due to an expected higher survival rate in patients treated with RAD without cells.

These unexpected findings, led CytoPherx, Inc. (Ann Arbor, Michigan) to develop a new therapeutic device called selective cytopheretic device (SCD) [262,263]. SCD is comprised of a synthetic membrane cartridge made with polysulfone fibers and a tubing system that allows its connection in series to a standard Continuous Renal Replacement Therapy (CRRT) device. The SCD cartridge works as an immunomodulatory device due to its capability to sequester and inhibit activated leukocytes, modutating the inflammation [262,264]. Safety of SCD device was proved in a phase IIa, single center study, where 12 patients were enrolled. The reported mortality of control-group was 78%, compared to 22% of the SCD treatment group [253].

A Phase-IIb multicenter US pilot study on 35 patients was performed to evaluate the safety and efficacy of the SCD treatment on patients requiring CRRT [264]. The results shown an improvement in patient outcomes treated with SCD + CRRT over standard of care therapy (CRRT alone) and a reduced mortality rate on day 60 (31.4% compared to 50%) [264].

In light of these results, an additional randomized trial on 134 patients where 65 received SCD therapy (NCT01400893) [265] was performed. Unfortunately, no significant difference in 60-day mortality was observed between the SCD group and control [266].

Another encapsulation system for external dialysis able to control and sustain delivery of secreted factors is under development by Sentien Biotechnologies (Fig. 2.8B). Sentien device, named SBI-101 (Sentinel™), now going through a phase I/II clinical trial (NCT03015623) [267], contains mesenchymal stem cell (MSC) seeded in an approved blood-filtration device [268].

Efficacy and pharmacodynamics responses to SBI-101 therapy will also be evaluated on 24 patients that will be enrolled by the end of 2018.

In Sentien devices, blood flows through the hollow fibers and therapeutic factors can be delivered into patient's blood, without any leakage of MSCs. SBI-101 offers two major advantages over traditional cell therapy administration: a) significantly extended duration of therapeutic activity by housing the MSCs in an extracorporeal device compared to traditional routes of administration of MSCs – injection or intravenous infusion where less than 1% of systemically administered MSCs persist for longer than a week following injection; b) overcomes MSC dosage limitations seen during injection or intravenous infusion.

A surgically implantable, artificial kidney is under investigation by Drs. Shuvo Roy and William Fissell at UC San Francisco for people with end-stage kidney disease [269]. This artificial kidney is composed by a silicon nanofilter to filter the blood and human kidney tubule cells embedded within microscopic scaffolding with the purpose of performing metabolic functions and reabsorbing water from the filtrate to control blood volume [270,271]. The artificial kidney is designed to be implanted near the patient's own kidneys and connected to the patient's blood supply and bladder. Clinical trials for the implantable artificial kidney are expected to start in 2018.

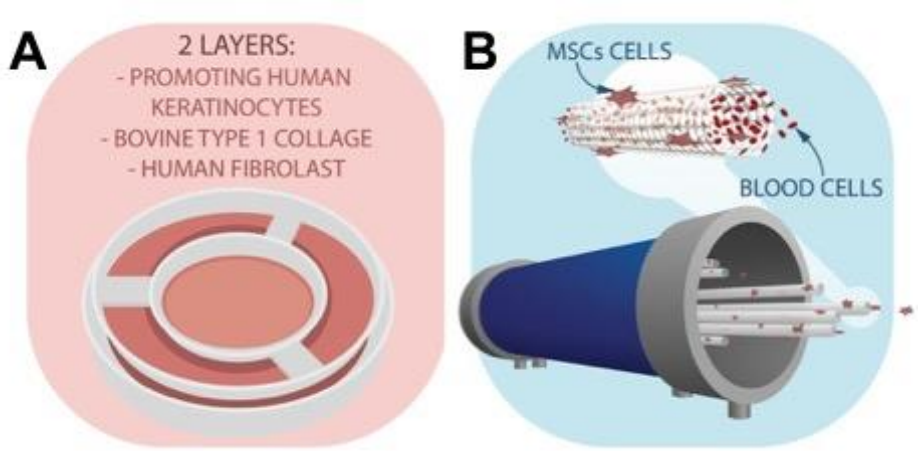

Figure 2.8: (A) Schematic of GINTUIT™ bioscaffold for wound regeneration consisting of allogeneic cultured keratinocytes and fibroblasts in bovine collagen) an allogeneic cellularized scaffold. (B) Sentien SBI-101 technology where MSCs are seeded into an extracorporeal device that delivers the factors secreted by the MSCs to the patient's bloodstream.

2.4.6 Cardiovascular Diseases

Cardiovascular diseases like myocardial infarction (MI), stroke and heart failure (HF) are leading causes of death worldwide [272]. As the damaged myocardium as well as the noncontractile scar tissue can significantly affect proper functioning of heart after MI and the regenerative capacity of endogenous cardiac tissue is limited, stem cell transplantation is explored as a potential treatment. Pluripotent stem cells (PSCs), including embryonic stem cells (ESCs) and induced pluripotent stem cells (iPSCs), have demonstrated the capability to differentiate into functional cardiomyocytes [273–275]. While PSCs may raise the concern of teratoma formation, administration of fully differentiated cardiomyocytes may not be useful as they do not integrate well with host cardiomyocytes and function in a coordinated fashion. Mesenchymal stem cells (MSCs) have shown to promote angiogenesis [276], prevent apoptosis [276], modulate immune response [277], recruit progenitor cells, and facilitate tissue remodeling [278] in such conditions. However, major challenges are the poor retention and survival of transplanted cells as well as adverse effects of inflammation and immunoreaction. Contractile nature of myocardium can mechanically disperse transplanted cells and the avascular, hostile and strong pro-inflammatory micro environment after MI can damage transplanted cells [279]. To address these challenges, various cell delivery and encapsulation strategies using natural or synthetic matrices, porous scaffolds, or cell sheets/patches are being investigated to improve cell retention and survival, as described below.

In a preclinical study by Levitt R.D. *et al.* encapsulated human MSC-treated hearts retained stem cells longer, showed improved revascularization, reduced scar formation, and resulted in improvement in left ventricular function as measured by transthoracic echocardiography (TTE) and cardiac magnetic resonance imaging (CMR) [280]. Tang *et al.* demonstrated that human cardiac stem cells (hCSCs) encapsulated in thermosensitive poly(N-isopropylacrylamineco-acrylic acid) or P(NIPAM-AA) nanogel transplanted in mouse and pig models of myocardial infarction (MI) preserved cardiac function and reduced scar size [281]. In

another in vivo study, Chi and others have demonstrated the potential for cardiac repair using bone marrow mesenchymal stem cells encapsulated in silk fibroin/hyaluronic acid patches in a rat model of myocardial infarction [282]. In 2002 Strauer *et al.* demonstrated the potential of cell therapy in myocardial regeneration and neovascularization in a clinical study using intracoronary administration of autologous mononuclear bone marrow cells in patients with MI. Since then numerous clinical studies [283] have investigated the safety and efficacy of different types of stem cells for cardiovascular applications demonstrating their great promise [283–287]; however issues related to long-term engraftment, optimal cell type, dose, route, and administration strategies are to be resolved and the promise of encapsulation is to be validated clinically to realize the full potential of stem cell therapy for cardiovascular diseases.

2.5 Key Challenges

In addition to the availability of good quality donor cells and appropriate delivery strategies, determination of the optimal site for cell delivery is a matter of intense research.

As described by *Pepper et all*., the optimal site should have an adequate tissue volume capacity and, in order to prevent hypoxia events, has to be in close proximity to vascular networks ensuring a sufficient oxygen supply to the graft. Moreover, has to be a site that is easily accessible via minimally invasive methods in order to allow for cell transplantation, biopsy and retrieve the graft [288]. Several other factors also have to be taken into consideration such as biocompatibility, safety, mechanical resistance and possibility of re-transplantation.

Some groups attribute graft failure to the lack of direct vascularization, with consequent gradual tissue necrosis and death. Consequently, a site in which encapsulated islets are in close contact with the blood-stream is obligatory for clinical application. Although the peritoneal cavity has been investigated in several studies with encapsulated cells because of accessibility and capacity to accommodate a large transplant volume, the optimal site for transplantation is yet to be determined. The subcutaneous tissue was shown to provide sufficient oxygen tension (20-40 mmHg) for the transplantation of cells such as pancreatic islets [149]. However, thus far, islet deployment into an unmodified subcutaneous site has not been successful in reversing diabetes in either animal models or in humans [147].

Various strategies are emerging, which allow to prevascularize the chosen site before transplantation [288,289]. In light of these, less vascular sites, such as the subcutaneous environment, become potentially suitable for cell transplantation. Further, successful deployment of cell

transplantation as a clinically viable approach to treating diseases entails the ability of, monitoring, retrieving, replacing, and supplementing cells with simple and minimally invasive procedures. Based on this requirement, numerous new cell delivery technologies and approaches are designed for subcutaneous transplantation.

Another critical limitation to the success of micro- and macroencapsulations is adverse tissue responses to the material of the system [173,290,291]. As an example, it has been shown that commercially available alginates can cause inflammatory responses due to ‘pathogen associated molecular patterns’ (PAMPs) contained within the alginate [148]. Further, many systems have been associated with protrusion of cells. Above a certain threshold, protrusion leads to strong inflammatory responses resulting in complete fibrosis of the capsules and necrosis of the transplanted cells. Mechanical properties might also be limiting factors. Different encapsulation systems are characterized by different elasticity and mechanical resistance. The optimal properties of encapsulation systems are also recipient and site dependent. The optimal mechanical parameters for cell survival are still unknown and difficult to determine.

While cell therapy offers a great promise for the treatment of many medical conditions, with different types of cells of various sources being tested concerns regarding ethical use and regulatory challenges are to be addressed as well.

2.6 Conclusions

Cell therapy and transplantation represent a vast research area. In this review, we presented only a subset of the current approaches by giving emphasis to the technologies at an advanced stage of development, under clinical evaluation, or already FDA approved. Despite several decades of intense research, drawing conclusions about which material, or if micro- or macroencapsulation is most appropriate for clinical use, is still difficult. Recent research indicates that cell encapsulation systems are possible solutions for many endocrine disorders for which the minute-to-minute regulation of metabolites is mandatory, and a structure similar to native organ is important. More generally, it is likely that these technologies may play a significant role in the next generation of therapeutics. Drug delivery may ultimately be achieved and finely controlled by cells as opposed to current modes of administration. This implies that drugs could be dosed exclusively when needed and at a precise amount in response to biological stimuli. It is clear that scalability and clinical translation of this biotechnologies will depend on cost-effectiveness together with establishing and satisfying a series of strict regulatory aspects. Indeed, one of the major challenges consists in moving from laboratory-based techniques to clinically acceptable large-scale practices operating under reproducibility, safety, and high-output requirements.

Chapter 3

NICHE fabrication and mechanical characterization

3.1. Introduction

Cell transplantation offers an attractive therapeutic approach for many endocrine deficiencies. Transplanted endocrine cells or engineered cells can act as biological sensors detecting changes in hormonal levels and secrete molecules in response to maintain homeostasis. Over decades of research efforts, transplantation of primary or genetically engineered cells of auto, allo- or xenogeneic origin has been shown to achieve localized and regulated 'de novo' delivery of a variety of therapeutic agents with the potential to cure diseases related to the endocrine system. However, widespread clinical application of cell transplantation remains limited by poor cell engraftment, dispersion, and graft immune rejection.

As reported in Chapter 2, several encapsulation strategies based on the encapsulation of cells within polymeric membranes, scaffolds or devices have been developed to offer isolation and protection of cells as well as to prevent their dispersion. However, due to the small dimension of the pores of their membranes (in the nanoscale), the majority of these systems do not allow for the vascularization and innervation of the graft, which are key for the long-term viability and function of the transplant. In fact, endocrine cells such as pancreatic islets in the body are irrigated by a dense network of capillaries that provide the highly needed oxygenation and delivery of nutrients. Tight engraftment with the vascular network allows cells to rapidly sense hormone fluctuations and respond accordingly.

To address all the aforementioned needs and challenges, here is presented the development of a 3D printed encapsulation platform technology (NICHE) for the transplantation of endocrine cells. Our NICHE is designed to allow vasculature and tissue ingrowth within the device in order to provide a highly vascularized and three-dimensional housing

environment required for long-term cell survival and function. The system is designed for subcutaneous implantation, and has ports for transcutaneous loading and refilling of cells. The subcutaneous environment is an ideal site for minimally invasive surgical insertion, cell supplementation, monitoring and rapid retrieval in case of need. Our system is fabricated in biocompatible polymer (polylactic acid, PLA), which offers a robust, yet flexible design to mechanically protect the graft from impacts. Further, a micro-chamber cell reservoir design promotes a homogeneous distribution of cells in close proximity to each other, while avoiding clustering.

In this chapter is presented the development, characterization and mechanical characterization in vitro and In Vivo evaluation of NICHE.

First, it's described the 3D printing and characterization of the polymeric structure, including the analysis of biocompatibility and degradation of the PLA. Second, is presented the mechanical properties of the encapsulation system in order to prove the safety for long term applications, both in vitro and in vivo. Third, using the experimental data previously obtained, we developed a finite element model (FEM) of the NICHE with the objective of optimizing device design by estimating the mechanical response of materials and tissues which is extremely challenging to be assessed in vivo.

3.2 Fabrication of the 3D printed NICHE:

Materials and Methods

NICHE and Dogbone fabrication

A 3D printer (Bioplotter, EnvisionTec, Gladbeck, Germany) with custom nozzle designed to improve the resolution of the printed filament was used. By adopting the Fused Filament Fabrication (FFF) method, parts were built layer-by-layer with a bottom-up approach by heating and extruding thermoplastic filament. A solid modeling software (SolidWorks®, Dassault Systèmes, Vélizy- Villacoublay, France) was used to create a 3D dataset for the fabrication process. Medical grade polylactic acid (PLA; Foster Corporation, Putnam, CT, USA) was used to fabricate the discoidal NICHE device, with a diameter of 10 mm, a thickness of 2.5 mm, and a cell reservoir volume of 200 µl. The cell reservoir consists of an array of square micro-chambers (300 µm × 300 µm) that promote a homogeneous distribution of transplanted cells in small aggregates across the structure. The micro- chambers are connected to the outside (subcutaneous tissue) via an array of square micro-channels presenting a nominal cross section of 100 µm × 100 µm and a length of ~50 µm. The device features a loading port (3 mm diameter) for transcutaneous cell loading and supplementation, as needed. Channel size and distribution were assessed via scanning electron microscopy (SEM, Nova NanoSEM, FEI, Oregon, USA). Twenty (20) micrographs were captured for each individual device (n=6 replicate devices) at random locations of the structure for size analysis. Images were processed using a Matlab (Mathworks, Natick, MA, USA) algorithm, the dimension and aspect ratio of each channel measured, and the channel size distribution computed. A set of 6

dogbone specimens with dimensions reported in Figure 1 were printed all with the same set up.

PLA material degradation

To assess the PLA material degradation, 3D printed NICHEs (n=10) were sterilized with 70% ethanol and ultra violet (UV) radiation, weighed, and completely immersed in glass tubes filled with 10 ml of 1X phosphate buffered saline (PBS; pH 7.0) and incubated at 37°C. Devices were recovered at 1, 2, 4, 6, 8, 12, and 16 weeks, dried, and then weighed (Mettler Toledo XPE56 Microbalance, Greifensee, Switzerland). Weight loss percentage (WI%) was calculated using the following equation:

$$\text{WI (\%)} = \frac{Wo - Wr}{W0} \; x \; 100$$

Where w_0 and w_r are the original and final device weight for the dry samples, respectively. To generate long term data, accelerated degradation conditions were used. 3D printed NICHE and rectangular samples (n= 20 each) were immersed in 10 ml of PBS and incubated at 70°C, with samples incubated at 37°C serving as controls. Degradation was assessed in terms of weight change every 2 days. Degradation test at 37°C was performed over a period of 365 days while that at 70°C was terminated when samples could no longer be weighed due to degradation. At each time point, SEM images and atomic force microscopy (AFM, BioScope Catalyst, Bruker Instruments, TX, USA) analyses (scanning region size) were used to evaluate microscopic structure changes.

Cell proliferation assay

To gain insight on the biocompatibility of the 3D printed PLA devices, MTT assays were performed with human umbilical vein endothelial cells (HUVEC) or mouse Leydig cells (TM3). HUVEC cells (ATTC, Manassas, VA, USA) were cultured in MEM medium (Sigma-Aldrich, St. Louis, MO,

USA) supplemented with 10% fetal bovine serum (FBS; Sigma-Aldrich, St. Louis, MO, US), 100 U penicillin, 1000 U streptomycin, and 2 mM L-glutamine at 37°C in a humidified atmosphere of 5% CO2. Leydig cells were cultured in a 1:1 mixture of Ham's F12 medium and Dulbecco's modified Eagle's medium with 2.5mM L-glutamine, 0.5mM sodium pyruvate, 1.2 g/l sodium carbonate and 15 mM HEPES, 92.5%, 5% horse serum, 2.5% fetal bovine serum. Media was replenished every 48 h and the cells passaged when 70-85% confluence was reached. For cell viability and growth analyses, cells were seeded at a density of 2 × 104 cells in 1 ml of media on the upper face of the polymers in wells of 24- well plate and incubated overnight to allow for cell adherence. Cells were seeded in triplicate for each time point. Proliferation was measured using WST-1 assay (Sigma Aldrich, St. Louis, MO, USA) on days 1, 4, 6, and 8 then normalized with respect to day 0. Absorbance was measured at OD 570/690 nm with Synergy™ HT Microplate Reader (Bio-Tech Instruments, Inc., USA).

3.3 Mechanical characterization

Materials and Methods

Uniaxial monotonic material testing

Tensile monotonic tests were performed according to ISO 527-2 and 527-3 Standard on a universal testing machine MTS Q Test/10 to determine stress-strain curve, and Young's modulus of 3D printed base material. Specimens were placed in the grips and pulled until failure. The machine was equipped with a 500 N load cell, and operated at a rate of 3 mm/min. A MTS clip-on extensometer (25 mm gage length, 50 mm extension) was adopted to monitor axial strain during testing. Tests were performed at 23±2°C both with dry samples or samples previously immersed in a sodium chloride solution 0.9% w/v NaCl for 24 h. Stress was calculated as the ratio between the load and the nominal cross-section area for each specimen. The elastic modulus *E* [MPa] was determined by considering the initial region of the stress σ/strain ε curve (strain ε up to 10%), where the material showed a proportional behavior. Three dry specimens and three wet ones were tested.

Mechanical characterization of subcutaneous tissue

While, the characteristics of human subcutaneous tissue may be different, for this pilot ex vivo evaluation, dermal chicken tissue was adopted. Triplicates of tissue-only samples (30x30x2 mm) were tested applying axial compressions to characterize the mechanical properties of the tissue. From experimental curves processing, calibration parameters for the tissue constitutive model were obtained for calibrating the constitutive material model for the numerical simulations.

Cell encapsulation system testing

3D printed PLA encapsulation systems were tested at 23±2°C in both dry and wet conditions for monotonic compression, creep and cyclic stress-strain behaviors. The testing load was applied at the center of the mesh, perpendicular to the mesh. Uniaxial central compression tests were run with a MTS QTest 10, 500 N load cell testing machine. For performing the creep and fatigue tests, an electromechanical testing machine (Bose Electroforce 5500 Framingham, US) equipped with a 200 N load cell was adopted. Samples were positioned horizontally on a circular metallic ring with an internal diameter of 8.5 mm and force was applied on the center of the devices with a 7 mm diameter spherical puncher (Figure 3A). Monotonic axial central compression tests were performed at a compression velocity of 2 mm/min until device failure. Monotonic central compression of 3D printed devices (in dry and wet conditions) with subcutaneous tissue interposed between puncher and device were also performed in a similar way with the same set up.

Creep central compression tests were performed by applying a constant load (2 and 3 N) in both dry and wet conditions for 2 hours. Fatigue testing was performed by applying two loads (2, 4 N in dry and wet condition) with a frequency of 1 Hz for a total of 100,000 cycles. Load and displacement data were acquired to evaluate the stiffness and hysteresis cycles. Four-point monotonic bending tests were performed utilizing the MTS Q/TEST 10 mechanical testing system equipped with a 500 N load cell and the samples were placed in a custom-made metallic holder (Figure 3.1B). Crosshead displacement speed was 2 mm/min.

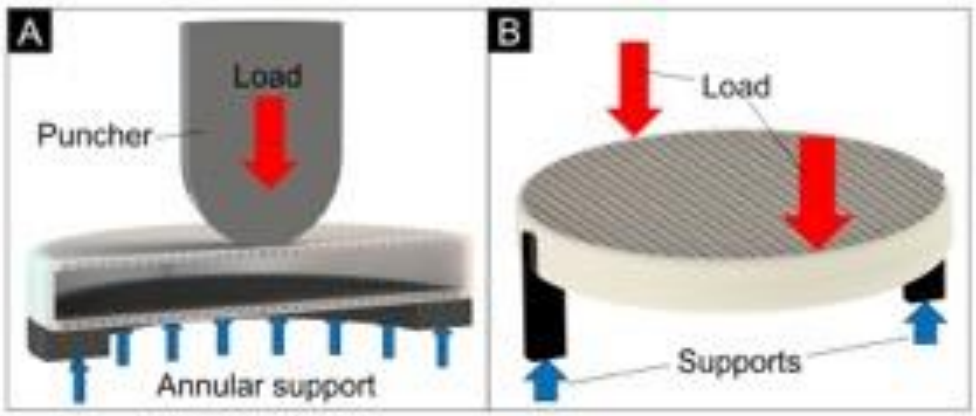

Figure 3.1: Experimental setup adopted for the compression testing (A) and four-point bending test (B) of the NICHE

In vivo implantation of NICHE in Yucatan minipigs

3D printed NICHEs were sterilized with 70% ethanol and ultra violet (UV) radiation in a sterile environment (clean room of the Houston Methodist Research Institute). Thereafter, NICHEs were filled with 300 µl platelet-rich plasma (PRP) alginate hydrogel (PRP, ZenBio, Inc., Durham, NC, USA) and were implanted in the dorsum of Yucatan minipigs (n=3). Four weeks after implantation, all NICHEs were retrieved to evaluate tissue infiltration within the device (n=1) and mechanical properties (n=2). Samples were fixed in 10% formalin overnight and stored in 10% sucrose solution at room temperature. Monotonic axial central compression tests of NICHEs were performed as previously described using chicken dermal tissue both above and below the NICHE. For histological analysis, the NICHE was embedded in OCT before cryosectioning (thickness of 7 µm) and stained via H&E and Picrosirius staining.

Finite Element Model simulations

All numerical simulations were carried out with ABAQUS Software (Dassault Systems).

At first, a set of FEM simulations was run for the tensile testing on dogbone specimens to validate the constitutive material model. Material

constitutive models, in dry and wet conditions, were calibrated with experimental stress-strain curves after the material testing under both conditions was completed. The dogbone specimen was modeled by means of three-dimensional solid elements (bricks). According to literature, the AM material was assumed to be homogeneous and isotropic as for metals [292] and for polymeric materials [293]. A load ramp was simulated, corresponding to loading experimental history on each specimen. A second set of numerical simulations of subcutaneous tissue compressions was carried out in order to calibrate the correct constitutive model of the tissue. The tissue specimen was modeled with three-dimensional hybrid solid elements (bricks). The Ogden model of hyper elasticity was used to simulate the behavior of the tissue [294,295]. In particular, the Ogden constitutive equation describes the nonlinear isotropic behavior of rubber like materials using the following incompressible strain energy function. The constitutive equation follows:

$$\phi = \frac{2\mu}{\alpha^2}(\lambda_1^\alpha + \lambda_2^\alpha + \lambda_3^\alpha - 3)$$

where ϕ is the strain energy density per undeformed unit volume, λ_1, λ_2, λ_3 are the principal stretch ratios (in a Cartesian reference frame), α is a strain hardening exponent and μ has the interpretation of the shear modulus under infinitesimal straining. A third set of simulations was run for the central compression testing on cell encapsulation systems, to estimate the stress distribution under central compression condition of the cell encapsulation system alone and wrapped in the tissue layer in for dry and wet conditions. The compression plates were modeled as rigid bodies. In particular the subcutaneous environment tests were modeled as shown in Figure 3.2B: the grey semilunar element represents the puncher; the purple lower element represents the device and the intermediate element represents the subcutaneous tissue.

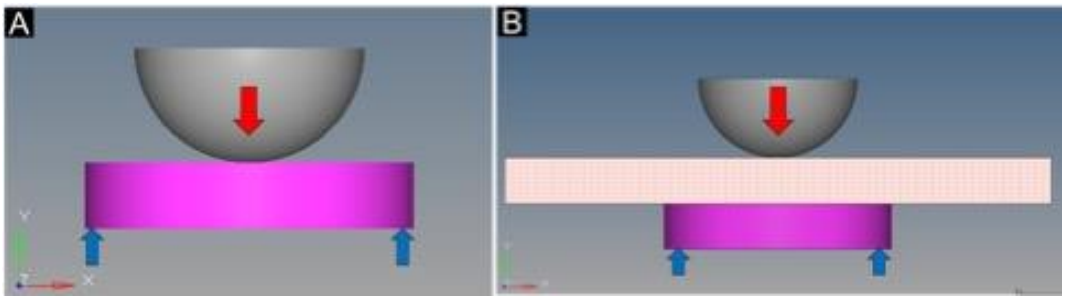

Figure 3.2: Simulation of central compression tests on encapsulation systems: model without skin layer (A) and with skin layer (B).

The cell encapsulation system was modeled by means of tetrahedral solid elements both in the annular strut and in the mesh parts (Figure 2A); displacements were fixed for circumferential nodes on the base of the annular ring. Constitutive material model of cell encapsulation system was adopted the average σ-ε curve obtained by means of experimental testing on dogbone specimen, validated by simulation of dogbone specimen monotonic testing. The spherical puncher was modeled as a rigid body. Contact zones were defined by creating contact surfaces characterized by a friction coefficient of 0.2 and using “contact pairs” interaction. Displacement boundary was applied on the puncher in order to simulate compression of the cell encapsulation system.

Numerical simulations were carried out with different displacements values: 1.23 mm and 1.12 mm, in dry and wet conditions respectively (without tissue layer), and 2.50 mm and 2.37 mm, in dry and wet conditions respectively for specimens with tissue layer. These values correspond to mean experimental displacements registered at failure loads of static capsule central compression (see Table 2). Stress and displacement distribution on the cell encapsulation systems were pointed out. In particular, Von Mises maximum stresses corresponding to failure experimental loads were used to compare uniaxial experimental testing failure stresses. According to literature [296] on FEM simulation of polymeric components and lattices, equivalent stresses based on energetic hypotheses well suit for large deformation applications and simple loading cases [297]. Experimental failure locations and maximum stress and stress nodes were then compared.

3.4. Results

NICHE structure characterization

We developed the NICHE as a cell encapsulation device for promoting in situ vascularization and supporting the viability and function of transplanted autologous cells in the subcutaneous environment. The device was 3D printed using biocompatible PLA in a discoidal shape presenting two loading ports incorporated on the upper face for transcutaneous cell loading (Fig. 2A). Primary design considerations for the device were to provide a robust yet flexible structure suitable for subcutaneous deployment, to hold enough cell volume in close proximity to vasculature while preventing cell dispersion. PLA filaments with diameter of 50 μm were deposited layer by layer forming 0° and 90° angle squares. Temperature of the 3D printer build plate was kept at 120°C to allow fibers to melt onto each other, which is fundamental to avoid free-space within layers that could decrease the mechanical properties of the NICHE. In order to facilitate the cell loading process, we developed a 3D printed external guide system that can be precisely superimposed on the skin above the implant. The guide features ports that coincide with the implant's ports, allowing drug, gel or cells to be loaded using a syringe. Excess injected components are vented out through the venting port. The internal structure of the NICHE is comprised of an array of micro-chambers (~300 x 300 μm2, 200 μm deep) designed to promote a homogeneous distribution of cells at loading to avoid clustering. Micro-chambers are connected to the external surface through square microchannels (Fig. 3.3A,B). The microchannels present a nominal cross section of 100 x 100 μm2 to allow for the penetration of subcutaneous microvessels, while avoiding cell leakage and dispersion (Fig. 3.3C). In this context, to characterize the microchannel size in preventing cell loss, we accounted for the size distribution of Leydig cell clusters measured in this study (peak ~200 μm) as well as pancreatic islets (peak ~150 μm)

(Fig. 2D). The microchannel size measurement showed a positive-skewed and sufficiently narrow Gaussian distribution (c = 1.4) with a population peak at ~125 µm (Fig. 3.3D). In the extreme scenario of unobstructed microchannels, such channel population would be sufficient to prevent the dispersion of a large percentage of cell clusters. However, as shown later in this paper, at the time of cell loading, the NICHE is vascularized with capillaries penetrating into the device through the microchannels. In this case, cell leakage is further impeded.

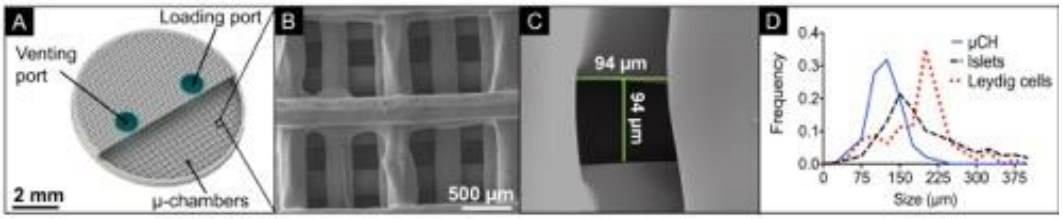

Figure 3.3 NICHE structure characterization. (A) 3D rendering of NICHE showing loading and venting ports and (B) SEM image of cell micro chambers and (C) microchannels. (D) Gaussian distribution of dimension of NICHE microchannels compared to pancreatic islets and Leydig cell clusters

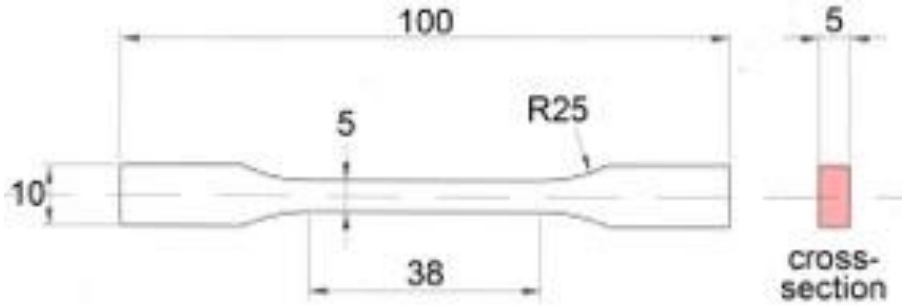

Figure 3.4: Dogbone specimen, dimensions in mm.

PLA degradation, mechanical characterization and biocompatibility

As the NICHE devices are intended for long term deployment, degradation of material is an important parameter to be evaluated. To assess the

compatibility of NICHE for long-term deployment, we first performed in vitro degradation test at 37°C as well as in accelerated conditions (70°C) in PBS, by assessing changes in specimen's weight. In vitro degradation at 70°C was shown in the literature to represent a viable test mimicking the mechanism of degradation at 37°C in vivo, in an accelerated timeframe]. On day 5, we observed 10% and 15% weight increases at 37°C and 70°C, respectively, attributable to initial water absorption in PLA bulk. This finding is consistent with previous reports [298,299]. At 37°C, the weight of the NICHE remained stable over 365 days with a slight decrease of ~1% per month (Fig. 3.5A). Samples incubated at 70°C became increasingly brittle and fractured by day 18. Based on PLA study by Weir et al.[298], 18-day degradation at 70°C corresponds to several years in vivo degradation condition. We analyzed the mechanical properties of PLA samples retrieved from 37°C degradation testing at day 365, as compared to fresh specimens (Fig. 3B). The destructive 3-point bending test showed that aged specimens were more brittle and withstood lower bending stresses (52.0 ± 15.6 MPa) as compared to the non-degraded controls (68.0 ± 25.6 MPa). Further, for aged specimens, cracks nucleated at the extrados rapidly propagated to the intrados leading to failure. In the fresh samples, fractures nucleated at the extrados did not propagate and samples continued to bend. In general, lower stiffness was observed in non-degraded samples, which is typical of plastic materials.

Aiming at evaluating the NICHE for endocrine cell transplantation, we used murine Leydig cells as a representative cell line. To ensure material biocompatibility with Leydig cells, we performed a cell viability assay on PLA over a period of 8 days. No significant differences were observed between cells cultured on PLA or in regular media (Fig. 3.5C), confirming that PLA does not impact negatively cell viability. Further, as endothelial cells are essential for vasculature network formation, we have previously demonstrated the cytocompatibility of PLA with human umbilical vein endothelial cells (HUVECs) with PLA via cell viability assay [36]. Our results are in accordance with the literature that the adopted PLA can be used for cell encapsulation applications.

Simultaneous to the degradation test, we assessed the changes in surface morphology under 37°C incubation condition for 365 days. SEM images showed clear surface degradation as indicated by a significant increase in the root mean square roughness RRMS (25.1 ± 6.2 nm) as compared to day 0 (RRMS=3.2 ± 0.4 nm) (Fig. 3.5D-G).

Overall while these tests highlighted the modes of PLA degradation, all samples retrieved on day 365 maintained integrity and sufficient mechanical properties in support of potential long-term applicability of the NICHE.

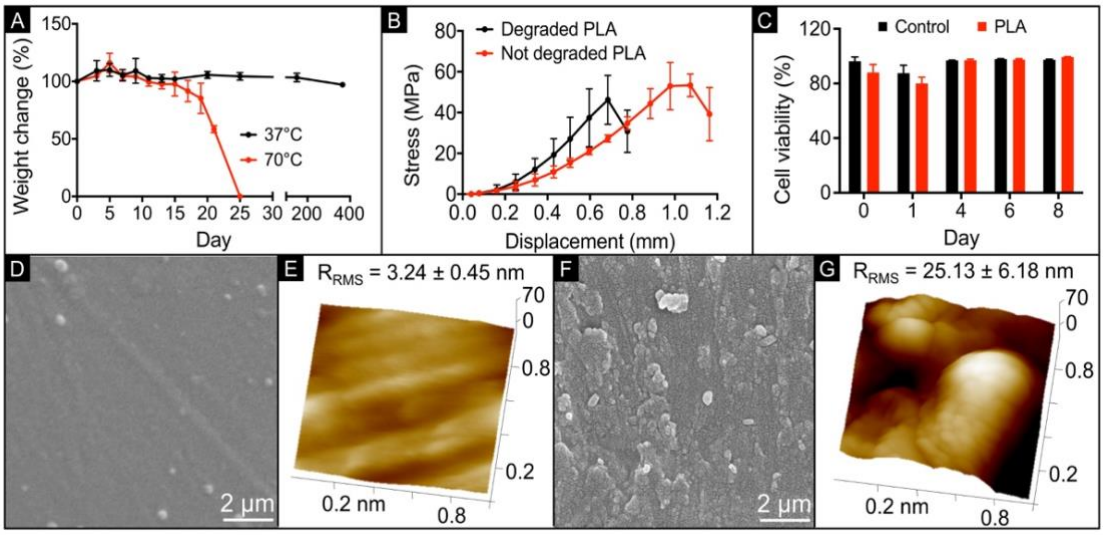

Figure 3.5: PLA characterization. (A) PLA degradation test under 37°C and 70°C showing weight change over time; (B) Three point bending monotonic tests of degraded and not degraded NICHEs; (C) viability of Leydig cell cultured on PLA and control media. (D) Baseline SEM image of PLA with (E) AFM analysis. (F) SEM image of PLA under 1 year degradation with corresponding (E) AFM analysis.

Dogbone base material monotonic tensile tests

The tensile stress-strain curves of base 3D-printed material are reported in Figure 3.6 and the mechanical properties are listed in Table 3.1. The material shows an elastic brittle behavior: linear elasticity is observed for part of deformation with a non-linear trend occurring shortly

prior to failure. The average and standard deviation of failure stress and strain are reported in Table 3.1. Mechanical properties quantified in terms of tensile strength (Rm) and Young's modulus (E) seem not to be affected by wet conditions. The small standard deviation indicates that the processing technique for dogbone specimens are affected by low density and small dimension of defects in the material.

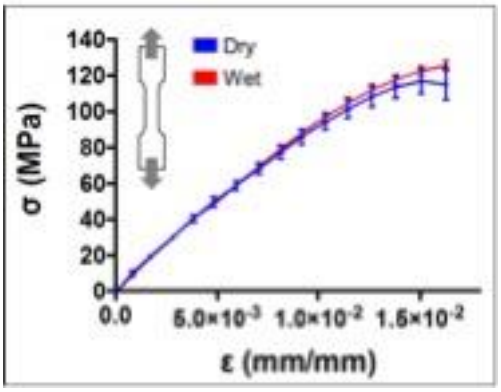

Figure 3.6: base material monotonic testing curves on dry (blue) and wet (red) specimens.

Table 3.1: base material monotonic testing results in dry and wet conditions

NICHE Dry conditions	Rm (MPa)	E (MPa)
1	123	11,210
2	124	10,845
3	107	11,530
Average	118	11,195
Standard deviation	9	343
NICHE Wet conditions	**Rm (MPa)**	**E (MPa)**
1	128	9,706
2	123	11,388
3	129	11,033
Average	127	10,709
Standard deviation	3	887

Static central compression of encapsulation system

Central compression results for the encapsulation systems in dry and wet conditions are shown in Figure 3.7A and B, respectively. In Table 3.2 the maximum compression forces in the two conditions are reported. Failure occurred in 30% cases in the circular connection region between the mesh and the ring and in 70% cases in the central mesh region, in the contact area between punch and mesh. It was observed that the wet specimens failed at a lower load in comparison with the dry specimens, along with a higher data scatter. No permanent deformations were observed in failed specimens, thus suggesting a brittle failure, in good agreement with the dogbone specimen testing results. No fragments were observed.

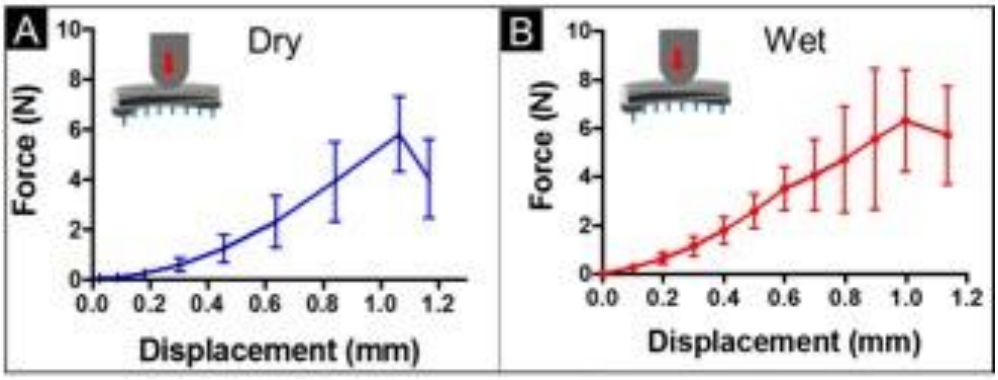

Figure 3.7: Static central compression curves for the encapsulation system in dry (A) and wet (B) conditions.

Table 3.2: maximum loads [N] for static capsule central compression

Sample	NICHE Dry	NICHE Wet	NICHE + Skin Dry	NICHE + Skin Wet
1	7.6	4.6	20.5	21.9
2	8.7	12.3	23.8	19.2
3	8.2	4.4	19.3	17.2
4	8.7	5.2	16.6	16.3
Average	8.5	6.6	20.0	18.6
Standard deviation	0.2	3.3	2.6	2.1
Average displacement (mm)	1.2	1.1	2.5	2.3

Static central compression of encapsulation system with the tissue layer

Encapsulation systems were tested ex-vivo for central compression, enveloped in a subcutaneous tissue. Results (Figure 3.8, Table 3.2) showed that these samples were able to endure higher values of maximum force.

This can be justified with lower local pressure on the mesh due to load distribution obtained by means of the intervening tissue. While no differences were observed in maximum force applied, failure for dry samples occurred at approximately 20% higher displacement as compared to wet samples. The higher displacement measured with the interpose dermal tissue in comparison to the capsule alone are ascribed to the displacement of the tissue itself under compression as shown in Section 3.5 below. Not significant permanent deformations were observed in failed specimens, thus suggesting a brittle failure, according to dogbone specimens testing results. No fragments were observed.

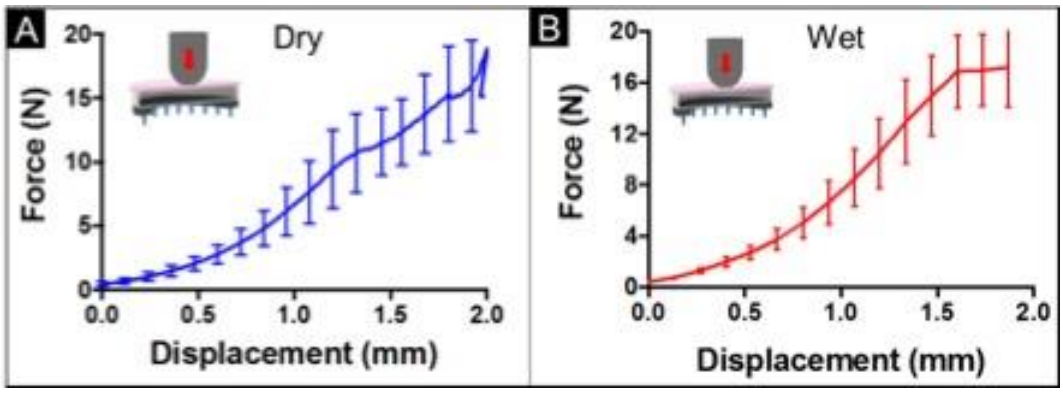

Figure 3.8: Static central compression curves for the encapsulation system, with tissue layer, in dry (A) and wet (B) conditions.

Static compression of encapsulation system enveloped in tissue layer and with infiltrated tissue.

To support viability and function of encapsulated cells and avoid hypoxia immediately after transplantation subcutaneously inserted NICHE are prevascularized to allow for tissue penetration and vessel formation within the device, prior to cell loading. Histological sections of NICHE retrieved on week 4 post subcutaneous implantation in Yucatan minipigs showed high levels of vascularization inside the device (Figure 3.9A,B). Further, high density of collagen Type I and II (Figure 3.9C) validated the presence of ingrown tissue. While the subcutaneous environment is typically poorly vascularized, our results showed that NICHE supplemented with PRP hydrogel was able to induce vascularization in and around the NICHE. Importantly, the results of the compression test showed that the ingrown tissue substantially contributes to the redistribution of stresses in the NICHE. In fact, the structure was able to withstand higher loads and deformations without failure (Figure 3.9D). These results are highly relevant as they indicate that during its intended deployment, both NICHE and ingrown tissue contribute to maintain mechanical stability and adequate support to encapsulated cells.

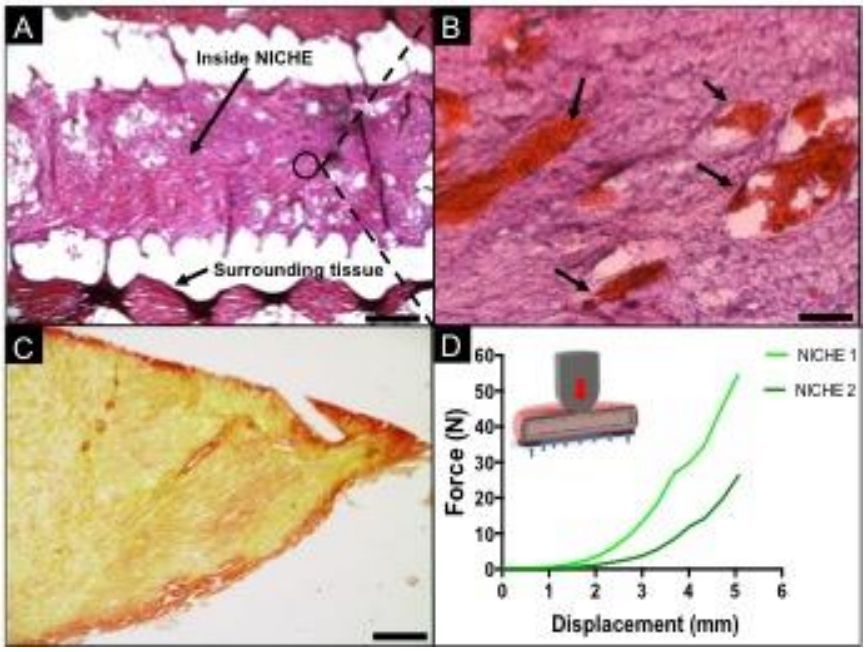

Figure 3.9: H&E images of vascularized NICHE retrieved from Yucatan minipigs after 4 weeks subcutaneous implantation (A, scale bar 500 µm), 40x

magnification of vascularized tissue within the device (B, scale bar 50 μm, black arrows show blood vessels); Picrosirius staining showing presence of collagen fibers: yellow, orange and reddish color within the NICHE (C, scale bar 500 μm). (D) Static central compression curves for NICHEs retrieved from subcutaneous implantation.

Chicken dermal tissue compression tests

Results from the tissue compression tests are shown in Figure 3.10. The material stress-strain behavior was modeled based on the Ogden hyperelastic behavior equation, and the results from our study demonstrated a similar material behavior to the data found in literature [294]. The Ogden curve calibration parameters, μ=0.007 and α=1.85, were obtained from experimental curves.

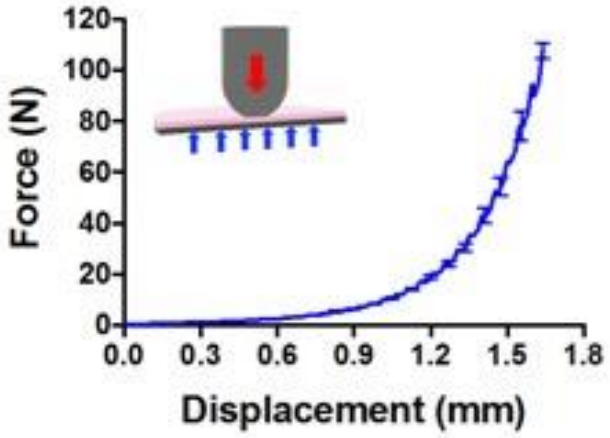

Figure 3.10: Tissue compression test curves.

Encapsulation system fatigue on central compression

Hysteresis cycles from the fatigue testing with dry and wet encapsulation systems are reported in Figure 3.11A and B. No samples survived the test. It was noticed that the damage increased gradually and cyclic strain accumulation was observed by gradual displacement of hysteresis cycles. This strain accumulation phenomenon (ratcheting) is well known for metallic materials [300] as well as polymeric materials [301,302]. It indicates that irreversible changes (damages) were taking place in the test specimens. Higher cyclic accumulation was observed in wet cell encapsulation systems. This phenomenon is probably due to the water adsorption in polymer material, which weakens the bonds between the molecules thus promoting deformation. Higher deformation achieved with the same number of cycles means that wet encapsulation systems, in a subcutaneous environment, can sustain higher deformations before failure. The increments of area of the cycles in the figure point to a progressive damage from the initial cycles (cycle 100) to later cycles (cycle 4000), which are more evident in wet specimens. Hysteresis area is another damage indicator [303,304]. Higher hysteresis area means higher dissipated energy, more damage and irreversible strain. Failure occurred in the mesh region, in the contact area between punch and mesh, for all specimens. Not permanent deformations were observed in failed specimens, thus suggesting a brittle failure, according to dogbone specimens testing results.

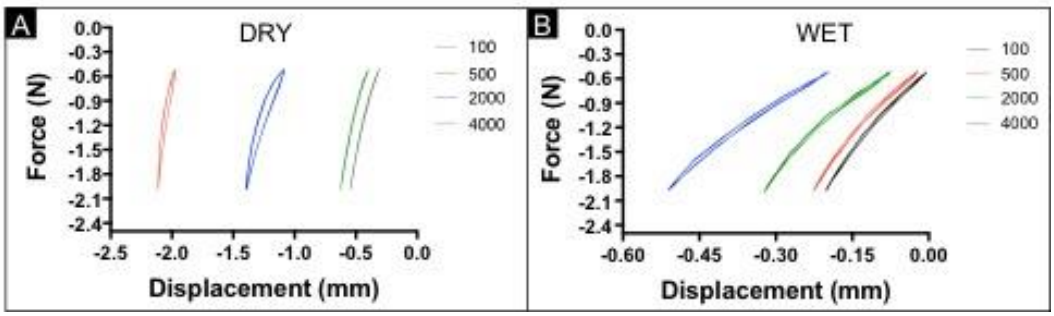

Figure 3.11: hysteresis cycles for dry (*a*) and wet (*b*) specimens during fatigue testing for cycle 100, 500, 2000 and 4000.

Encapsulation system creep tests

The instant stiffness curves from the creep tests with the dry and wet encapsulation systems at various load conditions are reported in Figure 3.12. Of the various load conditions tested, the dry specimen at 3 N failed during the first creep phase, while the specimen at 2 N abruptly failed during the second creep phase. Wet samples at 3N also failed within 800 sec but showing substantially larger displacements. By comparing the 2 N test results for dry and wet conditions, wet specimens showed shorter lives and higher displacements than dry specimens with the exception of one wet specimen for which failure occurred after the 3rd creep phase at approximately 5000 sec. A lower stiffness in subcutaneous conditions corresponds also to lower creep life. For creep loads higher than 2 N, device life dramatically shortens. Failure occurs in the mesh, which points to a brittle behavior of the mesh structure. Failure occurred in the circular connection region between the mesh and the ring for some specimens and in the central region for others. Neither fragments nor permanent deformations were observed in failed specimens, thus suggesting a brittle failure.

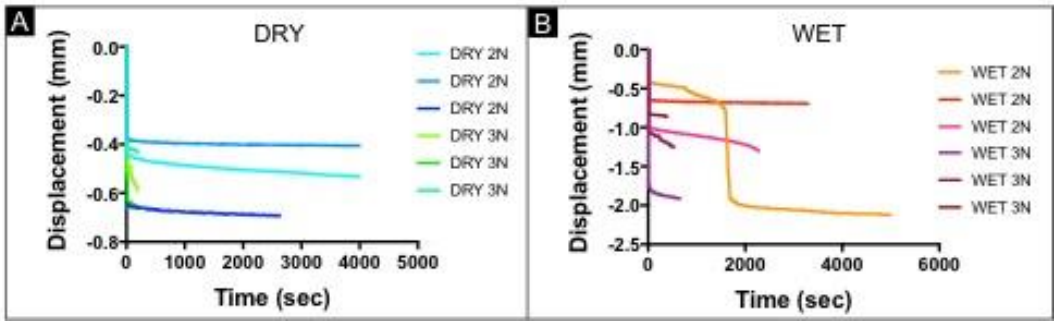

Figure 3.12: instant stiffness curves for dry (A) and wet (B) encapsulation system.

Encapsulation system monotonic bending tests

The bending force-displacement results in dry and wet conditions are plotted in Figure 3.13A and B respectively and the results summarized in Table 3.3 below. It was observed that, while the stiffness of dry and wet specimens remains the same, dry specimens were able to withstand a higher maximum load (38 N) before failure. It was also observed that the failure occurred in the mesh part of the devices. Not permanent deformations were observed in failed specimens, thus suggesting a brittle failure. No fragments were observed.

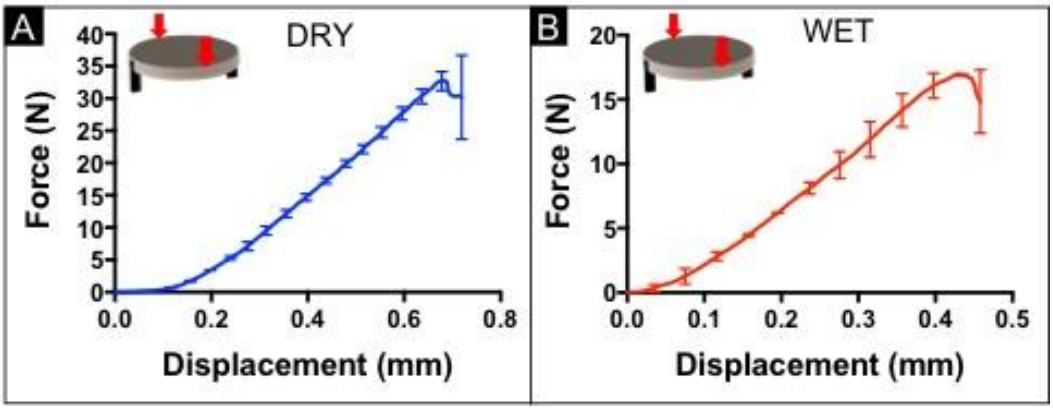

Figure 3.13: bending force-displacement curves for cell encapsulation systems in dry (A) and wet (B) conditions

Table 3.3: bending testing results of cell encapsulation system

NICHE Dry conditions	Max load (N)	Stiffness (N/mm)
1	17.1	26.3
2	18.3	31.6
3	19.0	31.9
Average	18.1	29.9
Standard deviation	0.96	3.15

NICHE Wet conditions	Max load (N)	Stiffness (N/mm)
1	44.5	35.2
2	31.3	27.8
3	40.1	29.0
Average	38.6	30.6
Standard deviation	6.72	3.97

FEM Results

In Figure 3.14A and B, the simulation results of the tensile testing on dogbone specimens are presented in dry and wet conditions, respectively. The stresses in the central part of the specimen, corresponding to the experimental tensile load to failure (N) were 129 MPa and 132 MPa respectively. The corresponding experimental failure stresses were 118±9 MPa and 127±3 MPa. The mismatch between experimental and numerical failure stress is lower than 10% and that may be due to the fact that dry and wet constitutive material models were defined on average experimental data.

Figure 14 shows the numerical-experimental comparison in terms of monotonic testing curves; the results from dry specimens are shown in Figure 3.15A while those from wet specimen in Figure 3.15B. Both graphs display the curves for all specimens obtained from experimental tests (continuous line) and the same results in relation to the numerical simulation (dot line). The numerical strain in the central cross section was calculated by the software. Experimental and numerical simulation curves for uniaxial testing show a good agreement both in the linear and nonlinear fields. The hypotheses of isotropic and homogeneous constitutive models are shown to be effective in the simulation of the uniaxial behavior on AM base material. The maximum difference between numerical and experimental data is lower than 10%, thus indicating a reliable behaviour of the constitutive model.

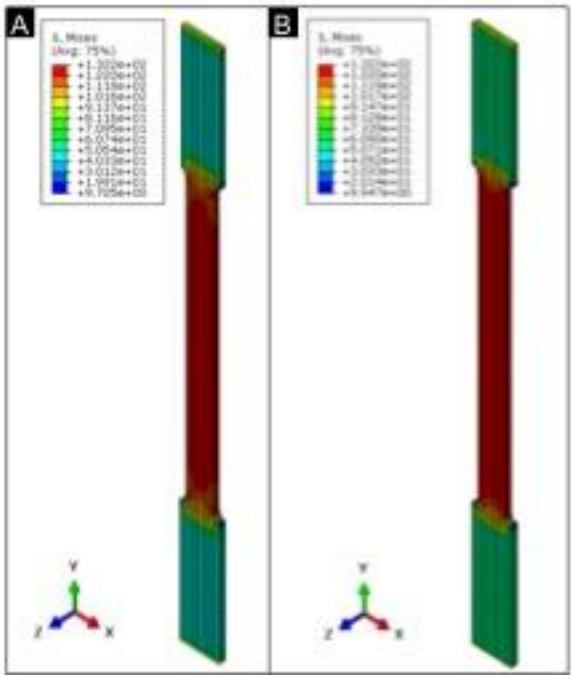

Figure 3.14: Simulated stress distribution of tensile testing simulation on dogbone specimens: dry (A) and wet (B) material

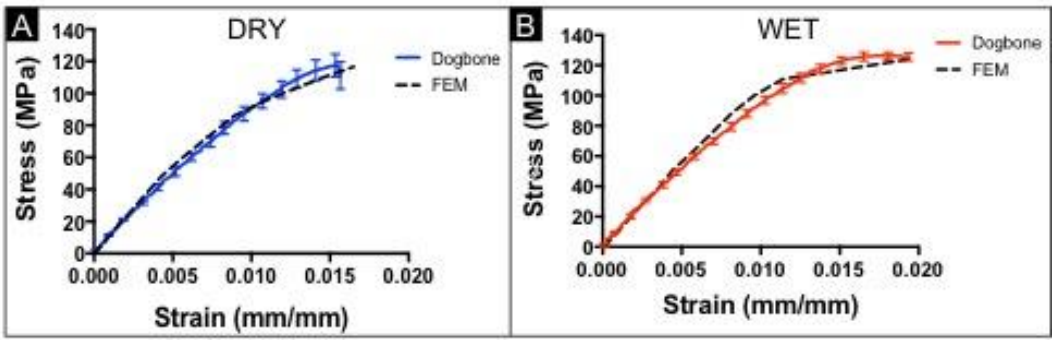

Figure 3.15: Comparison between experimental and numerical results: monotonic testing curves on dry specimens (A) and wet specimens (B)

The comparison between experimental and numerical curves related to the tissue compression tests are shown in Figure 3.16. Ogden parameters used for this model are: μ=0.007 and α=1.85 and were obtained from experimental testing data fitting. The maximum difference between numerical and experimental data is lower than 5%, indicating that the Ogden model well fits the experimental results.

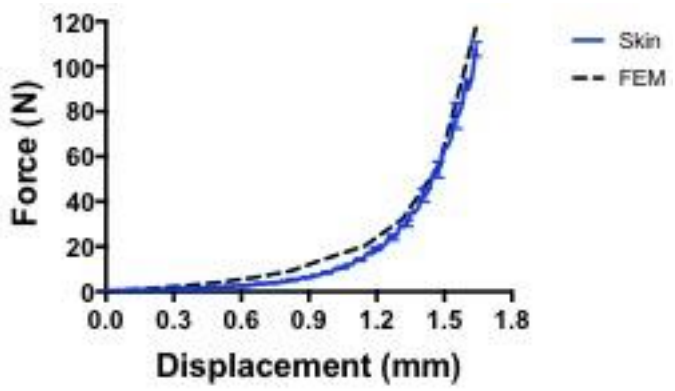

Figure 3.16: Comparison between experimental and numerical compression results of chicken dermal tissue

Results from the cell encapsulation system central compression simulations are presented in Figure 3.17 and Table 3.4. Figure 3.17 shows the calculated stress distribution on encapsulation systems for central compression static tests.

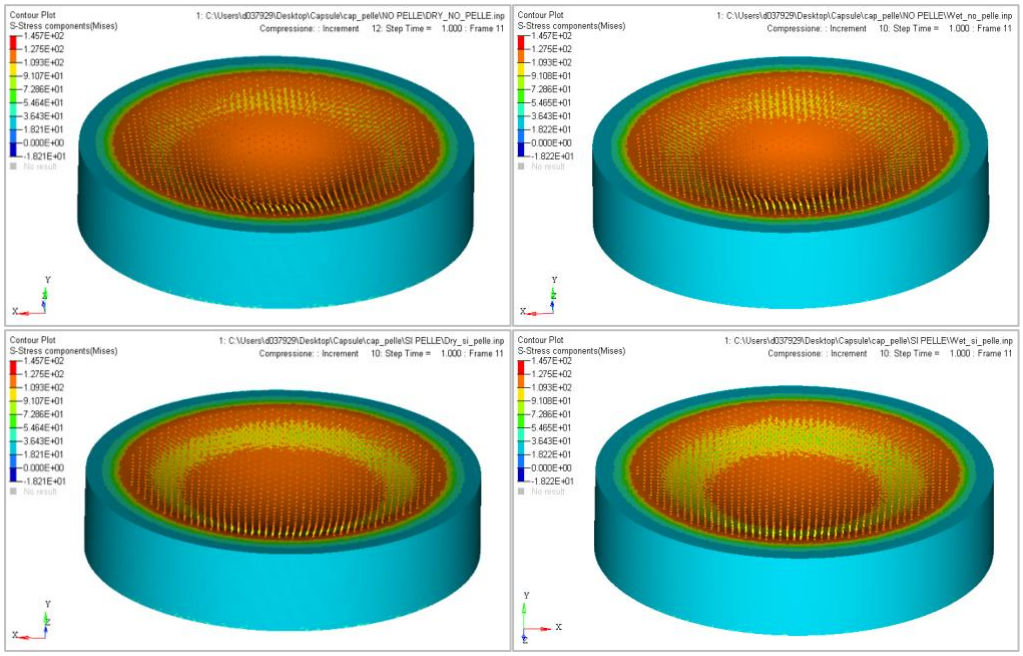

Figure 3.17: Stress distribution on encapsulation system due to compression static tests: simulations without tissue layer (up) and with tissue layer (down), for dry material (left) and wet material (right) respectively

It was observed that in wet conditions, for the same stress (127.5 MPa), the displacement values obtained for the encapsulation system, with or without the tissue, were different. The displacement values were about two times with the tissue, compared to that of device alone (1.12 mm). These displacements correspond to average failure load (last column in Table 3.4).

Table 3.4: Values of simulated displacements, stresses and contact area for different simulation conditions

Model	Max displacement (mm)	Max stress (Mpa)	Contact area (mm^2)	Experimental Load to failure (N)
Dry, no tissue	1.23	124.0	2.42	7.7
Wet, no tissue	1.13	127.5	2.39	5.8
Dry, with tissue	2.50	124.0	56.16	20.0
Wet, with tissue	2.37	127.5	52.16	18.7

This means that the skin layer allows a redistribution of the load, a better strain distribution and a decrease in the local stress with tissue layer. To obtain the same stress value, a higher deformation is needed if the tissue layer is interposed between the puncher and the encapsulation device. Similar results and displacement trends were observed in dry conditions, with and without the tissue, for a similar stress (124 MPa). A symmetrical distribution of the stress was also noticed, with most stressed areas located at the center and near the peripheral rim. They also corresponded to failure points on sample testing. According to experimental results, the stress calculated on cell encapsulation systems corresponding to failure load in dry and wet conditions is in the failure stress range obtained from uniaxial experimental testing on AM base material specimens. While experimental wet base material failure stress was 124 MPa, the corresponding simulated stress at failure in cell encapsulation systems was 127.5 MPa. Matching simulations with experimental results, for dry cell encapsulation systems, experimental

base material failure stress was 118 MPa, and the simulated stress corresponding to failure load was 124 MPa. This difference could be accounted for the numerical model approximation and the geometric reinforcement effects on the component structure.

The simulated contact area, displacement and stresses are also summarized in. For simulation, the contact area dramatically increased for devices with tissue layer, in comparison with those without the tissue. This result is in agreement with the decrement of maximum normal stress in case of subcutaneous tests simulations. The interposition of a high compliant layer redistributes local loads and allows a more favorable stress distribution. The comparison with experimental results provides two other conclusions: the first one is that the Von Mises equivalent stress well adapts for the estimation of stress in the presented loading condition for the cell encapsulation systems and the second is that the homogeneous isotropic constitutive model adopted for the simulation of complex stress distribution in the presented AM component well adapts for the description of the behavior of the cell encapsulation system.

Actually, the meshes can be represented as a sequence of beams connected in orthogonal directions and the stress shows one preferential direction (axial). The stress calculated using solid elements also for the mesh part of the cell encapsulation system follows this result and the equivalent stress is then almost coincident with uniaxial stress.

3.5. Discussion and Conclusions

In this chapter, we have demonstrated the development and proof of concept testing of the 3D printed NICHE. The NICHE can serve as a platform technology for the subcutaneous encapsulation of transplanted cells. Specifically, we adopted 3D printing to generate the NICHE with channel dimensions suitable for vasculature penetration while avoiding cell leakage.

3D printing technologies have been increasingly explored for clinical applications as it allows for the design and fabrication of complex 3D structures simulating body structures and organs, which can be patient specific [58,59]. Combining advanced imaging techniques, such as magnetic resonance imaging and computer tomography, computer-aided design software and 3D printing, is possible to develop customized, complex structures in a timely and cost-effective manner, as compared to traditional manufacturing processes. In the context of our cell macroencapsulation NICHE, 3D additive manufacturing allows for straightforward scalability and customization. Different device shapes and sizes can be generated depending on the anatomical features of the implantation site and the volume of cells required to be encapsulated.

Our choice of printable material (polylactic acid) was motivated by PLA's biocompatibility and adequate mechanical properties previously reported in the literature [60,61]. Importantly, PLA shows slow degradation kinetics: our results in accelerated degradation condition show that mechanical properties are potentially preserved for years, prior to any substantially noticeable weakening of the structure. However, in some instances, after cell engraftment and the formation of a subcutaneous organ-like structure, NICHE could degrade without affecting the function of the established system. In other cases, maintaining a bioinert structure could be beneficial. This is the case for diabetes, whereby

supplementation or replacement of cells may be required to adjust to the needs of patients and to address the systematic loss of viability that cells endure after transplantation over the years. In these cases, other bioinert materials could be used such as polyether ether ketone (PEEK) and polytetrafluoroethylene (PTFE), among others, which have been demonstrated in other cell delivery applications.

To further demonstrate the long-term application of the NICHE technology, we performed combining experimental testing and numerical simulations. Various numerical and experimental methods have been used in the literature to study the mechanical properties and fracture behavior of a wide range of materials and applications [305]. In several studies, stress-strain curves obtained by experimental testing were successfully adopted as constitutive model curve for numerical simulation obtaining good correlation with experimental results even in presence of voids and defects derived from manufacturing. In this context, material constitutive models can take into account the defects implicitly [306,307]. Alternatively, homogeneous material models can be used which macroscopically describe the global material behavior inclusive of defects [308,309]. In this study, we opted for the latter approach demonstrating its validity for a complex 3D-printed structure such as the NICHE.

The experimental mechanical testing was initiated with the calibration on the constitutive material model to be used in numerical FE analysis. Numerical simulation of the tensile testing on specimen validated the numerical model in case of uniaxial loading. In addition, a numerical FE structural model of the cell encapsulation system was implemented and results compared to the experimental results. Component simulation of central compression matched well with experimental results, thus allowing for validation of biaxial loading numerical modeling, both in dry and wet conditions.

As opposed to other rigid materials and subcutaneous implants developed for controlled drug delivery [162,164,310] in the case of the NICHE deformations are required for the system to conform to the surrounding tissues and avoid unwanted stress points that could damage

and ulcerate the tissues over time. Mechanical testing demonstrated that no device fragments were produced both in dry and wet conditions and no permanent deformations were developed indicating an elastic behavior of printed PLA. In the majority of the tested NICHEs, failure took place in the area where the load was applied and, in some cases, where the mesh is connected to the annular part of the capsule. In this location, the calculated stresses were lower than demonstrated failure stresses and these failures maybe expected from the presence of imperfections in 3D printed material. The test conditions with empty NICHE devices and central compression were chosen to simulate a worst-case scenario in terms of mechanical loading. In an in vivo scenario, the encapsulation devices is rapidly filled with blood vessels and tissue ingrowth. This engraftment process progressively takes place within approximately 3 weeks post device implantation. During this phase NICHE is mostly empty. Once the NICHE is fully engrafted, external forces and stresses from surrounding tissue are more uniformly distributed over the device structure. The results of compression testing of NICHEs retrieved from subcutaneous implantation in a porcine model, clearly demonstrated the combined effect of implant and tissue in withstanding the applied stresses to a substantially larger extent as compared to empty devices.

By comparing structural FEM simulations for the most critical mechanical conditions (empty capsule) while adopting homogeneous isotropic material properties derived from experimental testing of 3D printed dogbones, good agreement was found with the experimental results. While published data indicates that the subcutaneous loading of devices [292] could reach higher values than those obtained by experimental testing on cell encapsulation systems, the current results are encouraging. Importantly, NICHEs retrieved from the pig study were intact and did not display any deformation or signs of failure. Results obtained from wet specimen testing, which is more indicative of physiological conditions, show higher load to failure and displacement to failure values than dry specimen in monotonic, creep and fatigue testing conditions. Furthermore, the presence of a biological tissue layer, simulating the subcutaneous application, increased the load to failure and displacement

to failure values of monotonic tested specimens, probably due to the resulting stress distribution, as reported in similar conditions [308]. The FEM analysis, corroborated by experimental results, validates the stress distribution in cell encapsulation systems, justifying the differences in load to failure and displacement to failure results. Further in vivo studies using animal models with comparable subcutaneous conditions to humans are required for validation before clinical translation of the system. However, these encouraging preliminary data show the promise of the 3D printed NICHE for long term clinical subcutaneous implantation and transplantation of therapeutic cells. Additionally, the finite element model adopting constitutive mechanical properties experimentally obtained for 3D-printed PLA showed to be able to predict with fidelity the experimental mechanical test results for the NICHE. This FEM approach demonstrates a promising tool for the design and optimization of a wide spectrum of polymeric devices for implantable applications.

Chapter 4

Development and in vitro testing of human mesenchymal stem cells differentiated into islet-like insulin producing aggregates (ILIPAs) for diabetes treatment

1. Introduction

The current standard of care for Type 1 diabetes patients involves daily monitoring of blood glucose levels and the continuous injection of insulin, and, for patients with Type 2 diabetes, oral or injected therapeutics [311]. Both treatments have their respective side effects including ketosis and hypoglycemic coma.

Pancreas and islet transplants have shown success at re-establishing glucose control and reversing diabetic complications, but their routine clinical application is still inadequate, primarily due to the limited supply of cadaveric organs and loss of graft function over time due to immune rejection, lack of neovascularization, and loss of physiological architecture. Patients transplanted with cadaveric human islets can become insulin independent for about 5 years, but limited quantity and quality of donor islets make it an unrealistic cure [22].

Being the islet demand way larger than the number of pancreata available, several labs are working on the development of engineered insulin releasing β-cells that can potentially replace the need of pancreas donors.

The ideal therapy would restore insulin independency using autologous β-cells [312]. Since pluripotent stem cells were discovered, several have been the tentative to use these cells for disease treatment and drug screening.

In this chapter, first is presented the production and characterization of islet like insulin producing aggregates (ILIPAs) from stem cells collected from human bone marrow (BM-MSCs) as potential substitute of human pancreatic islets. Successively, is accessed the viability and insulin secretion of encapsulating ILIPAs in the NICHE devices, in vitro.

2. Materials and methods

Human pancreatic islets isolation and purification

Human pancreata (n=5) were obtained from heart-beating donors deceased by brain death with informed consent for transplant or research use from relatives of the donors. Human islets were isolated from cadaver donors using an adaptation of the automated method described by Ricordi et al.[313]

Islet cell culture

Aliquots from human islet isolations were then cultured in Memphis Serum-Free Medium (M-SFM) further supplemented with 10 U/mL heparin and 10 mM Niacin as described previously. Islet culture media was changed at day 1 post isolation and thereafter weekly for all islet preparations during the culture period. Islet tissue was cultured for 1-3 days prior to experimentation, to allow for sterility and viability testing. These islets were used as positive controls for BM-MSCs derived ILIPAs.

Isolation, expansion, and differentiation of BM-MSCs

Bone marrow samples (n=5) were recovered from leftover tissue in used bone marrow collection bag sets, properly consented for research utilization. Isolation, expansion, and differentiation of BM-MSCs was performed according to the procedures outlined by Gabr et al. [314]

Characterization of isolated MSCs by flow cytometry

For flow cytometric analysis, the MSCs at passage three were trypsinized, centrifuged at 300 g for 8 minutes, and resuspended in PBS

at a concentration of 1×10^6 cells/ml. 100 µl aliquots were labeled for 30 mins with antibodies against CD14, CD45 (FITC) or CD73, CD34 phycoerythrin (PE) (Becton-Dickinson, USA), or CD105 PE or CD90 (FITC) (Becton-Dickinson, USA), washed with 1ml of stain buffer (BD-Pharmingen, USA) and resuspended in 500 µl of stain buffer. The labeled cells were analyzed using an argon ion laser with a wavelength of 488 nm (FACS Calibur, Becton-Dickinson, USA). A total of 10,000 events were obtained and analyzed with the DIVA software program (Becton-Dickinson, USA). Control staining with appropriate isotype-matched monoclonal antibodies was included.

Differentiation of the MSCs to ILIPAs

After passage three, MSCs with appropriate CD profiles were seeded at a density of 1×10^5 cells/ml in serum-free, high glucose (450 mg/dL) D-MEM (25 mmol/L) containing 0.5 mmol/L β-mercaptoethanol (Sigma) and incubated for 2 days. The medium was replaced with serum-free, glucose-rich medium containing 1% nonessential amino acids (Sigma), 20 ng/ml basic fibroblast growth factor (Sigma), 20 ng/ml epidermal growth factor (Sigma), 2% B27 supplement (Gibco BRL, Life Technologies, UK) and 2 mmol/L L-glutamine (Sigma). The preparations were cultured for 8-10 days. Finally, the cells were cultured for an additional 8-10 days in serum free, high glucose D-MEM containing 10 ng/ml betacellulin (Sigma), 10 ng/ml activin-A (Sigma), 2% B27 supplement and 10 mmol/L nicotinamide (Sigma).

Immunolabelling

Immunohistochemistry was performed using primary antibodies against insulin (AB6995, Abcam, Cambridge, MA), and glucagon (AB92517, Abcam). For nanogold immunostaining, the ILIPAs were fixed in 2% formalin and 0.5% glutaraldehyde (EM grade from Ted Pella) in PBS overnight at 4°C. After washing 3 x 15 min with PBS containing

0.05% Tween 20 (Bio-Rad Laboratories, Hercules, CA, USA), ILIPAs were blocked for 6 hours in casein blocking buffer (BioRad) with 0.05% Tween 20 at room temperature. Subsequently samples were incubated with mouse monoclonal anti-c-peptide (1H8) antibody (Abcam, ab8297) at 1:50 dilution in blocking buffer, overnight at 4°C. The next day, samples were washed for several hours with PBS- 0.05% Tween 20 and incubated overnight at 4°C with anti-mouse antibody conjugated with 1.4 nm gold (Nanoprobes, Yaphank, NY, USA) diluted at 1:50 with blocking buffer. The next day, samples were washed 3 x 15 min with PBS-0.05% Tween 20, post-fixed for 20 min in 1% glutaraldehyde in PBS-0.05% Tween 20, washed 3 x 15 min in water, silver enhanced and either photographed as a whole mount or processed for electron microscopy without the osmium tetraoxide treatment, as described previously. Whole-mount immunostained ILIPAs were contrasted with 0.5% uranyl acetate only (without osmium tetraoxide) and embedded in Epon. Thin (70-100 nm) sections were examined and photographed in JEOL 1200 transmission electron microscope.

Microarray analysis

RNA was extracted using the Trizol Hybrid RNA Method and RNA quality was assessed on the Agilent Bioanalyzer RNA Amplification using the Ambion WT Expression Kit (Affymetrix). Fragmentation/Terminal labeling Hybridization to the Affy 1.1ST Human Plate on the GeneTitan.

Gene expression by RT-PCR

Total RNA (totRNA) was extracted in accordance with the manufacturer's instructions. Variable amounts of total RNA input were reverse transcribed using the iScript cDNA Synthesis kit (Bio-Rad), the amount defined by the respective samples concentration (from 5 – 1000 ng total RNA input).

TaqMan® (Life Technologies) analysis was performed on the Roche LightCycler 480 II Instrument with LightCycler® 480 Probes Master mix

(Roche). See supplementary table 2 for list of TaqMan® primers/probes analyzed. For more representative normalization, a cDNA master mix (cDNA, 2X Probes master mix, PCR-grade water) was prepared for each cDNA sample to which either query or normalizing TaqMan primers/probe were subsequently added. This procedure allows the query and normalizing primers/probe to interrogate the same cDNA master mix preparation, resulting in more accurate normalization. Normalized Cp values (Critical point; Cp_{query} - geometrix-mean ($Cp_{PPIA,}$ Cp_{18S}) were analyzed. In addition, relative quantitative RT-PCR (qPCR) gene expression for differentiated islet like pancreatic cells were analyzed against human islets served as a positive control and acinar and undifferentiated MSCs as a negative control.

NICHE surface patterning and modification

After fabrication as described in chapter 3, NICHE surface modification was performed using various agents as described below, to obtain suitable external charge and hydrophilicity for supporting cell growth and viability. All of the PLA NICHE were immersed in a 5 M NaOH (Macron Chemicals, PA, USA) solution in Millipore water for 4 hours under mild agitation, then rinsed, and dried at room temperature. A NICHE custom holder has been fabricated for running two 60-second cycles of Argon plasma (Ar) or Oxygen plasma (O_2) etching (30 Watt, 150 mTorr) (March plasma etcher, Nordson, Ohio, USA).

Five NICHEs were placed in a petri dish filled with a poly-L-lysine solution 0.01%, 150,000-300,000 MW (PLL, Sigma Aldrich), incubated for 5 minutes, and air dried at room temperature. A second group of five NICHEs were placed in a petri dish filled with endothelial cell attachment factor (ECAF, Sigma Aldrich, sterile-filtered liquid), followed by a ten-minute incubation, and drying at room temperature, as per manufacturer's instructions.

Cell viability in surface modified NICHE in vitro

For the in vitro cell viability study, flat PLA membranes (n=7) were printed (20 mm diameter, 1 mm thickness), treated with NaOH, Argon plasma, PLL, and ECAF (n=6 per each group), assembled into 6-well polystyrene cell culture inserts (Becton Dickinson, USA), and filled with $1.5x10^5$ human umbilical vein endothelial cells (HUVEC) in a volume of 1 ml of complete Endothelial Cell Basal Medium (EBM, Lonza, USA). All samples were incubated at 37 °C and 5% CO_2 for 7 days with a change of media at regular time intervals (2, 4, and 7 days). To assess viability, cells were rinsed with PBS buffer, trypsinized (Trypsin/EDTA solution), and quantified using Trypan blue solution.

Assessment of insulin secretion and content in vitro

Standard aliquots of 50 islets equivalent (IEQ) or 100 IEQ of ILIPAs were incubated for 60 minutes with low glucose (60 mg/dL, basal), followed by 60 minutes of high glucose (300 mg/dL, stimulated). Following high glucose incubation, islets were harvested and insulin was extracted in an ethanol–acid solution (165 mM HCl in 75% ethanol). The islets were then analyzed for insulin content using a specific ELISA assay (ALPCO Diagnostics, Windham, NH). The low glucose media used was standard alpha MEM supplemented with 5% Platelet Lysate (PL). The high glucose stimulation media was high glucose D-MEM (450 mg/dL glucose) supplemented with 5% PL.

ILIPAs insulin secretion in NICHE

In order to assess the long-term viability of ILIPAs when housed in the NICHE devices, we loaded multiple NGs (10 per group) with approximately 2,000 ILIPA constructs. The ILIPAs were loaded in a platelet lysate (PL) gel into the NICHE. Briefly, NICHEs were placed in the wells of a sterile 12-well suspension type plate (Sarstedt). ILIPAs were centrifuged and media was removed. The ILIPAs were mixed with

PL at a concentration that would allow for approximately 2,000 ILIPAs to be loaded in a volume of 200 uL (10,000 ILIPAs/mL). Three NICHE treatment types were tested in this evaluation. NICHEs without surface modification (untreated), NGs surface modified with Argon plasma, and NICHEs surface modified with Oxygen plasma. Once the PL-ILIPAs were loaded into the wells, 50 uL of Thrombin (2,000 units/mL, King Pharma, Bristol, TN) was mixed with the solution. The plates were placed in a 37°C, 5% CO_2 incubator for 60 minutes to allow the gel to completely form.

Once gelation was accomplished, the NICHEs were transferred into new microplates and 3 mL of alpha MEM with 5% PL was added to the wells. The media was replaced every 3-4 days for the next month. The NGs were tested weekly for insulin release using a perifusion type evaluation.

On days 7, 14, 21, and 28, the media was collected from the NICHE wells and saved for insulin analysis. The media was replaced with fresh media that represented the low glucose portion of the testing (100 mg/dL). The plates were incubated for 30 minute intervals, and the media was harvested for insulin analysis every thirty minutes for up to six hours. The media was changed to high glucose media at 90 minutes and remained so until the final incubation of the day. At this time, the media was replaced with low glucose media and the plates were returned to the incubator overnight. The following morning, media was collected and replaced with high glucose media again, with incubation extending up to another 3-4 hours.

Statistical analysis

Results are expressed as mean and standard deviation for at least three replicates. One-way nonparametric analysis of variance followed by the Tukey post-hoc test was assessed to verify statistical significance; $p < 0.05$ was considered statistically significant. Statistical analysis was performed using Prism 5 software (GraphPad Software Inc., San Diego, CA, USA).

3. Results

Morphological and phenotypical characterization of the cultured MSCs

During the MSC differentiation into ILIPA phase, cells gathered gradually in groups with the formation of three dimensional aggregates. At the end of the differentiation protocol, cells formed clusters with spheroidal morphology (Figure 4.1). A difference in the rate of growth or differentiation was observed between different donors (data not showed).

At the end of differentiation, immunofluorescent labeling and electron microscopy demonstrated c-peptide positive staining in the differentiated ILIPAs.

Furthermore, using immunohistochemistry we show that differentiated ILIPAs contain α-cells that are positively stained for glucagon and β-cells positively stained for insulin (Figure 4.2).

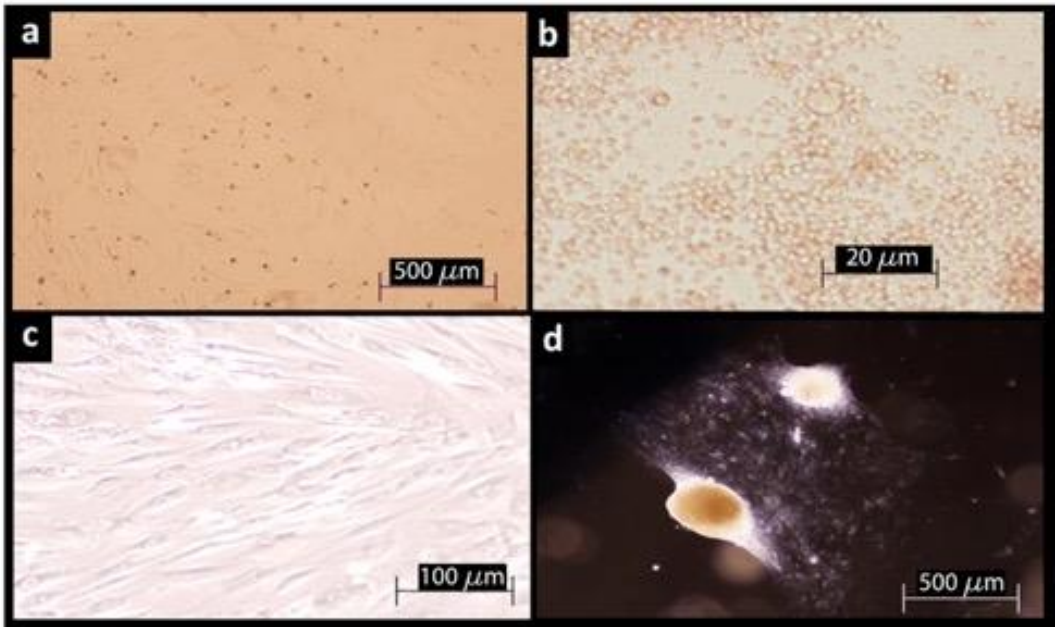

Figure 4.1: Morphological changes of bone marrow derived cells (MSCs) differentiated into functional islet-like structures (ILIPAs). (a) Bone marrow cells, (b) purified MSC, (c) undifferentiated MSCs, at the end of the expansion phase,

and (d) contrast phase microscopy showing aggregation of differentiating MSCs into insulin-producing ILIPA.

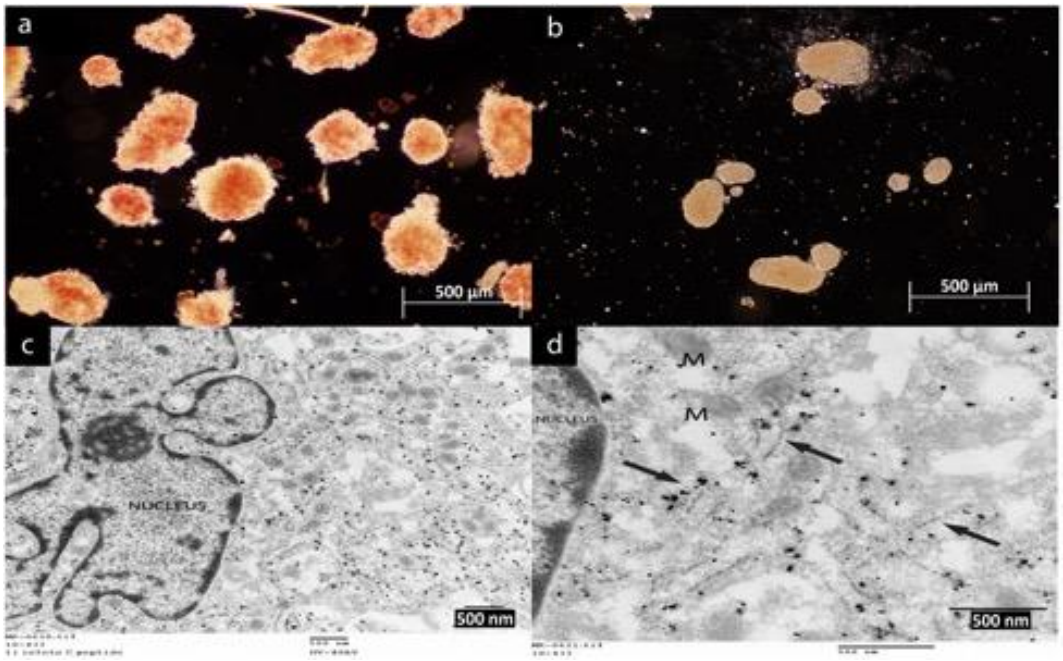

Figure 4.2: Differentiated ILIPAs (b) are similar in size to human islets (a). ILIPA EM photomicrograph (d) stained with gold nanoparticles labeled with antibodies to C-peptide (grey arrows) at the cisternae of rough endoplasmic reticulum (c).

Gene expression profile of human pancreatic islets and ILIPAs

Human islets (n=5) and ILIPAs (n=5) were analyzed for gene profile using high density Affymetrix U133A Gene Chips (analyzed by Gene Spring software). Genes that met the criteria for statistically significant differential expression ($p \leq 0.01$) at false discovery rate of 2%, were identified by the Welch t-test. This list was further refined by omitting those genes whose fold-difference of expression was less than two. Using Ingenuity Pathways Analysis software, we identified differential of gene expression in islets that play a role in insulin synthesis and secretion as well as glucose metabolism (Supplementary table 1 and Figure 4.3). While there was no difference in the insulin expression between islets and ILIPAs, islets had high relative levels of genes that

promote insulin production and secretion, such genes included ABCC8, PDX1, RFX6 PCSK1, SLC2A2, FOXA2, and SST.

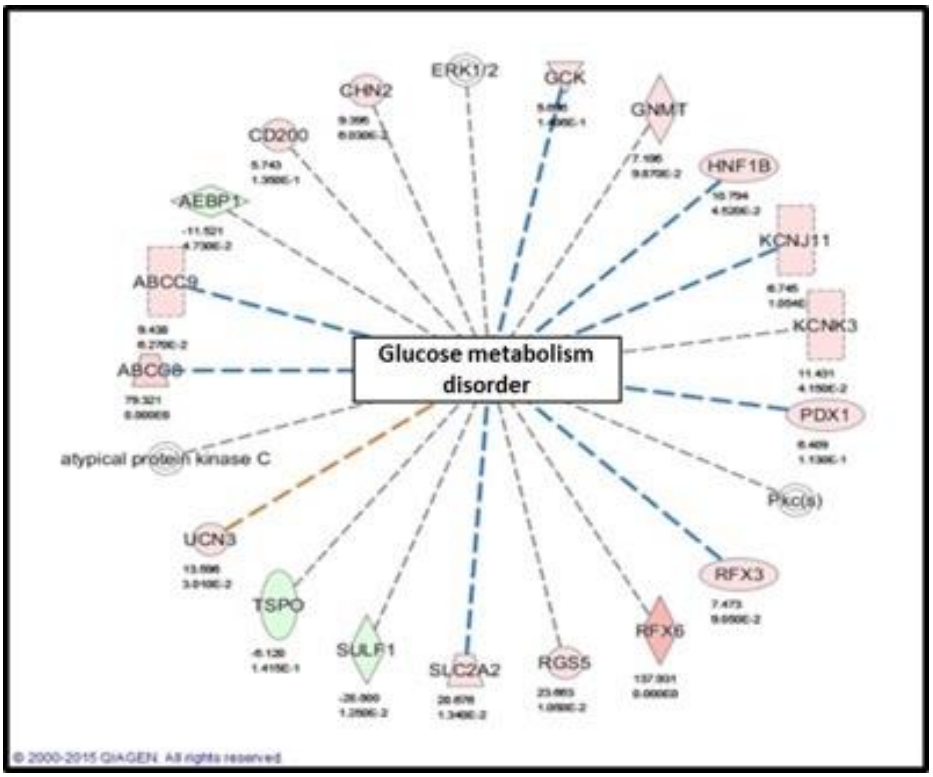

Figure 4.3: Glucose metabolism disorder network generated using Ingenuity Pathways Analysis software comparing human islets to ILIPAs. Upregulated genes are shown in red and downregulated genes in green. Genes that are important to glucose metabolism such as ABCC8, RFX6, and SLC2A2 are expressed much higher in the islets with fold changes of 79, 138, and 21, respectively.

RT-PCR of differentiated ILIPAs

Islet gene expression profile varies in different donors. To determine the variation in gene expression profile of different ILIPA preparations, we examined five differentiated ILIPA preparations and compared them to an average of five human islet preparations as a positive control and to undifferentiated MSCs and acinar cells as a negative control. We tested for genes that are crucial for insulin secretion and glucose metabolism and results expressed by previous gene expression array, such as Insulin, SST, ABCC8, SC2A2, PDX1, FOXA2, RFX6, and PSCK1. As

shown in figure 4, there is a wide variation between different ILIPA preparations, where two out of five have similar expression levels as the islets (Figure 4.4).

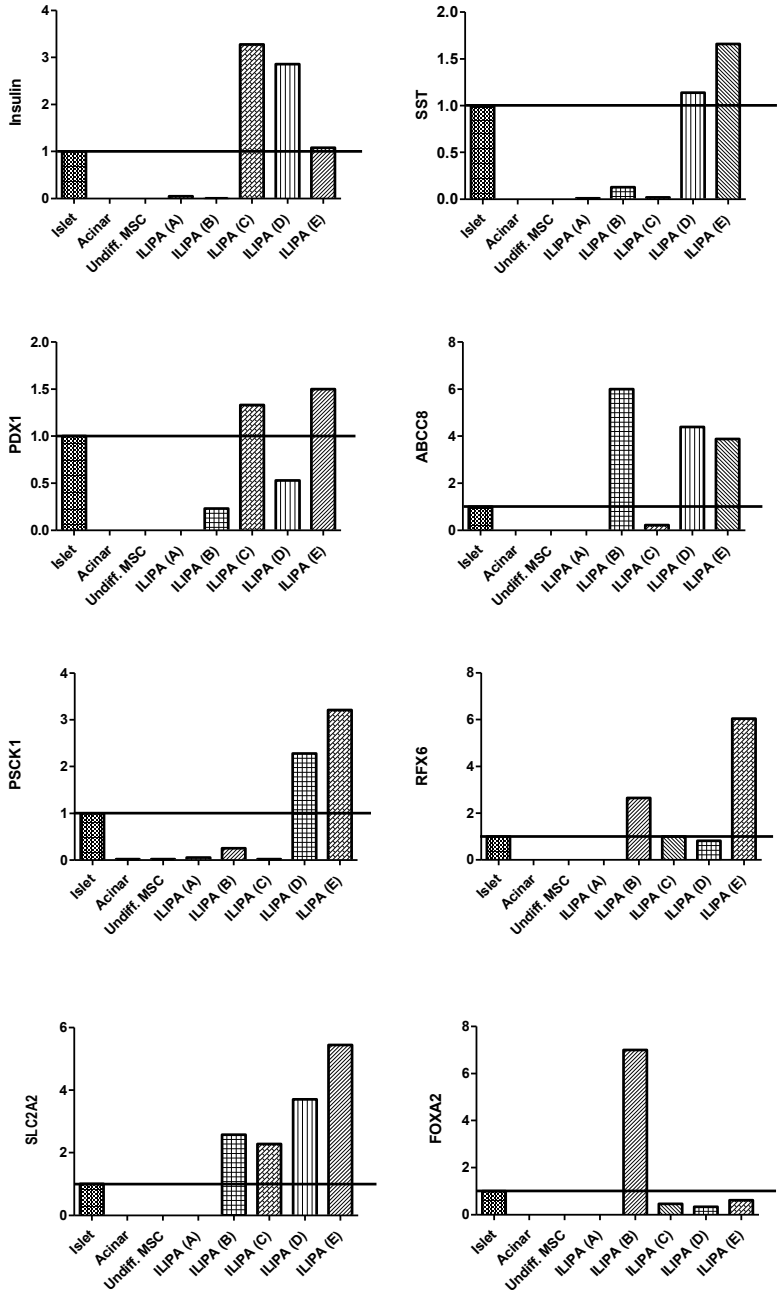

Figure 4.4: Real time PCR of islet's key transcription factors expression of acinar cells, undifferentiated MSC, and differentiated ILIPAs from 5 different donors, normalized to 5 different isolated human islets**.** The results are expressed as the fold change difference of islets to ILIPAs.

NICHE surface treatment and endothelial cell culture

Different surface treatments were tested to augment PLA NICHE hydrophilicity. All of the tested surface modifications reduce water contact angle on the polymer surface in the first week after treatment. The effect was higher when the NICHEs were treated with a combination of Ar plasma and ECAF ($p<0.001$), but this group lost the hydrophilic change in almost one week, becoming comparable to the other treated groups. All of the groups treated with Ar plasma maintained the surface characteristics, as shown by low contact angle at 1 month from the surface treatment ($p<0.01$), but only the combination with PLL and ECAF maintained the effectiveness at day 40 ($p<0.05$).

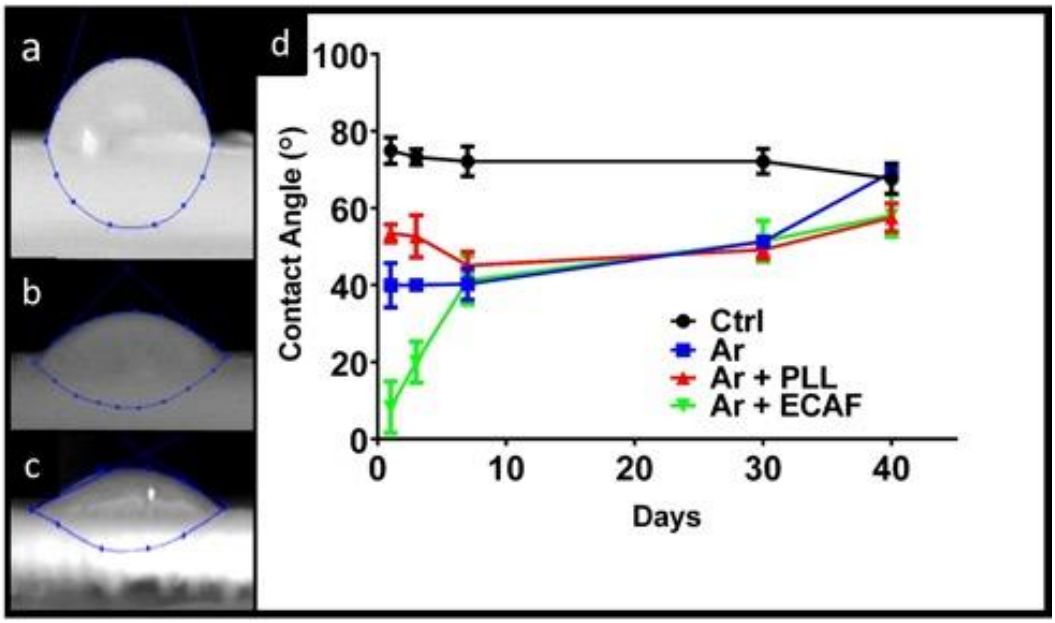

Figure 4.5: Comparison of hydrophilicity achieved by various surface modification techniques, as measured by water contact angle on day 1 (a=control, b=PLL, c=ECAF) and their stability over 40 days.

Cell proliferation and viability were tested in surface modified NGs using human umbilical vein endothelial cells (HUVECs). HUVECs were grown on NICHEs treated with PLL and Ar. Plasma treatment showed a slower growth compared to all the other surface treatments ($p<0.05$). All groups cultured in surface treated NICHEs showed a mean viability higher than 90%, and dimension comparable to control, with minor differences between the control and untreated NGs (16.81 μm vs. 15.54

μm, $p<0.05$). All cells cultured inside the NGs grew slower than the control group cultured in classical polystyrene well ($p<0.001$).

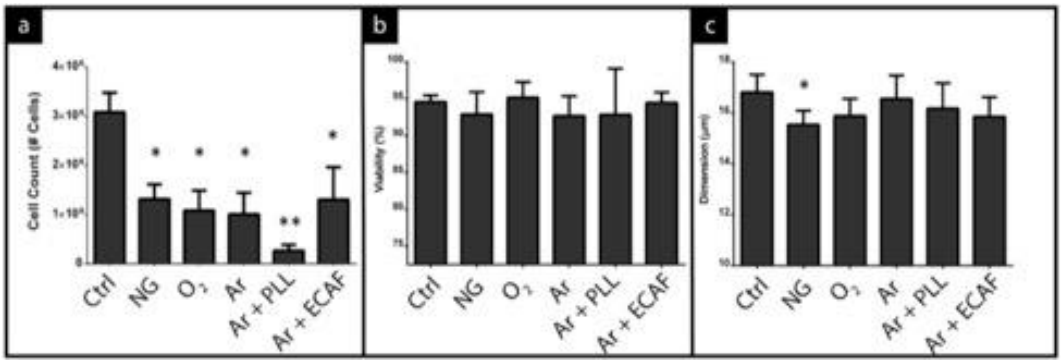

Figure 4.6: Effect of different polylactic acid surface modification techniques on HUVEC viability (a), growth (b), and dimension (c). * $p < 0.05$, ** $p<0.001$

Insulin secretion by ILIPAs in NICHE

A month long ILIPA culture was conducted in polymeric NGs with different surface treatments to understand long-term viability and insulin secretion in response to glucose stimuli.

ILIPAs showed an ability to produce steady levels of insulin throughout the testing process. The insulin accumulated in the testing media in a consistent manner showing spikes in insulin production and accumulation at time 0 (following weekend incubation) as well as following overnight incubation during the testing. These spikes seem constant during the entire duration of study, with a statistically non-significant reduction trend during week 4 in all groups. There were no differences in both basal insulin secretion or response to high glucose in argon or oxygen treated NICHEs. ILIPAs showed no significant difference in overall performance over the testing period when different types of surface treatments were compared and insulin release tracking was consistent for each NICHE cohort (Figure 4.7).

When comparing ILIPAs in the NG-PL to free ILIPAs tested in the same manner, we see a rapid drop in insulin levels for the free ILIPAs compared to those in the NICHE devices, presumably due to retention of insulin within the PL gel matrix (Figure 4.7A).

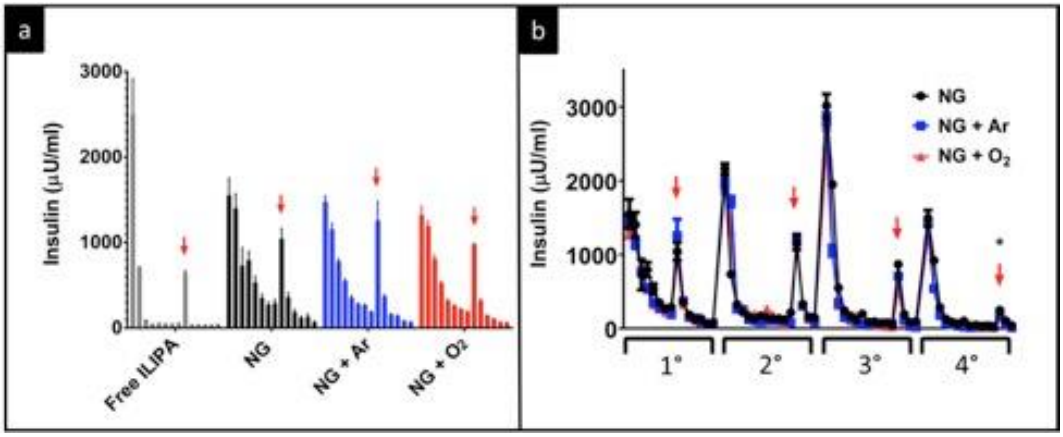

Figure 4.7: Effect of NICHE and surface modifications on ILIPAs' insulin secretions after glucose stimulation during the 1st week of culturing (a) and over a 4-week experiment (b). The overnight peaks are marked by red arrows.

4. Conclusion

Over the last few decades, islet and stem cell transplantation has been explored as a promising method to achieve strict control of blood glucose and as a potential cure for diabetes. Two key problems for these cell therapies are the lack of adequate islets or islet-like tissue and the need to use immunosuppressants. Here is presented the generation of human mesenchymal stem cells (MSCs). Since MSCs comprise only 0.001% to 0.01% of bone marrow mononuclear cells, in vitro expansion of these cells is necessary to obtain sufficient cell numbers for clinical use. Following the expansion phase, cells were driven to differentiate into islet-like insulin-producing aggregates (ILIPAs) that express pancreatic islet genes and secrete insulin. The premise of stem cell therapy for diabetes is the production of autogenous differentiated cells that mimic pancreatic islets and β-cells as a source of insulin for blood glucose homeostasis. Our data show that despite the success in creating ILIPAs that are capable of insulin and C-peptide production, there was a variation among cultures from different donors in key transcriptional factor expression such as PDX1, a factor responsible for the development of the pancreas in humans as well as maintaining insulin gene expression and β-cell survival. Down regulation in the expression of PDX1 could lead to β-cell failure and subsequently type 2 diabetes. RFX6 was another transcription factor upregulated in ILIPAs, commonly responsible for the regulation of insulin gene expression and secretion, and is thought to be involved in islet cell differentiation.

ILIPAs expressed SLC2A2, a gene that produces GLUT2, the specific glucose transporter in β-cells, responsible for glucose homeostasis by enabling transport across cell membranes, tuning insulin secretion. PCSK1, Proprotein convertase subtilisin kexin type 1 (PCSK1) belongs to the subtilisin-like proprotein convertase family that process latent precursor proteins, such as proinsulin, into their biologically active products. and ABCC8 a gene included ATP-binding cassette, sub-family

C (CFTR/MRP), member 8, which functions as a modulator of ATP-sensitive potassium channels and insulin release. Donor variability is a major concern. Our laboratory found that not all donor cells differentiate at the expected time frame; indeed, some took a longer time to reach the desired phase. Therefore, testing ILIPA preparation with RT-PCR for key genes required for healthy islet function could be essential for possible future clinical studies. RNA-seq could be a valid method to further characterize ILIPA gene expression and their biological characteristics, which will require larger quantity of cells.

3D NICHEs, after performing Plasma surface treatment, were adopted to encapsulate ILIPAs in order to evaluate cell viability and insulin release.

Plasma surface treatment, followed by surface functionalization with cationic groups have shown to greatly enhance biomimetic properties of PLA and the consequent affinity for the cells. Prior work with endothelial cells on oxygen plasma treated PLA scaffolds has shown increased cell proliferation over 4–6 days and increased angiogenesis in vivo at 12 days. This characteristic could be very useful for potential clinical application, permitting a better vascularization of PLA implanted devices used as cell reservoirs.

Xia *et al. [315]* showed rapid endothelialization of plasma treated PLA with functionalized –COOH groups to link gelatin or chitosan, while Zhu *et al.* showed similar results through aminolyzed PLA. A possible advantage of polymeric PLA implants is the local lactate release after degradation, which seems to improve angiogenesis and cutaneous wound healing in different mouse strains.

ILIPAs, either free or in NGs, did not show a measurable acute response to high glucose as a secretogogue, likely due to the lack of insulin storage granules in the ILIPA construct. However, all groups demonstrated very consistent low-level insulin production throughout the testing period and as such, may prove clinically useful as a replacement source of basal levels of insulin. All tissues tested resulted in a basal insulin level of 0.012-0.072 μU insulin per ILIPA (data not shown). An interesting observation was that free ILIPAs showed a quicker reduction in

insulin release than those housed in NICHEs, presumably due to insulin accumulation in the PL gel matrix in the latter. Also, ILIPA overnight incubation in NICHEs produced higher insulin spikes.

Chapter 5

NICHE validation In Vivo for insulin and testosterone release

5.1 3D printed vascularized device for subcutaneous transplantation of human islets

1. Introduction

In this chapter is presented the validation of NICHE as encapsulation system for subcutaneous engraftment of human pancreatic islets in an immunocompromised mouse model. After 3D printing, the devices were treated with Argon plasma and growth factor enriched platelet gel in order to improve polymer biocompatibility and enhance vessel formation within the NICHE. After achieving an optimal level of vascularization, human pancreatic islets were transplanted. As demonstrated by the detection of human insulin over the 22-weeks of the experiment, the device resulted to have protected the encapsulated islets from acute hypoxia and kept them functional. Moreover, the adaptability of the NICHE for long term applications was demonstrated by refilling some of the experimental groups via transcutaneous injection of additional islets.

2. Materials & Methods

NICHE devices suitable for rodent studies to hold up to 5,000 islets were printed as previously described in chapter 3. After fabrication, NICHE surfaces were treated with Argon and Oxygen plasma (March plasma etcher, Nordson). The power (30W) and gas flow (150mTorr) were kept constant, while changing the exposure time (30, 90, 120 and 150 seconds). The structure of the device was evaluated at different magnification by scanning electron microscopy (SEM) (Nova NanoSEM, FEI) for channel quality and size (Fig. 1c-d). Hydrophilicity was evaluated by measuring the water contact angle, as described previously in Chapter 4 and surface nanopattering and roughness were evaluated by atomic-force microscopy set in tapping mode (Fig. 1e-f, BioScope Catalyst, Bruker Instruments, Texas).

The function of the encapsulation devices was evaluated in nude mice (Nu/Nu, female, 8-10-week-old), after receiving approval by the Institutional Animal Care and Use Committee of Houston Methodist Research Institute. The devices were sterilized with 70% ethanol and UV before performing all the surface modification treatment with oxygen or argon plasma in a sterile environment (clean room of the Houston Methodist Research Institute). Thereafter, devices were filled with a platelet-lysate solution (ZenBio), under aseptic conditions and incubated overnight at 37 °C in a cell incubator to form the gel, with the addition of bovine thrombin (BioPharm Laboratories, LLC). The ready to be implanted devices were then packaged and transferred to the animal facility and the package opened in a sterile environment just before the implantation. Surface treated and sterilized devices, loaded with platelet-lysate matrix (PLM) enriched with VEGF at two different concentrations (0.5 and 5 µg/ml), were implanted subcutaneously in the mice dorsum (n=12 per group). At 1, 2, and 4 weeks post implantation, 4 mice per group were euthanized and the graft explanted for histological assessment of vascularization and innervation. The implant and surrounding tissues were

harvested, and processed for histopathology evaluation of tissue response to the implanted device with hematoxylin and eosin (H&E). This staining was used to analyze tissue morphology and to evaluate the presence of immune cells, vessels infiltration, and fibrotic response at the tissue-device interface. CD31 antibody (Abcam, ab28364) was used for immunohistochemistry (IHC) analysis and a pan-axonal antibody (Cambridge Bioscience, SMI-312R-100) with immunofluorescence (IF) to assess device vascularization and innervation respectively. CD31 expressing cells were counted separately in 10 high-power fields. (HPFs).

A second experiment was performed in nude mice (n=5 per group) to evaluate insulin release from human islets transplanted into a prevascularized device. Human pancreatic islets (2,000 IEQ per mice) were injected subcutaneously with a 22 G needle into the encapsulation system 4 weeks after device implantation or were inserted under the kidney capsule (positive control). Human insulin (ultra-sensitive human insulin ELISA kit, Alpco) and blood glucose (OneTouch® Glucometer, Johnson and Johnson) levels were assessed weekly and body weight was monitored throughout the experiment. Intra peritoneal glucose tolerance test (IPGTT) was performed weekly to stimulate insulin secretion from the transplanted islets. Blood was collected using retro-orbital method, under topical anaesthesia and aseptic techniques. A subsequent test was performed on the same animal cohort to demonstrate the subcutaneous refillability of the implant. Twelve weeks after the first injection, additional human islets (2,000 IEQ per mice) were injected trancutaneously in all groups where the insulin production was lower than 0.125 µIU/ml.

Statistical analysis was performed using Student's two tailed paired t-test. Results are presented as mean and standard error of the mean (SEM). A value of $p<0.05$ was considered statistically significant. GraphPad Software, Inc. was used for the analysis.

3. Results

Transplantation of cells on porous biomaterials has emerged as a promising strategy for long-term function facilitating rapid tissue ingrowth, vascularization and innervation providing oxygen, nutrition, and waste removal [147]. Recognizing such needs for an islet and cell encapsulation system, we are working on new strategies to deliver cells subcutaneously [35–37]. The architecture of the proposed device is designed to maintain pancreatic islets close to blood vessels, but separated from each other to mimic the physiological architecture in the pancreas and avoid cell crowding.

To increase the biointegration of the NICHE, we decided to use PLA, which is a widely adopted polymer in biomedical devices, biocompatible, and presents good elasticity and mechanical strength suitable for subcutaneous implantation as previously described in Chapter 3 and 5. Due to the chiral nature of lactic acid, PLA is hydrophobic with low cell adhesion properties. Surface treatment with plasma improves the low surface free energy of different materials and offers a solvent-free technique capable of changing the wettability, surface roughness and surface chemistry of polymers, enhancing cell proliferation and viability [315,316]. Plasma activation also increases PLA's surface free energy forming a broad variety of functional groups on the surface, including polar groups, which drastically change wettability and have a positive effect on material–cell interactions. Previous work from our group demonstrated that plasma treatment substantially increased the hydrophilicity of the surface and reduced the contact angle, which remained stable over 30 days in phosphate buffered saline (PBS) [36]. Here we looked at the effect of plasma exposure time on surface patterning and roughness and compared Oxygen and Argon treatments. Since UV light sterilization methods showed to increase polymer wettability without affecting morphology and mechanical properties, we decide to evaluate the effect of the surface modification only at the end of plasma treatment. As shown in Fig. 5.1E,

both treatments increased surface roughness, reaching a maximum value, after which the roughness diminished with continued exposure, possibly due to eventual etching of the crystalline regions. It was also noticed that the Oxygen treatment cause deeper patterns (4.63 nm with Argon and 26.45 nm with Oxygen, $p<0.01$, Fig. 1F), which has been demonstrated to be beneficial for cell attachment and proliferation. For this reason, a 120 seconds Oxygen treatment was selected for the following experiments [317] .

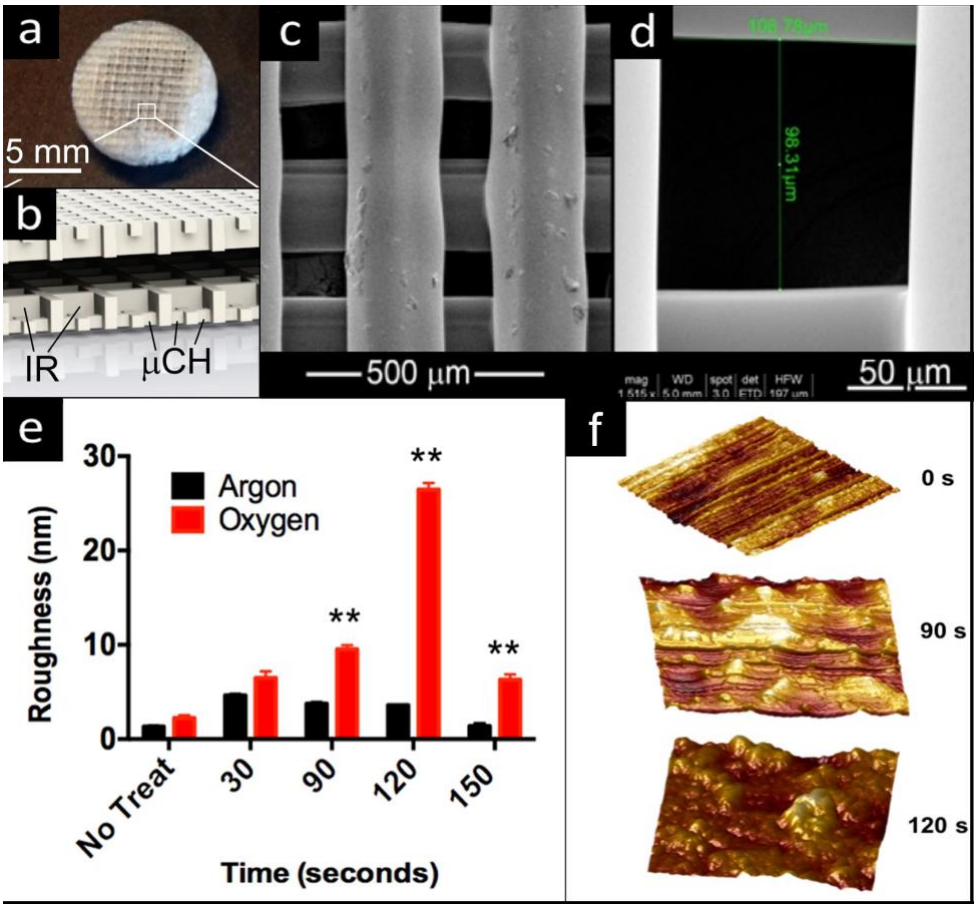

Figure 5.1. Mouse prototype of the 3D-printed NICHE (A) and rendering of the structure (B) that includes insulin reservoirs (IR) and microchannels (□CH). Magnification of the microchannels under SEM (C) and (D). PLA superficial roughness measurements after Argon and Oxygen plasma treatments, changing time of application (0, 30, 90, 120, and 150 seconds) (E). AFM pictures of PLA surface treated with Oxygen plasma after 0, 90 and 120 seconds (F). Average and SEM are represented. ** $p<0.01$.

We then investigated the in vivo vascularization and innervation of Oxygen treated devices after subcutaneous implantation in nude mice. Nude mice were selected for these studies with the novel encapsulation device as they show an inflammatory response to a foreign body, but allow for transplantation with human islets without the need for immunosuppression. It has been broadly demonstrated that vascularization of the graft is the key for successful engraftment of islet transplants [288,289]. Prevascularization could mitigate the issue of acute hypoxia which was shown to result in islet apoptosis and graft failure. To stimulate neovascularization and to support the islet viability and function for a period of time after transplantation we tested devices loaded with biological gels with different VEGF concentrations. An acute inflammatory response to the foreign body was present in the first week after device implantation, mainly in the VEGF groups, and subsided with time, leaving a rim of vascularized connective tissue around the device at week 4 (Fig. 2). Indeed, the neutrophils, which are considered to have an impact on the development of the inflammatory response leading to the formation of the fibrotic capsule, were almost absent from the second week (Fig. 5.2 A-I). The red arrows in Fig. 5.2 indicate the protrusion of the surrounding subcutaneous tissue into the devices. Tissue samples were taken from the side of the device closer to the skin, representing the subcutaneous environment. We noticed a positive trend between VEGF concentration and the number of vessels stained by CD31 (Fig. 5.2J-M), but there was no statistically significant difference between the groups after 1 week, probably for the limited number of animals per group. After 4 weeks, we noticed calcification in the VEGF 5 µg/ml sample as evident by the dark spots in high density close to the tissue-implant interface (Fig. 2I, black arrow). It has been already shown that VEGF is involved in the calcification process of cartilage and at similar concentration it was tested to induce bone response to implanted craniofacial implants. It was observed that in 4 weeks the subcutaneous tissue and the inside of the device were also vascularized with lower concentration of VEGF (Fig. 5.2N-O). Based on these results, 0.5 µg/ml VEGF was selected for further studies.

Finally, we also found nerve bundles in the proximity of the device (Fig. 5.2P-Q). These may have reached the device and the transplanted islets. However, further long-term studies are necessary to prove and quantify islet innervation, considering the slower rate of growth of nerves compared to vessels.

After proving the device vascularization, we performed a second experiment injecting human islet into a prevascularized device previously loaded with the VEGF rich matrix. By the time of the islet injection the gel was already degraded, releasing growth factors (Fig. 5.2N).

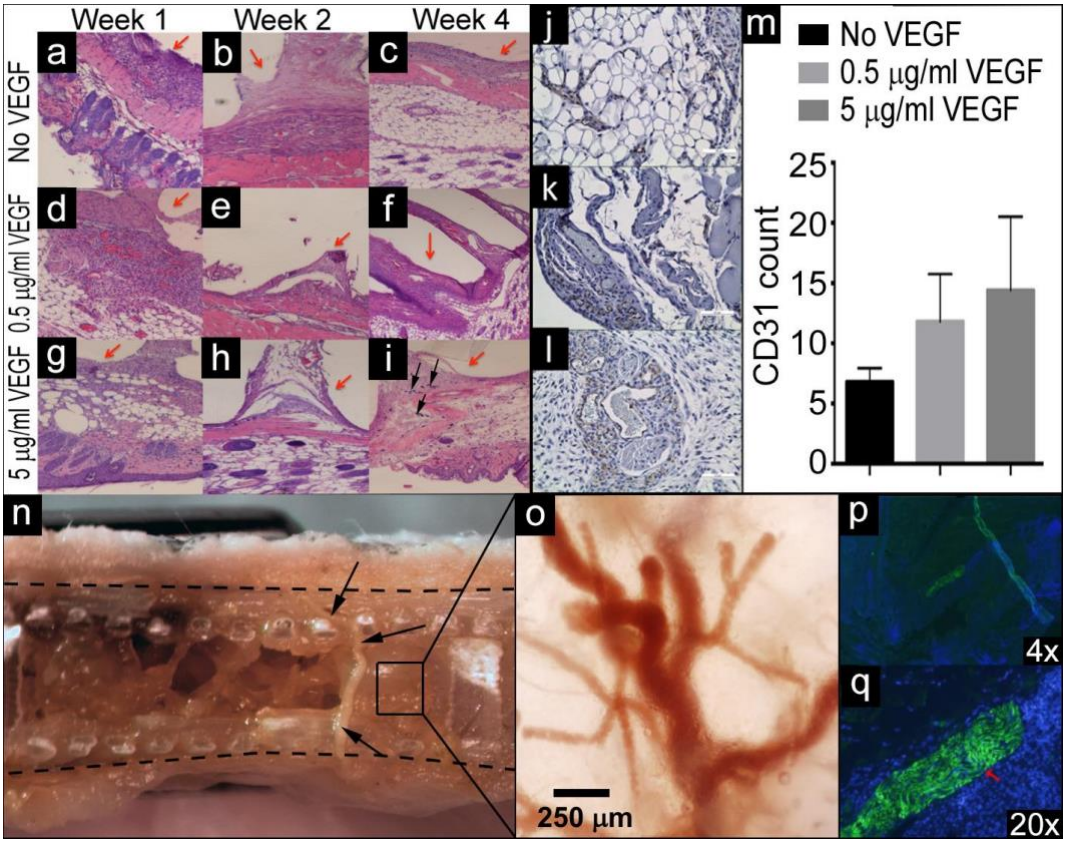

Figure 5.2. H&E of the tissue surrounding the device at 4x. Tissue response at the device-subcutaneous tissue interface is shown (red arrow, A-I). Different concentrations of VEGF were tested and device retrieved after 1, 2, and 4 weeks from the implantation. Diffuse spots of calcification (black arrows) were present at week 4 with the highest VEGF concentration (I). CD31 staining of tissue (J-L). Scale bar is 50 μm. Average and SEM of the CD31 count for high power field (M). Representative optical microscope visualization of the tissue collected from the device reservoir (VEGF 0.5 μg/ml group), showing the presence of mature vessels (N-O) Dotted lines represent device-subcutaneous tissue interface and the black arrows follow the path of a vessel through the polymeric scaffold.

Neurofilament staining (SMI312-R, in green) indicates the proximity of subcutaneous nerve bundles to the encapsulation device (P-Q).

We observed detectable levels of human insulin from week 4, but at lower levels compared to the positive control ($p<0.001$). As described in various islet encapsulation models, there is a lag time for adequate function until the transplanted islets are vascularized [15,288]. The prevascularization of the device appeared to have helped encapsulated islets to overcome the initial post implant injury, but it takes longer for the transplanted cells to develop mature vasculature and be functional. The lower insulin level detected after IPGTT in the device group as compared to the kidney capsule control could be ascribed to a non-complete vascularization of islets in the device. Although prevascularized, it is expected that islets will need to fully connect to the vasculature post transplantation. The duration of this process is compatible with the 2 weeks timeframe observed in Fig. 5.3 for an increase in insulin secretion in the device group. As the platelet lysate matrix is expected to be resorbed within few days from device implantation, we do not expect that islets were affected in their function by residual PLM. A second load of islets (2,000 IEQ) into vascularized devices increased the insulin levels (~10 µIU/ml) to values that were comparable to the kidney capsule transplantation (Fig. 5.3a, $p>0.05$). The total number of islets loaded was 4,000 IEQ per device, less than the theoretical maximal loadable volume according to the three-dimensional structure of device and the presence of a vascularized environment. Nevertheless, it was not possible to estimate exact volume of vessels and tissue present in the device at the time of the second islet loading, and this could have an effect on the distribution and the packing density of the islets in the device. Further studies are required to understand the optimal timing and the amount of islets needed to obtain a valid insulin secretion after multiple loading of islets. Achieving this could help adapting the insulin output to patient physiology and clinical need. Additionally, the devices were well tolerated and animals showed comparable basal glucose level (Fig. 5.3b) and weight (Fig. 5.3c),

demonstrating that the presence of additional islets is not associated with hypoglycemia.

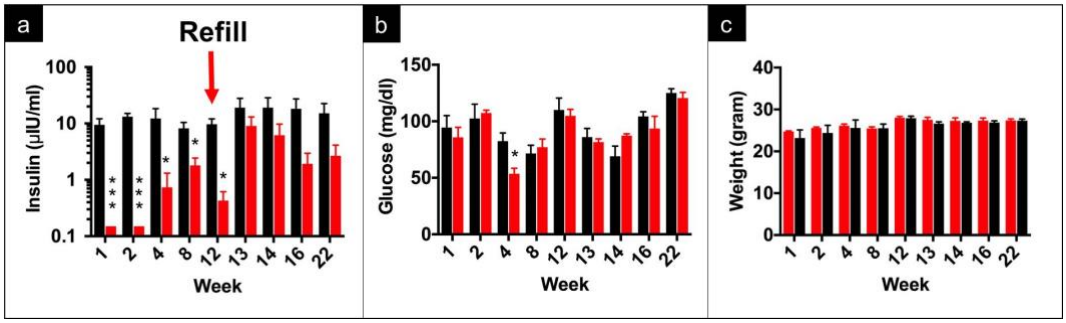

Figure 5.3. Insulin release from kidney capsule (black) and encapsulation device (red) after glucose stimulation (A). On week 12 all the animal with insulin level below 0.125 uU/ml where treated by refilling the implant with additional 2000 IEQ (red arrow). Basal blood glucose levels (B) and body weight (C). Average and SEM are represented. * $p<0.05$; *** $p<0.001$.

4. Conclusion

In this study, we showed that the subcutaneous implantation of a 3D printed and functionalized NICHE generates adequate and prompt vascularization of the graft. Vascularization was enhanced by the ability to dispense pro-angiogenic factors, such as VEGF, which is also known to increase islet viability and function [318]. In addition, the device could protect the graft, while the islets are being vascularized, from initial transplant site stressors and support their long-term survival. The transcutaneous refillability of the device offers opportunities for cell supplementation, without surgical retrieval and re-implantation, to accommodate for changing physiological needs. This will be of significant advantage in the case of the growing children with diabetes. Moreover, the reservoir structure permits the potential retrievability of the graft, which is important for stem cell derived engineered cells, undergoing malignant or other unwanted transformations. A current limitation of this device is the lack of immunoprotection of the transplanted cells. The priority of this work was to prove the vascularization and function of the device without compounding with the risk of immune rejection. For this reason, we used an immunodeficient animal model. A different device design can incorporate a strategy for local delivery of immunomodulators, which will expand its use in immunocompetent diabetic animals [319]. Further studies in diabetic animal models are required to evaluate the full potential of this versatile encapsulation device for diabetes cell therapy.

5.2 Transcutaneously refillable, 3D-printed biopolymeric encapsulation system for the transplantation of endocrine cells.

1. Introduction:

The NICHE is designed to be a technological platform for the encapsulation of a large range of cell lines. The encapsulation of human pancreatic islets or ILIPAs for diabetes treatment has been the first field of application. However, several other endocrine disorders can benefit from this solution, among them male hypogonadism is a disorder that affects more than 34% of men between 45-54 years old [320,321]. Nowadays, male hormone replacement therapy (testosterone replacement therapy) via oral, nasal or injection are the only treatment options available. However, Testosterone therapy carries various risks, including also heart attack [322].

Therefore, there is the need to develop novel alternative treatment solutions in order to restore the testosterone levels. Recent developments in the production of Leydig cells derived from bone marrow, adipose tissue, umbilical cord, and the testes have shown promise for future therapy for primary hypogonadism. However, as described in the case of islet transplantation, there is the need of an encapsulation system in order to support long-term graft viability and functionality.

In this chapter is presented the vascularization and testosterone release of Leydig cells encapsulated in 3D printed NICHEs In Vivo.

First, is described the modification of NICHE with a platelet-rich plasma (PRP) based hydrogel and coating designed to promote rapid biointegration of the device after implantation.

Second, is investigated the device compatibility in vitro and with the CAM assay using human pancreatic islets and mouse Leydig cells as representatives of endocrine cells.

Finally, NICHE is implanted subcutaneously in a castrated Rag1 -/- mouse model, assessing vascularization, engraftment with Leydig cells, function in terms of testosterone secretion, and device retrievability.

NICHE was designed to be used according to the protocol shown in figure 5.4.

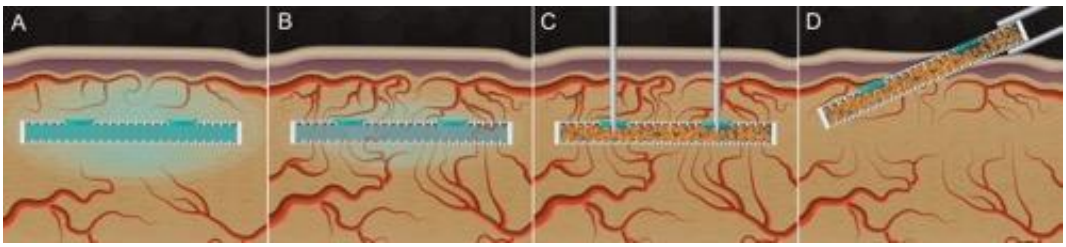

Figure 5.4: Deployment protocol for the NICHE. (A) Subcutaneous implantation and local release of growth factors to stimulate angiogenesis. (B) NICHE vascularization with vessel penetration inside the NICHE reservoir across microchannels. (C) Once the vascularization is completed, cells are transcutaneously inserted via injection. (D) Subcutaneous implantation allows for the complete retrieval of NICHE and transplanted cells if needed.

2. Materials and Methods

Device coating

After fabrication as described in Chapter 3, NICHEs were sterilized using 70% ethanol and UV in a sterile environment (clean room of the Houston Methodist Research Institute). Thereafter, the surfaces of devices were treated with a polyvinylpyrrolidone (PVP)-based platelet rich plasma (PRP, ZenBio, Inc., Durham, NC, USA) or platelet lysate (PL, ZenBio, Inc., Durham, NC, USA). Six (6) devices of each type of coating (PVP only, PVP + PRP and PVP + PL) were prepared. PLA devices were then immersed in 70% ethanol (Fisher Scientific, Hampton, NH, USA) for 4 h under mild agitation, rinsed, dried at room temperature. Three devices were coated with PVP solution (Sigma-Aldrich, St. Louis, MO, US) incubated for 5 min, and air-dried at room temperature (RT). The PLA devices were coated with one of three solutions of PVP, PVP + PRP, and PVP + PL, and allowed to dry at RT overnight (n=3 devices per group). Once coated with solutions, the PLA devices were placed on Polydimethylsiloxane (PDMS) templates containing micro sized vertical posts. The PDMS templates were fabricated via photo- and soft lithography as previously described. To evaluate the degradation kinetics and release of proteins and growth factors from the coating, all samples were individually immersed in 750 µl of 1X PBS for 7 days under gentle agitation at 37°C. Protein release in the sink solution was measured at day 1, 2, 3, 5 and 7 via a µBCA protein assay kit (Thermo Fisher Scientific Inc., USA). SEM micrographs were also collected to directly image coating degradation over time.

Hydrogel preparation

Growth factor rich hydrogels were prepared by crosslinking alginate-PRP/PL solutions with calcium chloride. 300 µl of 1.2% alginate/PRP or PL solution was added to the wells of a 24-well plate, stirred for 10 min at room temperature followed by addition of 80 µl of 15% 1M calcium chloride in 1X PBS ($CaCl_2$; Fisher Chemical, Hampton, NH, USA). Alginate solutions were prepared by mixing alginic acid sodium salt (Sigma-Aldrich, St. Louis, MO, USA) with either 1.2% w/v PRP (ZenBio, Inc., Durham, NC, USA) or PL (ZenBio, Inc., Durham, NC, USA) and stirred overnight at 37°C. The alginate/PRP or PL solution was agitated on a shaker at 400 rpm for 10 mins at 37°C to ensure homogeneous cross-linking.

Hydrogel in vitro degradation, in vitro

PRP/PL hydrogels (n=6 per group) were weighted and placed in the wells of a 12-well plate 1 ml 1X PBS and incubated at 37°C. Hydrogel samples were weighed on day 1, 2, 3, 5, 7, 10, and 13, to evaluate the gel stability and degradation. Quantification of protein release from the hydrogels were performed by collecting 500 µl of the supernatant and was analyzed using micro-BCA assay (Micro BCA™ Protein Assay Kit, Thermo Fisher Scientific Inc., USA). The removed supernatant was replaced with 500 µl of fresh 1X PBS.

Isolation of human pancreatic islets and culture

Pancreata were procured from heart beating cadaveric multi-organ donors perfused in situ by aortic flushing with cold preservation solution, placed in a container of cold preservation solution and packed in wet ice. Upon arrival at Methodist Hospital Islet Center the pancreata were digested using a modification of the islet isolation procedure described by Ricordi et al. After isolation islets were suspended and cultured in Memphis serum free media (M-SFM at 24°C, 5% CO_2 prior to use.

Pancreatic islet viability on hydrogel

1 ml PRP hydrogels (n=4 per time point) were prepared, as described previously, in 24-well plates. 200 islet equivalents (IEQ) in M-SFM were seeded per well over PRP hydrogel. Islets seeded directly in M-SFM in the 24-well plate were treated as control. On days 3, 7, 14 and 28, islet viability was tested by the Dye exclusion technique using fluorescein diacetate (FDA, Sigma Chemical Co.) and propidium iodide (PI, (Sigma Chemical Co) and images were captured by fluorescence microscopy (TiEclipse, Nikon instruments, Inc.). The islets were microscopically evaluated and measured for FDA (bright green fluorescence) and PI (red/orange fluorescence) dye uptake. Islets with greater than 25% PI dye uptake were scored as non-viable. At least 50 islets were assessed per well.

Glucose-stimulated insulin release from pancreatic islets on hydrogel

200 IEQ were seeded on 24-well plates with PRP gel in 24-well plates, as in the viability assay. On days 3, 7, 14 and 28, insulin secretion in response to a secretogogue was evaluated by a sequential static incubation method. The insulin content (IC) was determined after extraction of islets with acid ethanol. For the static incubation, islets were washed twice in low glucose media to remove M-SFM. The islets were then incubated for one hour in low glucose media (60 mg/dl) at 37°C / 5% CO_2. After removal of pre-incubation media, an additional aliquot of low glucose media was added to the wells. Following 1-hour incubation, the supernatant was collected for insulin analysis by ELISA (ALPCO Diagnostics, Windham, NH, USA). The centrifuge tube was rinsed with high glucose media (300 mg/dl) to recover any islets that may have been removed during media collection. The recovered islets were transferred to a microwell plate and incubated for one hour (37°C / 5% CO_2). The media was again collected for insulin analysis. An acid/alcohol solution was used to collect all of the remaining islets in each well. After vortexing, the islets

were frozen at -20°C overnight. The following day, after vortexing the supernatant was collected for IC measurement by ELISA [low glucose, high glucose and insulin content].

Leydig cell WST-1 proliferation assay and testosterone release ELISA analysis

The proliferative behavior of Leydig cells on PRP hydrogels was analyzed via WST-1 Cell Proliferation Assay (Sigma Aldrich, St. Louis, MO, USA) over a period of 28 days. 1000 Leydig cells were seeded per well in 1 ml media (day 0) on top of PRP hydrogel in a 24-well plate. 24 h after stimulating cells with 6 mIU/200 µl horse human chorionic Gonadotropin (hCG; Sigma-Aldrich, Missouri, USA), WST-1 reagent was added. After 2-hour incubation at 37°C, an area scan absorbance measurement was performed at 450 nm and 690 nm using the Synergy H4 Hybrid Multi-Mode Microplate Reader (Biotek Instruments Inc., Winooski, VT, USA). Using the area scan measurement, the absorbance readings at 9 areas in each well were used to calculate the mean absorbance per well. Triplicates of each condition were performed. A graph was plotted with OD_{690} reference values subtracted from OD_{450} values and normalized to absorbance on day 0. The procedure was repeated on days 1, 5, 9, 13, 21 and 28. Using the same culture conditions of the Leydig cell proliferation assay, on days 2, 6, 10, 14, 22 and 28, the entire 1 ml of supernatant was collected (and replaced by fresh culture media), which was used to quantify testosterone release via ELISA (ENZO Life Sciences, New York, USA).

Chorioallantoic membrane assay

Fertilized chicken eggs were purchased from Charles River (Norwich, Connecticut, USA). The chick chorioallantoic membrane (CAM) assay was performed as described previously. On embryonic day 7, PRP hydrogel alone or PRP hydrogel + PRP coated NICHE was placed on top of the CAM (n=20) with a silicone ring around the gel to demarcate its location.

The CAM, hydrogel or NICHE-hydrogel (n=6) were harvested on days 1,3, and 5 post cells seeding and analyzed via optical microscope to evaluate the degree of vascularization, followed by histological analysis via H&E staining after Optimal Cutting Temperature (OCT) cryoembedding.

In vivo bioluminescence imaging

1 x 10^6 luciferase-overexpressing Lewis lung carcinoma (LLC) cells were suspended in 30 µl 1X PBS and 20 µl Matrigel (Corning, Tewksbury, MA, USA) were grafted on the CAM with or without PRP hydrogel within a silicone ring. As a negative control, we cultured 1 x 10^6 LLC cells on PRP hydrogel with 100 µl media supplementation, compared to cells in media only and PRP only. Bioluminescence imaging was performed in a Caliper in vivo imaging system (IVIS) Spectrum (PerkinElmer, Inc., Waltham, Massachusetts, USA) on day 3 after cell seeding. Exposure time was 1 second and 5 minutes after adding 100 µl D-luciferin (15 mg/ml). The region of interest (ROI) was quantified by the Lumina software (PerkinElmer, Waltham, MA, USA) and data was plotted with Prism (Graphpad Software, Inc., La Jolla, California, USA).

In vivo NICHE assessment

Sterilized 3D printed NICHEs containing 300 µl PRP hydrogel supplemented with 0.5 µg/ml of VEGF were implanted in the dorsum of ten castrated *Rag1-/-* male mice, after collecting blood samples for baseline testosterone measurements. 4 weeks after implantation, 2 mice were euthanized to evaluate the vascularization within the NICHE, and devices with surrounding tissue were harvested for histological evaluation. On week 4, 6 x 10^6 Leydig cells were transplanted via transcutaneous injection through the loading port of the NICHE in the 6 remaining mice. On week 10, NICHEs were retrieved and mice were euthanized on week 12. Blood was sampled weekly (50 µl) 4 hours after subcutaneous hCG injection to stimulate testosterone production from day 0 till week 12. Testosterone level was measured via ELISA (ENZO Life Sciences,

Farmingdale, New York, USA).

Histological analysis

NICHEs collected from the mice were fixed in 10% formalin overnight, transferred to 10% sucrose solution for 2 days and then stored in 1% sucrose solution. NICHEs were then embedded in OCT and stored in -20°C. 4 hrs. before cryo-sectioning, samples were transferred to -80°C. Samples were sectioned at 7 µm thickness and stained via H&E, CD31 (ab28364, Abcam, Cambridge, UK) and HSD3B (ab65156, Abcam, Cambridge, UK). Vasculature formation within the NICHE was assessed on week 4 by quantification of CD31 staining intensity. Presence of functional Leydig cells was determined by HSD3B staining. Rabbit anti-mouse FITC conjugated antibodies (ab6717, Abcam) were used as secondary antibody for immunofluorescence staining.

Statistical analysis

Results are expressed as mean ± SEM. All statistical analyses were performed using GraphPad Prism 7 software (GraphPad Software Inc., San Diego, CA, USA). Student t-tests or one-way ANOVA were performed to determine the significant difference between groups. *P* values of less than 0.05 were considered statistically significant, whereby symbols indicating statistical significance are as follow: n.s., not significant, * $P \leq 0.05$, ** $P \leq 0.01$, *** $P \leq 0.001$, **** $P \leq 0.0001$.

3. Results

NICHE coating characterization and degradation

To promote neovascularization and rapid bio-integration of the device upon implantation using growth factor release, 3D printed NICHEs were coated with a solution of polyvinylpyrrolidone (PVP) containing either platelet-rich plasma (PRP) or platelet lysate (PL). PVP is a water-soluble biocompatible polymer widely used in biomedical applications as a binding and solubilizing agent. PRP and PL contain growth factors that stimulate vasculature formation and innervation [323]. SEM analysis of the treated NICHE demonstrated a uniform, smooth surface coating (Fig. 5.5A) with a thickness of approximately 30 μm (Fig. 4B). The coating was patterned with monodispersed pores of average size of 45-50 μm in regular arrays (Fig. 5.5A, C). The outer surface of the coated device was imprinted with the circular posts on the PDMS template to enhance the coating efficiency. In addition, patterned micro-chambers on the surface formed a uniform non-porous layer which improved the release kinetics of growth factor. To evaluate coating degradation over time, we analyzed samples in PBS at 37°C via SEM and measured protein release from PRP or PL coated NICHEs. SEM analysis showed near complete degradation of both coatings by day 5 (Fig. 5.5D, E). Protein quantification showed a burst protein release in the first 2 days, reaching 80.7 ± 5.4% for PVP-PRP and 93.7 ± 4.7% for PVP-PL, respectively. While PVP-PL reached a complete plateau by day 3, a slower release of proteins from the PVP-PRP samples extended until day 7 (Fig. 5.5F). Based on the better release kinetics of proteins, we selected PVP-PRP as the coating of choice for the following analysis in vivo.

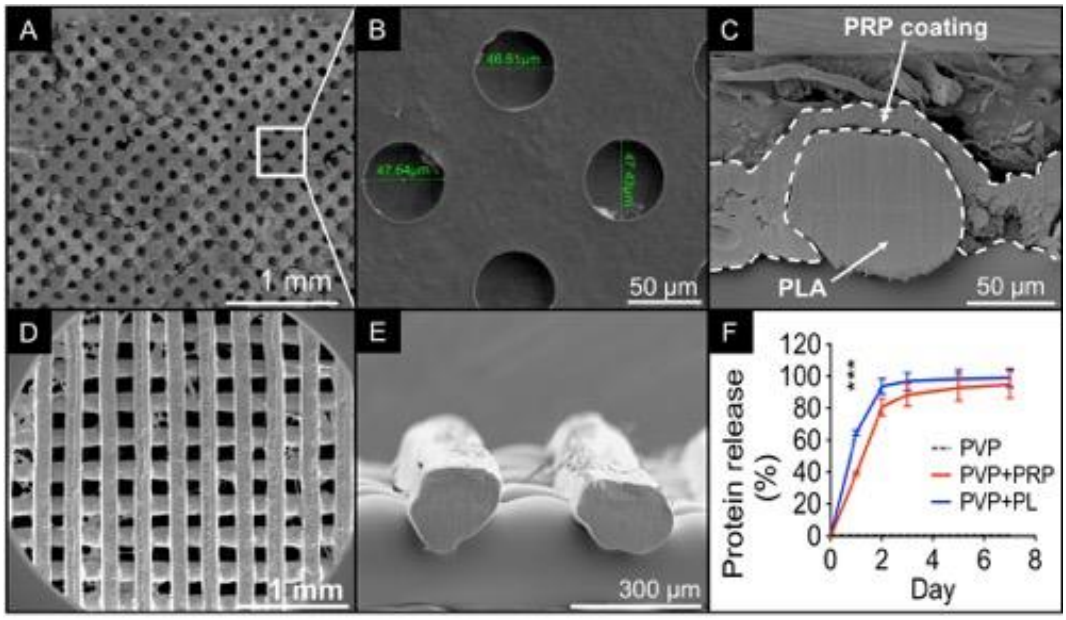

Figure 5.5: PRP coating of NICHE. (A) Baseline SEM images of NICHE coated with PVP-PRP coating, (B) with mean pore size of 47.6 µm and (C) cross section of PRP coating. (D,E) Day 7 SEM images of the degraded coating. (F) In vitro protein cumulative release from coating over 7 days.

Hydrogel degradation analysis

With the objective of promoting angiogenesis within the NICHE, we tested PRP or PL hydrogels, to be loaded in the device at time of implantation. We evaluated the degradation of both hydrogel formulations in PBS at 37°C in terms of mass changes (Fig. 5.6A) and growth factor release capability (Fig. 5.6B). Mass loss profiles demonstrated a quicker degradation of PL hydrogel with an 80% weight reduction in the first 5 days of testing as compared to 20% for PRP hydrogel. While by day 9 PL was almost completely degraded (90% weight loss), and PRP hydrogel retained 50% of its initial weight. By day 13, both hydrogels were completely degraded.

Protein release from the PRP hydrogel was sustained over 11 days in a constant manner (Fig. 5.6B). In contrast, PL hydrogel presented a linear protein release for 5 days, corresponding to 80% mass loss (Fig. 5.6A), and reached a plateau thereafter. In light of slower degradation and sustained protein release, PRP hydrogel was selected as the most

suitable constituent in the NICHE to support vascularization and engraftment.

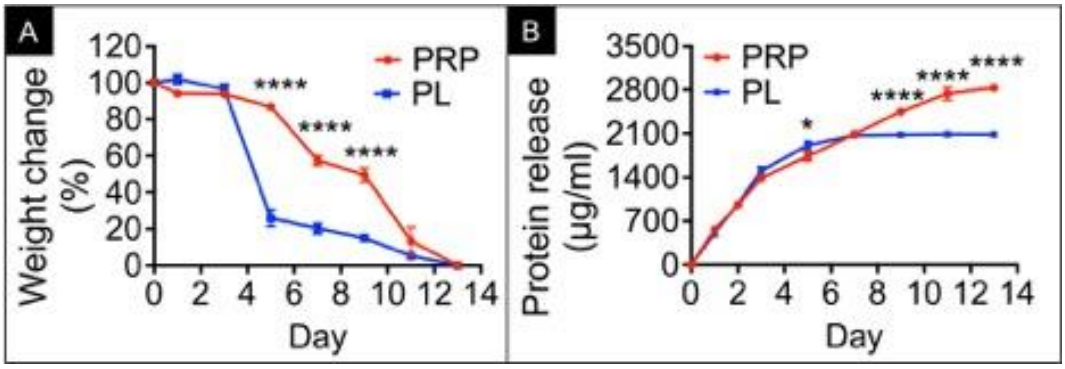

Figure 5.6: PRP and PL hydrogel in vitro stability. PRP and PL hydrogel (A) weight change and (B) protein release over 13 days

Cell viability and hormone secretion in PRP hydrogel

In the intended in vivo deployment of NICHE, PRP hydrogel is expected to completely degrade by 2-3 weeks post-implantation, after which cells are transplanted into the device for encapsulation [35]. To ensure cytocompatibility of hydrogel degradation by-products or in the event of residual hydrogel by the time of cell transplantation, we performed a 14-day experiment to test viability and function of two representative endocrine cell types – murine Leydig cells and human pancreatic islets, as an additional relevant endocrine cell that could be of potential applicability.

Results demonstrate that Leydig cells on PRP hydrogels have similar viability (Fig. 5.7A) and testosterone release (Fig. 5.7B) as compared to cells with media (control). Consistent with literature reports, we observed cluster formation of Leydig cells in PRP hydrogel by day 4. In the case of human islets, over the course of 14 days, we observed comparable viability of islets cultured in media and PRP hydrogel via dye exclusion using fluorescein diacetate and propidium iodide analysis (Fig. 5.7C,D). While quantitative assessment of insulin secretion via ELISA showed that islets cultured in PRP hydrogel exhibited an upward trend of insulin release throughout the 14 days as opposed to islets cultured in media only (Fig. 5.7E), there was no statistically significant difference between the two

groups. Overall, these results demonstrate that both islets and Leydig cells remained viable and functional activity was maintained in PRP hydrogel.

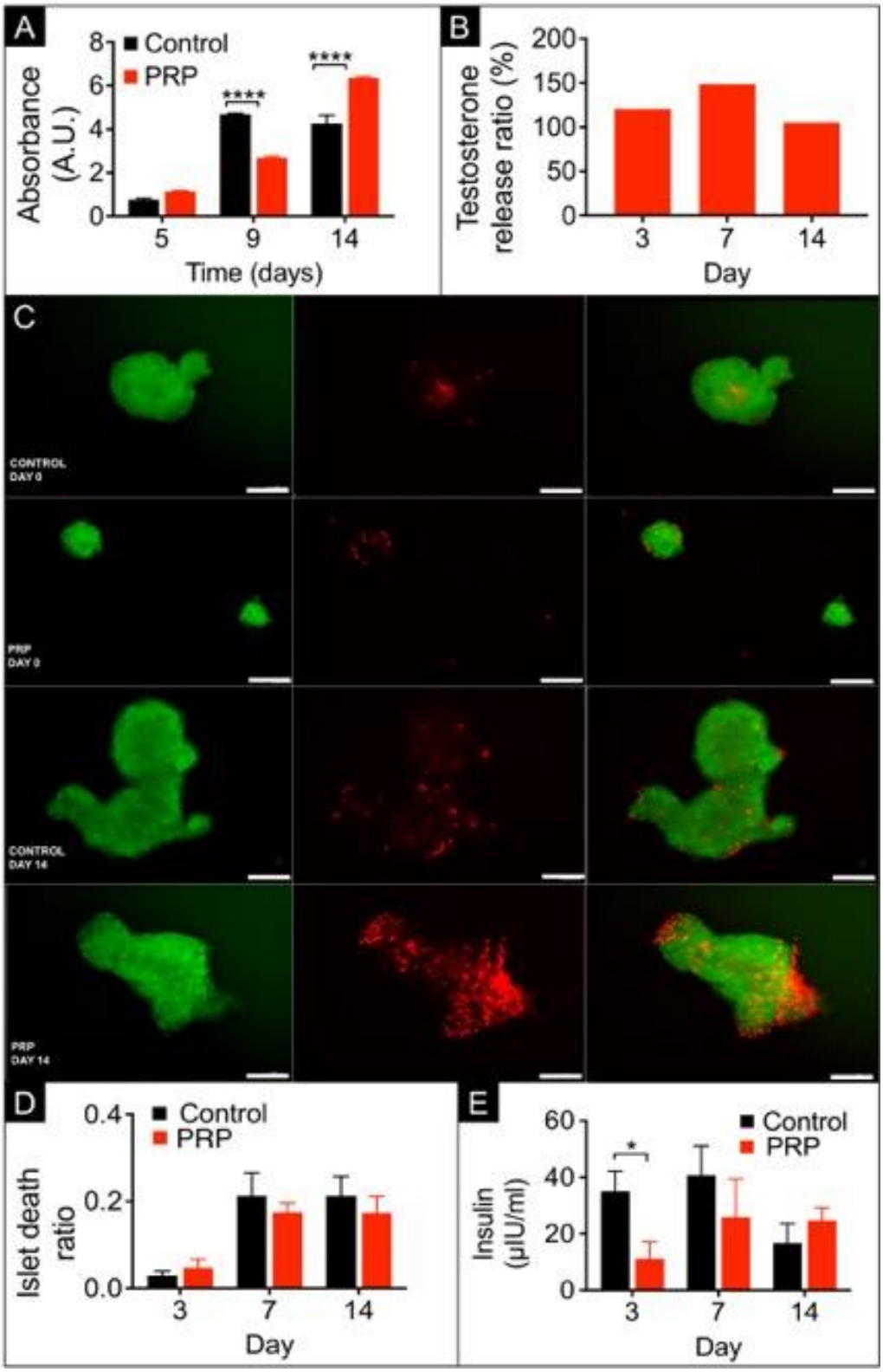

Figure 5.7: Leydig cell and human pancreatic islet culture. (A) Leydig cell viability on PRP hydrogel and (B) testosterone release over 14 days. (C) Fluorescein diacetate and propidium iodide analysis of human islets in PRP and

control over 14 days (Scale bar represents 100 μm). (D) Islet death ration between PRP hydrogel and control group with (E) insulin release level.

Vascularization of PRP hydrogel

For initial assessment of the ability of PRP hydrogel to stimulate vascularization in vivo, we used a chick CAM model, which is an established, rapid, and cost effective assay to visualize and evaluate angiogenesis [324]. After placing PRP hydrogel samples onto the CAM (Fig. 5.8A), we monitored them for signs of vascularization using optical microscopy. Hydrogels appeared stable in morphology on day 1 and 3, on day 5, and clear signs of incorporation within the CAM were observed (Fig. 5.8B,C), suggestive of CAM vasculature infiltration into the gel (Fig. 5.8C). Hydrogel samples retrieved from the CAM on day 1, 3, and 5 confirmed the observation in vivo, with clear presence of vasculature penetration into the gel across the CAM (Fig. 5.8C). Next, to determine if PRP hydrogel could stimulate vasculature penetration through the NICHE's microchannels into the gel, PVP-PRP-coated NICHE containing PRP hydrogel within were overlaid onto the CAM (Fig. 5.8D). We observed signs of angiogenesis by day 3, with progressive vasculature formation by day 5 surrounding the PLA microchannels (Fig. 5.8D). Histological analysis of the explanted device showed endothelial cell infiltration into the hydrogel (Fig. 5.8E). Additional histological analysis of cross sections of the retrieved samples confirmed direct vessel connection of hydrogel with the CAM (Fig. 5.8F). To further validate our findings, we established an in vivo cell viability test on CAM. Luciferase-expressing Lewis lung carcinoma (LLC) cells were seeded either directly onto the CAM (positive control), or placed onto a layer of PRP hydrogel laid onto the CAM (Fig. 5.8G). Bioluminescence imaging analysis showed that both groups of cells were viable after 3 days on the CAM, while cells in PRP without CAM were not viable. This demonstrated that PRP hydrogel was rapidly vascularized providing support to the LLC cells to a similar extent to cells directly in contact with the CAM. In the negative control, cell seeded on PRP

hydrogel (Fig. 5.8G) in cell culture plates demonstrate loss of viability in absence of vascular tissue supplying cells with oxygenation and nutrients.

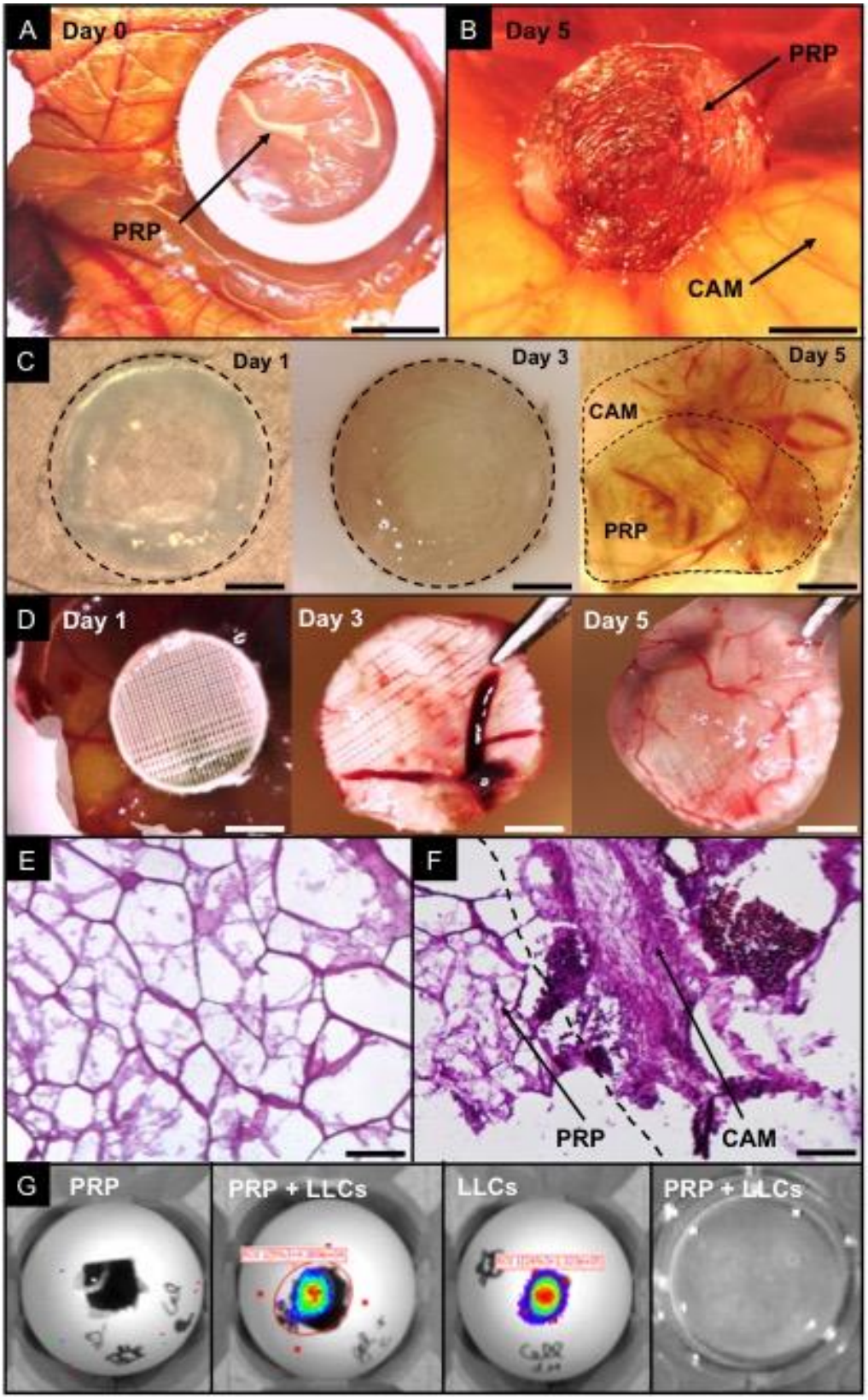

Figure 5.8: PRP hydrogel vascularization on CAM. (A) PRP hydrogel at day 1 and (B) day 5 (scale bar represents 4 mm). Optical microscopy images of (C)

harvested PRP and of (D) NICHEs on day 1, 3 and 5 (scale bar represents 4 mm). H&E images of (E) PRP hydrogel at 20x and (F) cross section showing intersection between PRP and CAM indicated by the dotted line (scale bar represents 200 µm). (G) IVIS analysis of PRP only on CAM, LLC cells only cultured on CAM, LLC cells + PRP hydrogel on CAM and LLC cells on PRP hydrogel in a well of a 24-well cell culture plate.

In vivo validation of NICHE

To investigate the function of our encapsulation system in vivo, we subcutaneously implanted sterile NICHEs filled with PRP-VEGF hydrogel in castrated Rag1-/- mice (n=10). VEGF was used as an additional stimulant for vessel formation. Rag1-/- mice were used because despite being immunocompromised, they maintain intact innate immunity and foreign body response, which is ideal for assessing the biocompatibility of the NICHE. NICHEs were implanted free of cells to achieve a pre-vascularized bed for the cell transplant. To establish the suitable time for Leydig cell transplantation, we harvested the devices from 2 mice each on weeks 2 and 4, to visualize and assess tissue growth and vascularization within the NICHE. At week 2, retrieved samples exclusively showed presence of hydrogel and low tissue and vasculature formation was observed. Therefore, histological images were difficult to obtain. In contrast, histological sections obtained from NICHEs retrieved on week 4 and stained with H&E and CD31 showed high levels of vascularization (Fig. 5.9A-F). While the subcutaneous environment is typically poorly vascularized, our data showed that VEGF-supplemented PRP hydrogel was able to induce vascularization in and around the NICHE. Immunofluorescent analysis of CD31 in histological sections from NICHEs implanted for 4 weeks (Fig. 8D) and week 14 (Fig. 5.9E,F) showed progressive vasculature network formation within the devices over time. Importantly, we did not observe immune infiltration, suggesting the biocompatibility of the NICHE. Picro siruis staining of tissues within the device further confirmed vascularized environment, with collagen formation inside of the NICHE (Fig. 5.9G-I).

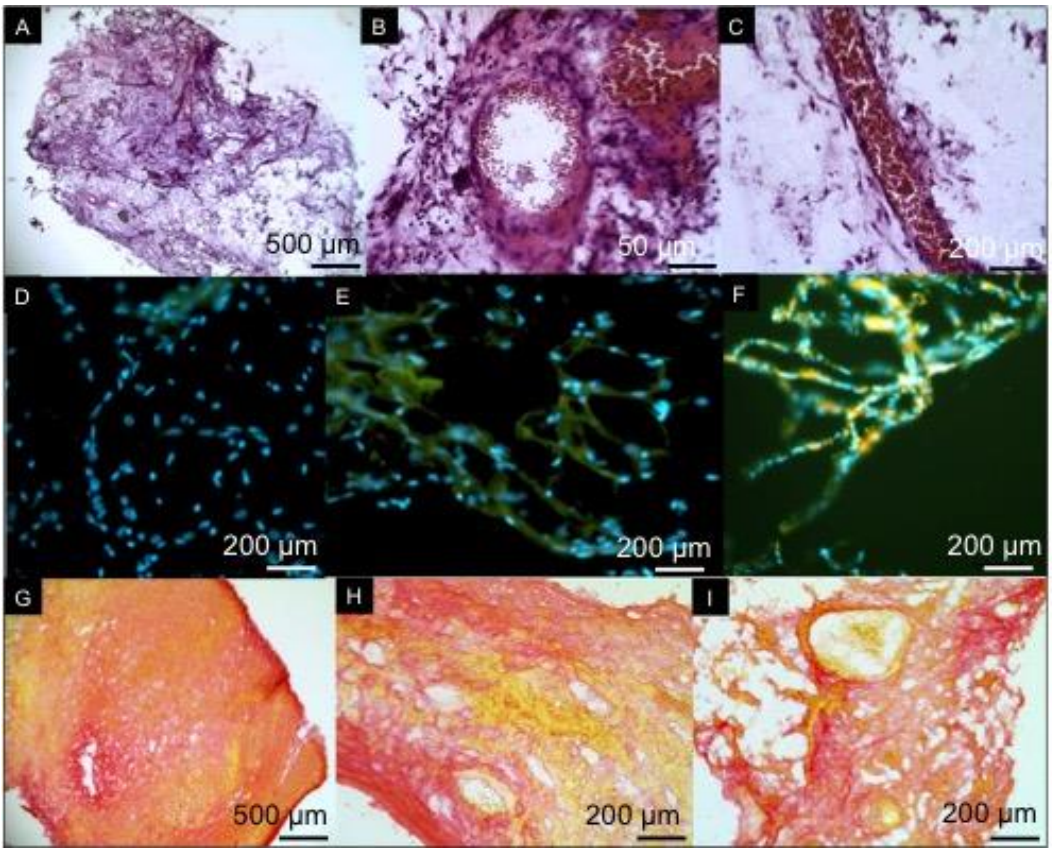

Figure 5.9: Vascularized tissue formation within the NICHE. (A) H&E staining of internal tissue retrieved on week 4 showing vessels penetration at 4x, (B,C) magnified cross section of vessels containing red blood cells at 20x. (D-F) CD31 (green) staining of blood vessels within the NICHE with DAPI counterstain (nuclei). (G-I) Picro sirius staining showing collagen I and II formation of blood vessels and surrounding tissues.

Upon determining that the implanted devices were vascularized within 4 weeks, we transplanted testosterone-secreting Leydig cells into the NICHE devices via transcutaneous injection through the NICHE loading port. Normal function of encapsulated Leydig cells over the 7-week transplantation was evaluated by weekly blood samples to measure testosterone levels using ELISA. ELISA analysis confirmed little to no testosterone up to 4 weeks prior to cell transplantation in the castrated mice. Throughout the 7 weeks of transplantation, testosterone levels ranged from 1.5 ng/ml to 2.2 ng/ml (Fig. 5.10A). Our results are comparable to physiological testosterone levels of non-castrated mice, which are around 1.2-1.5 ng/ml. Upon NICHE implantation, mouse total body weight stabilized and upon NICHE retrieval, increased to up to 28 g

(Fig. 5.10B). 7 weeks after cell transplantation, evaluation of the tissue within the device showed extensive vasculature formation (Fig. 5.10C-E). Further, immunohistochemical staining of HSD3b (a marker for Leydig cells), confirmed presence of cells within the vascularized tissue in the NICHE (Fig. 5.10F-H). Overall, this study demonstrated the capability of the NICHE to provide a pre-vascularized and physiological like environment conducive for the preservation of viability and functionality of encapsulated cells.

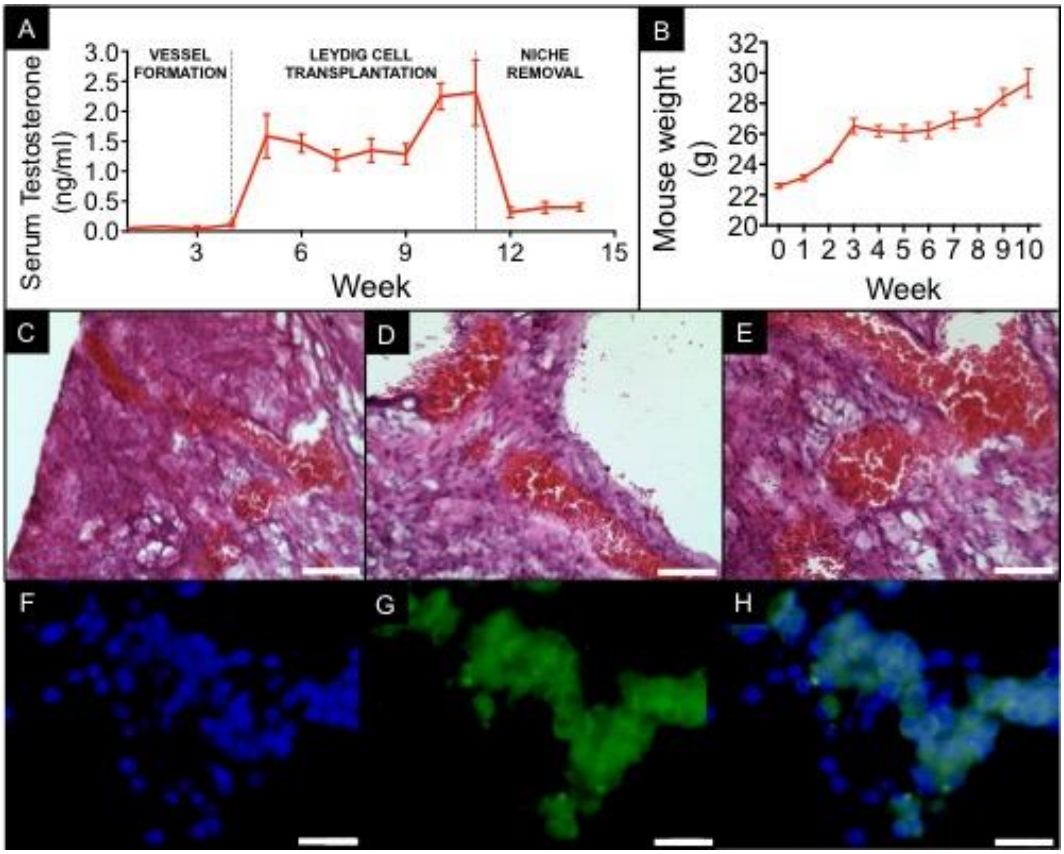

Figure 5.10: Leydig cell transplantation in NICHE. (A) serum testosterone levels and (B) body weight of castrated mice before device implantation, after cell transplantation and device retrieval. (C-E) H&E staining of vascularized tissue and (F-H) HSD3b staining within NICHE on week 14. (Scale bar represents 200 μm).

4. Discussion

Here we demonstrated that our PVP-PRP coating strategy provides a first line approach for stimulating rapid biointegration and vascularization of the structure. The flexibility of this coating technology permits for modification of thickness and porosity, and consequently control of degradation rate and growth factor release to tailor to different clinical needs. The same applies for the PRP-hydrogel matrix incorporated inside the NICHE. As demonstrated with the CAM assay and the rodent study, we were able to achieve a high level of vasculature density within the NICHE triggered by device coating and PRP-VEGF- combination hydrogel. In certain instances, as in the case of pancreatic islets transplantation, graft innervation to replicate the structure of islets in the pancreas would be beneficial [325,326]. For this, the growth factor and hydrogel cocktail in coating and hydrogel can be engineered to deliver local gradients of nerve growth factor (NGF) and glial cell line-derived neurotrophic factor (GDNF). Additionally, PRP hydrogels could contain perfluorocarbons to support oxygenation of cells to avoid acute hypoxia immediately post transplantation [327].

For the transplantation site, we chose the subcutaneous environment as it provides flexibility for the implantation of devices of various size and dimensions, has an adequate vascular network, and is easily accessible through minimally invasive surgical techniques. Several other sites, including the peritoneal cavity, have been investigated because of the higher density of blood vessels, and the capacity to accommodate large transplant volumes. However, invasive surgery procedures are required for graft insertion, retrieval, and refilling.

In the above mentioned in vivo study, at week 4, we were able to successfully execute transcutaneous cell loading in the pre-vascularized NICHE, using an external guide. No significant challenges were experienced during loading. Additional transcutaneous cell loading could

be performed for cell supplementation at need. Pediatric diabetic patients represent a clear example of individuals for whom the ability of replenishing and supplementing cells could present a clear advantage to address the changing physiological needs in terms of hormone secretion [328,329]. Post-transplant hypoxia and loss of cell function were not observed as cells became functional soon after transplantation, achieving plasma testosterone levels of approximately 1.3 ng/ml, which are in line with physiological levels for intact *Rag1-/-* mice [330]. Notably, substantially increased testosterone levels (2.3 ng/ml) were measured 5 weeks after cell transplantation. This increase suggests that Leydig cells required this timeframe to colonize the NICHE and form larger clusters as observed by immunohistochemical analysis. There was low level mononuclear cell (MNL) infiltration into areas within the NICHE device and no neutrophils in regions surrounding the device.

Biocompatibility of the adopted material and absence of adverse reaction to the transplanted cells were further demonstrated with the lack of fibrotic tissue surrounding the NICHE and no overgrowth of the surrounding tissue within the implant. These aspects are of additional advantage allowing for further refilling of the implant with additional cell dosage. However, if some tissues need to be removed to refill the NICHE with fresh cells, transcutaneous injection of clinically-approved dosage of collagenase may be used, a technique already adopted for treatment of several clinical conditions [331]. A limit of our model is the absence of a valid adaptive immune response in *Rag 1-/-,* which have limited a potential role of lymphocytes on the device biointegration. On the other side, this is still a good model to test foreign body response [332]. Further experiments are needed to prove a similar behavior of the implant in different animal models, but implants of similar materials were well-tolerated in other work from our group.

12 weeks after NICHE implantation, we demonstrated the ability to retrieve the implant via an endoscopic subcutaneous surgery. The procedure was well tolerated by the animals, which healed within 3 days post NICHE removal. The ability of retrieving transplanted cells is of particular

importance for treatments adopting stem cell-derived transplants, for which the long term fate is still uncertain and there is a risk for teratoma or cancerous tissue formation [211]. As expected, testosterone levels decreased substantially after device retrieval. However, as testosterone did not completely revert to basal level we cannot preclude the possibility of minor cell injection outside the device that could have occurred during cell loading. To optimize the loading protocol for future testing we are considering to change the positioning of the ports to the periphery of the NICHE. This modification would allow us to transplant cells via needles presenting multiple openings. In this way, cells would be simultaneously injected in different regions of the NICHE, reducing the volume released from each opening and consequently, the hydrostatic pressure on cells at injection.

Several encapsulation systems have been developed for cell transplantation. Among them, PEC-Encap™ of Viacyte, MAILPAN® of Defymed, βAir of Beta-O_2 Technologies and others have reached advance pre-clinical testing and clinical trials. A large percentage of these approaches rely on semipermeable polymeric membrane to act as a physical barrier to prevent immune rejection of the transplant in allo- and xeno transplantations. The major challenge of this approach is the limited supply of oxygen and nutrients to the transplanted cells due to the physical separation from the surrounding vasculature [333].

In contrast, our approach is fully focused on achieving proper vascularization of cells. In the context of autologous transplantation, the NICHE allows for direct contact of the transplanted cells with vascular network resulting in an adequate supplementation of oxygen and nutrients. In the case of allo- or xeno- transplantation, the NICHE can be modified to provide local delivery of immune suppressants. We are currently working on the second generation of NICHE, which implements a nanofluidic drug delivery system for sustained release of immunosuppressants *in situ [162,164]*. This novel approach could allow non-autologous cell transplantation while avoiding systemic administration of immunosuppressant drugs and related adverse effects.

Chapter 5

Summary and future prospective

In this thesis, the development and validation of the NICHE as a novel macroencapsulation system for autologous cell transplantation was detailed.

First the potential of adopting 3D printing technology to manufacture and customize the structure of the NICHE was demonstrated. As discussed in chapter 3, 3D printing allows for the design and fabrication of complex structures mimicking body structures and organs, which can be rapidly and inexpensively generated to be patient specific. Moreover, 3D additive manufacturing allows for straightforward scalability and customization of devices in terms of shape and size depending on the anatomical features of the implantation site and the volume of cells required to be encapsulated. These properties offer substantial advantages with respect to traditional manufacturing processes. In this work PLA was adopted, which showed to be biocompatible and suitable for long term applications in terms of polymeric degradation rate and mechanical properties.

Second, NICHE vascularization and engraftment was achieved subcutaneously using two immune compromised murine models. This investigation was of crucial importance as obtaining proper engraftment is determinant for the successful transplantation of cells and supporting their viability and function long-term. It was shown that transplanted cells were able to thrive thanks to a direct access to blood vessels and supply of oxygen and nutrients.

Third, two cells line (human pancreatic islets and Leydig cells) were used, to validate the NICHE capability to release insulin (up to 10 µIU/ml) and testosterone (up to 2.2 ng/ml), respectively. It is important to note that the presented NICHE was designed for the encapsulation of autologous cells only. In fact, it allows for the direct contact of the transplanted cells with blood vessels and did not provide any immunoisolating mean to protect cells from rejection.

The results achieved provide substantial evidence of the potential of the NICHE to promote the formation of an ideal environment for the transplanted cells, able to support their viability and functionality for long-term applications.

To enable heterologous cell transplantations, Grattoni's team is working on the development of an advanced version (NICHE-2) that includes a reservoir to house transplanted cells in a fully prevascularized environment (as presented in this thesis), and a drug reservoir for the constant and sustained release of immunosuppressive drugs *in situ* through a nanofluidic silicon membrane. Figures 5.11 A and B schematically show the differences between the two NICHE architectures. Both systems include microwells that promote a homogeneous distribution of cells in the device while avoiding clustering. Further, they prevent loss and dispersion of transplanted cells while allowing blood vessel penetration into the device, transcutaneous cell loading, easy retrieval, and addition or replenishment of cells at need.

In the case of NICHE-2, sustained drug release through a nanofluidic membrane, which is under investigation for the controlled release of immunosuppressants. The objective is to abrogate graft rejection by achieving effective concentration of immunosuppressants locally, while minimizing systemic drug exposure and associated adverse effects. Importantly, the system allows for transcutaneous drug replenishment once the drug reservoir is depleted. This allows for extending the immunosuppressive regimens for years without requiring surgical substitution of the implant. Notably, the membrane could be used for the local sustained delivery of immune suppression in cocktail with growth factors and nutrients to provide additional support to the transplanted cells.

In light of the promising results, the NICHE exemplifies a clinically translatable strategy for preserving viability and function of transplanted cells. This technological platform may offer exciting potential for clinical

adoption in relevant medical areas of diabetes, hypogonadism, hypothyroidism, cancer, and neurological diseases, among others.

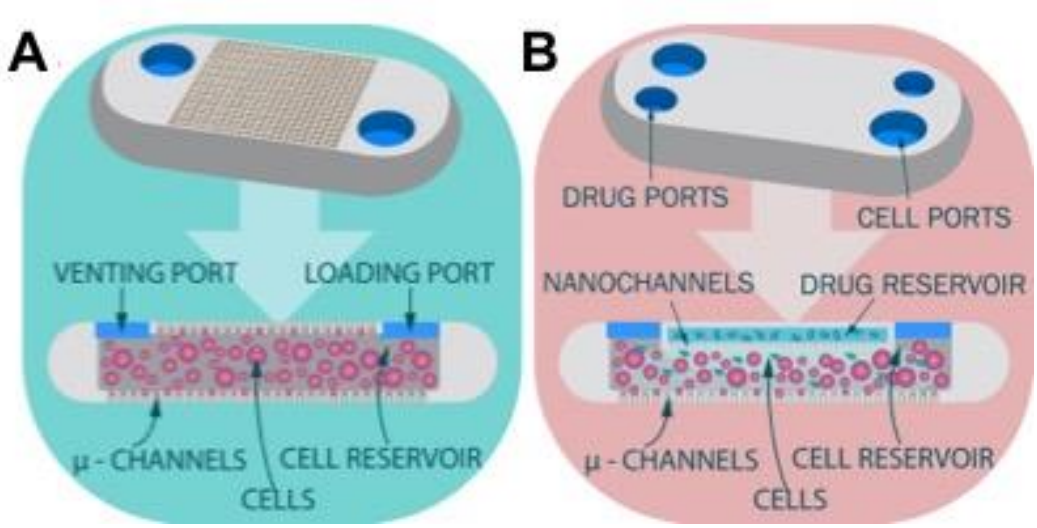

Figure 5.11 *(A) NICHE-1 encapsulation system consists of a reservoir that houses autologous insulin producing cells in a prevascularized environment. (B) Schematic of NICHE-2 composed by a fully vascularized cell reservoir for heterologous cells and a drug reservoir for the constant and sustained release of immunosuppressive drugs in situ through a nanofluidic silicon membrane.*

References

[1] Gene Therapy and Cell Therapy Defined | ASGCT - American Society of Gene & Cell Therapy, (n.d.). http://www.asgct.org/general-public/educational-resources/gene-therapy--and-cell-therapy-defined (accessed September 21, 2017).

[2] Cell-Based Therapeutics: The Next Pillar of Medicine | Science Translational Medicine, (n.d.). http://stm.sciencemag.org/content/5/179/179ps7 (accessed January 10, 2018).

[3] Z. Baimakhanov, K. Yamanouchi, Y. Sakai, M. Koike, A. Soyama, M. Hidaka, M. Takatsuki, F. Fujita, K. Kanetaka, T. Kuroki, S. Eguchi, Efficacy of Multilayered Hepatocyte Sheet Transplantation for Radiation-Induced Liver Damage and Partial Hepatectomy in a Rat Model, Cell Transplant. 25 (2016) 549–558. doi:10.3727/096368915X688669.

[4] A.M.J. Shapiro, M. Pokrywczynska, C. Ricordi, Clinical pancreatic islet transplantation, Nat. Rev. Endocrinol. 13 (2017) 268–277. doi:10.1038/nrendo.2016.178.

[5] W. Zhang, H. Ouyang, C.R. Dass, J. Xu, Current research on pharmacologic and regenerative therapies for osteoarthritis, Bone Res. 4 (2016) 15040. doi:10.1038/boneres.2015.40.

[6] E. Fastag, J. Varon, G. Sternbach, Richard Lower: the origins of blood transfusion, J. Emerg. Med. 44 (2013) 1146–1150. doi:10.1016/j.jemermed.2012.12.015.

[7] Ullmann E., Officielles Protokoll der kk Gesellschaft der Ärzte in Wien., Wien Klin Wochenschr 190215 707. (n.d.).

[8] W. Druml, C. Druml, Emerich Ullmann (1861-1937): not only a pioneer of kidney transplantation, J. Nephrol. 17 (2004) 461–466.

[9] A. Carrel, The transplantation of organs: a preliminary communication. 1905 [classical article], Yale J. Biol. Med. 74 (2001) 239–241.

[10] P. Niehans, Introduction to cellular therapy, Pageant Books, 1960.

[11] T.M. Chang, SEMIPERMEABLE MICROCAPSULES, Science. 146 (1964) 524–525.

[12] D.J. Han, D.E. Sutherland, Pancreas Transplantation, Gut Liver. 4 (2010) 450–465. doi:10.5009/gnl.2010.4.4.450.

[13] A. Frank, S. Deng, X. Huang, E. Velidedeoglu, Y.-S. Bae, C. Liu, P. Abt, R. Stephenson, M. Mohiuddin, T. Thambipillai, E. Markmann, M. Palanjian, M. Sellers, A. Naji, C.F. Barker, J.F. Markmann, Transplantation for Type I Diabetes, Ann. Surg. 240 (2004) 631–643. doi:10.1097/01.sla.0000140754.26575.2a.

[14] D.E.R. Sutherland, R.W.G. Gruessner, D.L. Dunn, A.J. Matas, A. Humar, R. Kandaswamy, S.M. Mauer, W.R. Kennedy, F.C. Goetz, R.P. Robertson, A.C. Gruessner, J.S. Najarian, Lessons Learned From More Than 1,000 Pancreas Transplants at a Single Institution, Ann. Surg. 233 (2001) 463–501.

[15] A.R. Pepper, B. Gala-Lopez, O. Ziff, A.J. Shapiro, Current status of clinical islet transplantation, World J. Transplant. 3 (2013) 48–53. doi:10.5500/wjt.v3.i4.48.

[16] Williams: St. Matthew - Google Scholar, (n.d.). https://scholar.google.com/scholar_lookup?title=Notes+on+diabetes+treated+with+extract+and+by+grafts+of+sheep%E2%80%99s+pancreas&author=Williams+P&publication_year=1894&journal=Br+Med+J&volume=2&pages=1303-304 (accessed September 21, 2017).

[17] J.S. Najarian, D.E. Sutherland, D. Baumgartner, B. Burke, J.J. Rynasiewicz, A.J. Matas, F.C. Goetz, Total or near total pancreatectomy and islet autotransplantation for treatment of chronic pancreatitis, Ann. Surg. 192 (1980) 526–542.

[18] D.W. Gray, G.L. Warnock, R. Sutton, M. Peters, P. McShane, P.J. Morris, Successful autotransplantation of isolated islets of Langerhans in the cynomolgus monkey, Br. J. Surg. 73 (1986) 850–853.

[19] A.G. Tzakis, C. Ricordi, R. Alejandro, Y. Zeng, J.J. Fung, S. Todo, A.J. Demetris, D.H. Mintz, T.E. Starzl, Pancreatic islet transplantation after upper abdominal exenteration and liver replacement, Lancet Lond. Engl. 336 (1990) 402–405.

[20] C. Ricordi, T.B. Strom, Clinical islet transplantation: advances and immunological challenges, Nat. Rev. Immunol. 4 (2004) 259–268. doi:10.1038/nri1332.

[21] A.M.J. Shapiro, J.R.T. Lakey, E.A. Ryan, G.S. Korbutt, E. Toth, G.L. Warnock, N.M. Kneteman, R.V. Rajotte, Islet Transplantation in Seven Patients with Type 1 Diabetes Mellitus Using a Glucocorticoid-Free Immunosuppressive Regimen, N. Engl. J. Med. 343 (2000) 230–238. doi:10.1056/NEJM200007273430401.

[22] D.C. Brennan, H.A. Kopetskie, P.H. Sayre, R. Alejandro, E. Cagliero, A.M.J. Shapiro, J.S. Goldstein, M.R. DesMarais, S. Booher, P.J. Bianchine, Long-Term Follow-Up of the Edmonton Protocol of Islet Transplantation in the United States, Am. J. Transplant. Off. J. Am. Soc. Transplant. Am. Soc. Transpl. Surg. 16 (2016) 509–517. doi:10.1111/ajt.13458.

[23] G. Orive, R.M. Hernández, A.R. Gascón, R. Calafiore, T.M.S. Chang, P. De Vos, G. Hortelano, D. Hunkeler, I. Lacík, A.M.J. Shapiro, J.L. Pedraz, Cell encapsulation: promise and progress, Nat. Med. 9 (2003) 104–107. doi:10.1038/nm0103-104.

[24] R.T. Prehn, J.M. Weaver, G.H. Algire, The diffusion-chamber technique applied to a study of the nature of homograft resistance, J. Natl. Cancer Inst. 15 (1954) 509–517.

[25] G.J. Lim, S. Zare, M.V. Dyke, A. Atala, Cell Microencapsulation, in: Ther. Appl. Cell Microencapsul., Springer, New York, NY, 2010: pp. 126–136. doi:10.1007/978-1-4419-5786-3_11.

[26] P. de Vos, H.A. Lazarjani, D. Poncelet, M.M. Faas, Polymers in cell encapsulation from an enveloped cell perspective, Adv. Drug Deliv. Rev. 67 (2014) 15–34. doi:10.1016/j.addr.2013.11.005.

[27] A. Abuchowski, PEGylated Bovine Carboxyhemoglobin (SANGUINATE^{TM}): Results of Clinical Safety Testing and Use in Patients, Adv. Exp. Med. Biol. 876 (2016) 461–467. doi:10.1007/978-1-4939-3023-4_58.

[28] F. Meng, G.H.M. Engbers, J. Feijen, Biodegradable polymersomes as a basis for artificial cells: encapsulation, release and targeting, J. Controlled Release. 101 (2005) 187–198. doi:10.1016/j.jconrel.2004.09.026.

[29] Z. Rong, M. Wang, Z. Hu, M. Stradner, S. Zhu, H. Kong, H. Yi, A. Goldrath, Y.-G. Yang, Y. Xu, X. Fu, An effective approach to prevent immune rejection of human ESC-derived allografts, Cell Stem Cell. 14 (2014) 121–130. doi:10.1016/j.stem.2013.11.014.

[30] C.-F. Lee, Y.-C. Lo, C.-H. Cheng, G.J. Furtmüller, B. Oh, V. Andrade-Oliveira, A.G. Thomas, C.E. Bowman, B.S. Slusher, M.J. Wolfgang, G. Brandacher, J.D. Powell, Preventing Allograft Rejection by Targeting Immune Metabolism, Cell Rep. 13 (2015) 760–770. doi:10.1016/j.celrep.2015.09.036.

[31] G. Orive, E. Santos, J.L. Pedraz, R.M. Hernández, Application of cell encapsulation for controlled delivery of biological therapeutics, Adv. Drug Deliv. Rev. 67 (2014) 3–14. doi:10.1016/j.addr.2013.07.009.

[32] A. Murua, A. Portero, G. Orive, R.M. Hernández, M. de Castro, J.L. Pedraz, Cell microencapsulation technology: towards clinical application, J. Control. Release Off. J. Control. Release Soc. 132 (2008) 76–83. doi:10.1016/j.jconrel.2008.08.010.

[33] A. Acarregui, A. Murua, J.L. Pedraz, G. Orive, R.M. Hernández, A perspective on bioactive cell microencapsulation, BioDrugs Clin. Immunother. Biopharm. Gene Ther. 26 (2012) 283–301. doi:10.2165/11632640-000000000-00000.

[34] G. Orive, R.M. Hernández, A. Rodríguez Gascón, R. Calafiore, T.M.S. Chang, P. de Vos, G. Hortelano, D. Hunkeler, I. Lacík, J.L. Pedraz, History, challenges and perspectives of cell microencapsulation, Trends Biotechnol. 22 (2004) 87–92.

[35] M. Farina, A. Ballerini, D.W. Fraga, E. Nicolov, M. Hogan, D. Demarchi, F. Scaglione, O.M. Sabek, P. Horner, U. Thekkedath, O.A. Gaber, A. Grattoni, 3D Printed Vascularized Device for Subcutaneous Transplantation of Human Islets, Biotechnol. J. (2017). doi:10.1002/biot.201700169.

[36] O.M. Sabek, M. Farina, D.W. Fraga, S. Afshar, A. Ballerini, C.S. Filgueira, U.R. Thekkedath, A. Grattoni, A.O. Gaber, Three-dimensional printed polymeric system to encapsulate human mesenchymal stem cells differentiated into islet-like insulin-producing aggregates for diabetes

treatment, J. Tissue Eng. 7 (2016) 2041731416638198. doi:10.1177/2041731416638198.

[37] O.M. Sabek, S. Ferrati, D.W. Fraga, J. Sih, E.V. Zabre, D.H. Fine, M. Ferrari, A.O. Gaber, A. Grattoni, Characterization of a nanogland for the autotransplantation of human pancreatic islets, Lab. Chip. 13 (2013) 3675–3688. doi:10.1039/c3lc50601k.

[38] D.F. Emerich, M.D. Lindner, S.R. Winn, E.Y. Chen, B.R. Frydel, J.H. Kordower, Implants of encapsulated human CNTF-producing fibroblasts prevent behavioral deficits and striatal degeneration in a rodent model of Huntington's disease, J. Neurosci. Off. J. Soc. Neurosci. 16 (1996) 5168–5181.

[39] Y. Uteza, J.-S. Rouillot, A. Kobetz, D. Marchant, S. Pecqueur, E. Arnaud, H. Prats, J. Honiger, J.-L. Dufier, M. Abitbol, M. Neuner-Jehle, Intravitreous transplantation of encapsulated fibroblasts secreting the human fibroblast growth factor 2 delays photoreceptor cell degeneration in Royal College of Surgeons rats, Proc. Natl. Acad. Sci. 96 (1999) 3126–3131. doi:10.1073/pnas.96.6.3126.

[40] C.A. Tobias, N.O. Dhoot, M.A. Wheatley, A. Tessler, M. Murray, I. Fischer, Grafting of Encapsulated BDNF-Producing Fibroblasts into the Injured Spinal Cord Without Immune Suppression in Adult Rats, J. Neurotrauma. 18 (2001) 287–301. doi:10.1089/08977150151070937.

[41] N.C. Hunt, R.M. Shelton, D.J. Henderson, L.M. Grover, Calcium-Alginate Hydrogel-Encapsulated Fibroblasts Provide Sustained Release of Vascular Endothelial Growth Factor, Tissue Eng. Part A. 19 (2012) 905–914. doi:10.1089/ten.tea.2012.0197.

[42] R. Bottino, M. Trucco, Use of genetically-engineered pig donors in islet transplantation, World J. Transplant. 5 (2015) 243–250. doi:10.5500/wjt.v5.i4.243.

[43] L.S. Gazda, J. Collins, A. Lovatt, R.W. Holdcraft, M.J. Morin, D. Galbraith, M. Graham, M.A. Laramore, C. Maclean, J. Black, E.W. Milne, D.G. Marthaler, H.V. Vinerean, M.M. Michalak, D. Hoffer, S. Richter, R.D. Hall, B.H. Smith, A comprehensive microbiological safety approach for agarose encapsulated porcine islets intended for clinical trials, Xenotransplantation. 23 (2016) 444–463. doi:10.1111/xen.12277.

[44] V. Delaune, T. Berney, S. Lacotte, C. Toso, Intraportal islet transplantation: the impact of the liver microenvironment, Transpl. Int. Off. J. Eur. Soc. Organ Transplant. 30 (2017) 227–238. doi:10.1111/tri.12919.

[45] B.L. Strand, A.E. Coron, G. Skjak-Braek, Current and Future Perspectives on Alginate Encapsulated Pancreatic Islet, Stem Cells Transl. Med. 6 (2017) 1053–1058. doi:10.1002/sctm.16-0116.

[46] D.V. Goeddel, D.G. Kleid, F. Bolivar, H.L. Heyneker, D.G. Yansura, R. Crea, T. Hirose, A. Kraszewski, K. Itakura, A.D. Riggs, Expression in Escherichia coli of chemically synthesized genes for human insulin, Proc. Natl. Acad. Sci. U. S. A. 76 (1979) 106–110.

[47] E. Piller Puicher, R. Tomanin, M. Salvalaio, A. Friso, G. Hortelano, O. Marin, M. Scarpa, Encapsulated engineered myoblasts can cure Hurler syndrome: preclinical experiments in the mouse model, Gene Ther. 19 (2012) 355–364. doi:10.1038/gt.2011.94.

[48] A. Lathuilière, S. Cosson, M.P. Lutolf, B.L. Schneider, P. Aebischer, A high-capacity cell macroencapsulation system supporting the long-term survival of genetically engineered allogeneic cells, Biomaterials. 35 (2014) 779–791. doi:10.1016/j.biomaterials.2013.09.071.

[49] A. Lathuilière, V. Laversenne, A. Astolfo, E. Kopetzki, H. Jacobsen, M. Stampanoni, B. Bohrmann, B.L. Schneider, P. Aebischer, A subcutaneous cellular implant for passive immunization against amyloid-β reduces brain amyloid and tau pathologies, Brain J. Neurol. 139 (2016) 1587–1604. doi:10.1093/brain/aww036.

[50] M. Costantini, S. Testa, P. Mozetic, A. Barbetta, C. Fuoco, E. Fornetti, F. Tamiro, S. Bernardini, J. Jaroszewicz, W. Święszkowski, M. Trombetta, L. Castagnoli, D. Seliktar, P. Garstecki, G. Cesareni, S. Cannata, A. Rainer, C. Gargioli, Microfluidic-enhanced 3D bioprinting of aligned myoblast-laden hydrogels leads to functionally organized myofibers in vitro and in vivo, Biomaterials. 131 (2017) 98–110. doi:10.1016/j.biomaterials.2017.03.026.

[51] Microfluidic Encapsulation of Human Mesenchymal Stem Cells for Articular Cartilage Tissue Regeneration - ACS Applied Materials & Interfaces (ACS Publications), (n.d.). http://pubs.acs.org/doi/abs/10.1021/acsami.7b00728?mi=aayia761&af=R&

AllField=nano&target=default&targetTab=std (accessed September 21, 2017).

[52] R.E. Vandenbroucke, E. Dejonckheere, P. Van Lint, D. Demeestere, E. Van Wonterghem, I. Vanlaere, L. Puimège, F. Van Hauwermeiren, R. De Rycke, C. Mc Guire, C. Campestre, C. López-Otin, P. Matthys, G. Leclercq, C. Libert, Matrix metalloprotease 8-dependent extracellular matrix cleavage at the blood-CSF barrier contributes to lethality during systemic inflammatory diseases, J. Neurosci. Off. J. Soc. Neurosci. 32 (2012) 9805–9816. doi:10.1523/JNEUROSCI.0967-12.2012.

[53] M. Brkic, S. Balusu, E. Van Wonterghem, N. Gorlé, I. Benilova, A. Kremer, I. Van Hove, L. Moons, B. De Strooper, S. Kanazir, C. Libert, R.E. Vandenbroucke, Amyloid β Oligomers Disrupt Blood-CSF Barrier Integrity by Activating Matrix Metalloproteinases, J. Neurosci. Off. J. Soc. Neurosci. 35 (2015) 12766–12778. doi:10.1523/JNEUROSCI.0006-15.2015.

[54] E.C.M. de Lange, Potential role of ABC transporters as a detoxification system at the blood-CSF barrier, Adv. Drug Deliv. Rev. 56 (2004) 1793–1809. doi:10.1016/j.addr.2004.07.009.

[55] Patent US20080119909 - Cell implantation to prevent and/or treat hearing loss - Google Patents, (n.d.). https://www.google.com/patents/US20080119909 (accessed September 21, 2017).

[56] S.J.M. Skinner, M.S. Geaney, P.L.J. Tan, R.K. Shepherd, L.N. Pettingill, J.K. Andrew, C. Thanos, D. Emerich, Cell implantation to prevent and/or treat hearing loss, US20080119909 A1, 2008. http://www.google.si/patents/US20080119909 (accessed January 10, 2018).

[57] A. Aliaghaei, H. Digaleh, F. Khodagholi, A. Ahmadiani, Encapsulated Choroid Plexus Epithelial Cells Actively Protect Against Intrahippocampal Aβ-induced Long-Term Memory Dysfunction; Upregulation of Effective Neurogenesis with the Abrogated Apoptosis and Neuroinflammation, J. Mol. Neurosci. MN. 56 (2015) 708–721. doi:10.1007/s12031-015-0492-y.

[58] C.G. Thanos, D.F. Emerich, B.E. Bintz, M. Goddard, J. Mills, R. Jensen, M. Lombardi, S. Hall, K. Boekelheide, Secreted products from the porcine

choroid plexus accelerate the healing of cutaneous wounds, Cell Transplant. 18 (2009) 1395–1409. doi:10.3727/096368909X12483162197402.

[59] C.V. Borlongan, C.G. Thanos, S.J.M. Skinner, M. Geaney, D.F. Emerich, Transplants of encapsulated rat choroid plexus cells exert neuroprotection in a rodent model of Huntington's disease, Cell Transplant. 16 (2008) 987–992.

[60] J.E. Lee, K.M. Taylor, R.H. Walanj, B.B.J. Lam, Treatment of cns disease with encapsulated inducible choroid plexus cells, US20160361365 A1, 2016. http://www.google.com/patents/US20160361365 (accessed September 21, 2017).

[61] Safety and clinical effects of NTCELL® [immunoprotected (alginate-encapsulated) porcine choroid plexus cells for xenotransplantation] in patients with Parkinson's disease (PD): 81 to 130 weeks follow-up, MDS Abstr. (n.d.). http://www.mdsabstracts.org/abstract/safety-and-clinical-effects-of-ntcell-immunoprotected-alginate-encapsulated-porcine-choroid-plexus-cells-for-xenotransplantation-in-patients-with-parkinsons-disease-pd-81-to-130-weeks-fol/ (accessed January 10, 2018).

[62] C.V. Borlongan, S.J.M. Skinner, M. Geaney, A.V. Vasconcellos, R.B. Elliott, D.F. Emerich, Intracerebral Transplantation of Porcine Choroid Plexus Provides Structural and Functional Neuroprotection in a Rodent Model of Stroke, Stroke. (2004). doi:10.1161/01.STR.0000138954.25825.0b.

[63] X.-M. Luo, H. Lin, W. Wang, M.S. Geaney, L. Law, S. Wynyard, S.B. Shaikh, H. Waldvogel, R.L.M. Faull, R.B. Elliott, S.J.M. Skinner, J.E. Lee, P.L.-J. Tan, Recovery of Neurological Functions in Non-Human Primate Model of Parkinson's Disease by Transplantation of Encapsulated Neonatal Porcine Choroid Plexus Cells, J. Park. Dis. 3 (2013) 275–291. doi:10.3233/JPD-130214.

[64] S.J. Kesseli, K.A. Smith, T.B. Gardner, Total Pancreatectomy with Islet Autologous Transplantation: The Cure for Chronic Pancreatitis?, Clin. Transl. Gastroenterol. 6 (2015) e73. doi:10.1038/ctg.2015.2.

[65] M.D. Li, H. Atkins, T. Bubela, The global landscape of stem cell clinical trials, Regen. Med. 9 (2014) 27–39. doi:10.2217/rme.13.80.

[66] A.J. Vegas, O. Veiseh, M. Gürtler, J.R. Millman, F.W. Pagliuca, A.R. Bader, J.C. Doloff, J. Li, M. Chen, K. Olejnik, H.H. Tam, S. Jhunjhunwala, E. Langan, S. Aresta-Dasilva, S. Gandham, J.J. McGarrigle, M.A. Bochenek, J. Hollister-Lock, J. Oberholzer, D.L. Greiner, G.C. Weir, D.A. Melton, R. Langer, D.G. Anderson, Long-term glycemic control using polymer-encapsulated human stem cell-derived beta cells in immune-competent mice, Nat. Med. 22 (2016) 306–311. doi:10.1038/nm.4030.

[67] F.W. Pagliuca, J.R. Millman, M. Gürtler, M. Segel, A. Van Dervort, J.H. Ryu, Q.P. Peterson, D. Greiner, D.A. Melton, Generation of Functional Human Pancreatic β Cells In Vitro, Cell. 159 (2014) 428–439. doi:10.1016/j.cell.2014.09.040.

[68] O. Karnieli, Y. Izhar-Prato, S. Bulvik, S. Efrat, Generation of insulin-producing cells from human bone marrow mesenchymal stem cells by genetic manipulation, Stem Cells Dayt. Ohio. 25 (2007) 2837–2844. doi:10.1634/stemcells.2007-0164.

[69] A.M. Madec, R. Mallone, G. Afonso, E. Abou Mrad, A. Mesnier, A. Eljaafari, C. Thivolet, Mesenchymal stem cells protect NOD mice from diabetes by inducing regulatory T cells, Diabetologia. 52 (2009) 1391–1399. doi:10.1007/s00125-009-1374-z.

[70] P. Fiorina, M. Jurewicz, A. Augello, A. Vergani, S. Dada, S. La Rosa, M. Selig, J. Godwin, K. Law, C. Placidi, R.N. Smith, C. Capella, S. Rodig, C.N. Adra, M. Atkinson, M.H. Sayegh, R. Abdi, Immunomodulatory function of bone marrow-derived mesenchymal stem cells in experimental autoimmune type 1 diabetes, J. Immunol. Baltim. Md 1950. 183 (2009) 993–1004. doi:10.4049/jimmunol.0900803.

[71] Y. Ding, D. Xu, G. Feng, A. Bushell, R.J. Muschel, K.J. Wood, Mesenchymal stem cells prevent the rejection of fully allogenic islet grafts by the immunosuppressive activity of matrix metalloproteinase-2 and -9, Diabetes. 58 (2009) 1797–1806. doi:10.2337/db09-0317.

[72] D.M. Berman, M.A. Willman, D. Han, G. Kleiner, N.M. Kenyon, O. Cabrera, J.A. Karl, R.W. Wiseman, D.H. O'Connor, A.M. Bartholomew, N.S. Kenyon, Mesenchymal stem cells enhance allogeneic islet engraftment in nonhuman primates, Diabetes. 59 (2010) 2558–2568. doi:10.2337/db10-0136.

[73] D. Lu, B. Chen, Z. Liang, W. Deng, Y. Jiang, S. Li, J. Xu, Q. Wu, Z. Zhang, B. Xie, S. Chen, Comparison of bone marrow mesenchymal stem cells with bone marrow-derived mononuclear cells for treatment of diabetic critical limb ischemia and foot ulcer: a double-blind, randomized, controlled trial, Diabetes Res. Clin. Pract. 92 (2011) 26–36. doi:10.1016/j.diabres.2010.12.010.

[74] R.H. Lee, M.J. Seo, R.L. Reger, J.L. Spees, A.A. Pulin, S.D. Olson, D.J. Prockop, Multipotent stromal cells from human marrow home to and promote repair of pancreatic islets and renal glomeruli in diabetic NOD/scid mice, Proc. Natl. Acad. Sci. U. S. A. 103 (2006) 17438–17443. doi:10.1073/pnas.0608249103.

[75] T.M. Kauer, J.-L. Figueiredo, S. Hingtgen, K. Shah, Encapsulated therapeutic stem cells implanted in the tumor resection cavity induce cell death in gliomas, Nat. Neurosci. 15 (2012) 197–204. doi:10.1038/nn.3019.

[76] N.-C. Cheng, W.-J. Lin, T.-Y. Ling, T.-H. Young, Sustained release of adipose-derived stem cells by thermosensitive chitosan/gelatin hydrogel for therapeutic angiogenesis, Acta Biomater. 51 (2017) 258–267. doi:10.1016/j.actbio.2017.01.060.

[77] Y. Xu, G. Balooch, M. Chiou, E. Bekerman, R.O. Ritchie, M.T. Longaker, Analysis of the material properties of early chondrogenic differentiated adipose-derived stromal cells (ASC) using an in vitro three-dimensional micromass culture system, Biochem. Biophys. Res. Commun. 359 (2007) 311–316. doi:10.1016/j.bbrc.2007.05.098.

[78] P. de Vos, A.F. Hamel, K. Tatarkiewicz, Considerations for successful transplantation of encapsulated pancreatic islets, Diabetologia. 45 (2002) 159–173. doi:10.1007/s00125-001-0729-x.

[79] Improving cell encapsulation through size control: Journal of Biomaterials Science, Polymer Edition: Vol 13, No 7, (n.d.). http://www.tandfonline.com/doi/abs/10.1163/156856202760197410 (accessed January 24, 2018).

[80] D. Chicheportiche, G. Reach, In vitro kinetics of insulin release by microencapsulated rat islets: effect of the size of the microcapsules, Diabetologia. 31 (1988) 54–57.

[81] Diabetes: Encapsulating the problem | Nature, (n.d.). https://www.nature.com/articles/540S60a (accessed January 24, 2018).

[82] A.A. Tomei, V. Manzoli, C.A. Fraker, J. Giraldo, D. Velluto, M. Najjar, A. Pileggi, R.D. Molano, C. Ricordi, C.L. Stabler, J.A. Hubbell, Device design and materials optimization of conformal coating for islets of Langerhans, Proc. Natl. Acad. Sci. U. S. A. 111 (2014) 10514–10519. doi:10.1073/pnas.1402216111.

[83] R. Calafiore, Microencapsulation for the cell therapy of type 1 diabetes mellitus: The interplay between common beliefs, prejudices and real progress, J. Diabetes Investig. (2017). doi:10.1111/jdi.12788.

[84] E.C. Opara, J.P. McQuilling, A.C. Farney, Microencapsulation of Pancreatic Islets for Use in a Bioartificial Pancreas, in: Organ Regen., Humana Press, Totowa, NJ, 2013: pp. 261–266. doi:10.1007/978-1-62703-363-3_21.

[85] Polyelectrolytes for cell encapsulation - ScienceDirect, (n.d.). http://www.sciencedirect.com/science/article/pii/S1359029405000270 (accessed January 10, 2018).

[86] A. Renken, D. Hunkeler, Polyvinylamine-based capsules: A mechanistic study of the formation using alginate and cellulose sulphate, J. Microencapsul. 24 (2007) 323–336. doi:10.1080/02652040601162350.

[87] K.K. Hall, K.M. Gattás-Asfura, C.L. Stabler, Microencapsulation of islets within alginate/poly(ethylene glycol) gels cross-linked via Staudinger ligation, Acta Biomater. 7 (2011) 614–624. doi:10.1016/j.actbio.2010.07.016.

[88] S.M. Luna, M.E. Gomes, J.F. Mano, R.L. Reis, Development of a Novel Cell Encapsulation System Based on Natural Origin Polymers for Tissue Engineering Applications, J. Bioact. Compat. Polym. 25 (2010) 341–359. doi:10.1177/0883911510372173.

[89] R. Krishnan, M. Alexander, L. Robles, C.E. Foster 3rd, J.R.T. Lakey, Islet and Stem Cell Encapsulation for Clinical Transplantation, Rev. Diabet. Stud. RDS. 11 (2014) 84–101. doi:10.1900/RDS.2014.11.84.

[90] P. Juárez, G. Alberto, M. Spasojevic, M.M. Faas, P. de Vos, Immunological and Technical Considerations in Application of Alginate-Based

Microencapsulation Systems, Front. Bioeng. Biotechnol. 2 (2014). doi:10.3389/fbioe.2014.00026.

[91] S.V. Bhujbal, B. de Haan, S.P. Niclou, P. de Vos, A novel multilayer immunoisolating encapsulation system overcoming protrusion of cells, Sci. Rep. 4 (2014) 6856. doi:10.1038/srep06856.

[92] J.L. Wilson, M.A. Najia, R. Saeed, T.C. McDevitt, Alginate encapsulation parameters influence the differentiation of microencapsulated embryonic stem cell aggregates, Biotechnol. Bioeng. 111 (2014) 618–631. doi:10.1002/bit.25121.

[93] T. Desai, L.D. Shea, Advances in islet encapsulation technologies, Nat. Rev. Drug Discov. 16 (2017) 338–350. doi:10.1038/nrd.2016.232.

[94] U. Barkai, A. Rotem, P. de Vos, Survival of encapsulated islets: More than a membrane story, World J. Transplant. 6 (2016) 69–90. doi:10.5500/wjt.v6.i1.69.

[95] C.J. Young, L.A. Poole-Warren, P.J. Martens, Combining submerged electrospray and UV photopolymerization for production of synthetic hydrogel microspheres for cell encapsulation, Biotechnol. Bioeng. 109 (2012) 1561–1570. doi:10.1002/bit.24430.

[96] H.-F. Lu, E.D. Targonsky, M.B. Wheeler, Y.-L. Cheng, Thermally induced gelable polymer networks for living cell encapsulation, Biotechnol. Bioeng. 96 (2007) 146–155. doi:10.1002/bit.21121.

[97] R.M. Olabisi, Cell microencapsulation with synthetic polymers, J. Biomed. Mater. Res. A. 103 (2015) 846–859. doi:10.1002/jbm.a.35205.

[98] Safety and Efficacy of PEG-Encapsulated Islet Allografts Implanted in Type I Diabetic Recipients - Full Text View - ClinicalTrials.gov, (n.d.). https://clinicaltrials.gov/ct2/show/NCT00260234 (accessed January 24, 2018).

[99] L.M. Weber, K.S. Anseth, Hydrogel encapsulation environments functionalized with extracellular matrix interactions increase islet insulin secretion, Matrix Biol. J. Int. Soc. Matrix Biol. 27 (2008) 667–673. doi:10.1016/j.matbio.2008.08.001.

[100] L. Gasperini, J.F. Mano, R.L. Reis, Natural polymers for the microencapsulation of cells, J. R. Soc. Interface. 11 (2014). doi:10.1098/rsif.2014.0817.

[101] X.T. Fu, S.M. Kim, Agarase: Review of Major Sources, Categories, Purification Method, Enzyme Characteristics and Applications, Mar. Drugs. 8 (2010) 200–218. doi:10.3390/md8010200.

[102] E.B. Hunziker, Articular cartilage repair: basic science and clinical progress. A review of the current status and prospects, Osteoarthritis Cartilage. 10 (2002) 432–463. doi:10.1053/joca.2002.0801.

[103] B. Salmons, E. Maria Brandtner, J. Dangerfield, W. Günzburg, Encapsulation of Insulin Producing Cells for Diabetes Treatment Using Alginate and Cellulose Sulphate as Bioencapsulation Polymers, Diabetes Res. Treat. 1 (2014) 1–7. doi:10.14437/DRTOA-1-102.

[104] biopharma-reporter.com, Cell-in-a-Box: PharmaCyte seeks FDA advice for inoperable cancer trial, Biopharma-Reportercom. (n.d.). https://www.biopharma-reporter.com/Article/2017/01/06/Cell-in-a-Box-PharmaCyte-seeks-FDA-advice-for-inoper-cancer-trial (accessed January 10, 2018).

[105] M. Löhr, Z.T. Bago, H. Bergmeister, M. Ceijna, M. Freund, W. Gelbmann, W.H. Günzburg, R. Jesnowski, J. Hain, K. Hauenstein, W. Henninger, A. Hoffmeyer, P. Karle, J.C. Kröger, G. Kundt, S. Liebe, U. Losert, P. Müller, A. Probst, K. Püschel, M. Renner, R. Renz, R. Saller, B. Salmons, I. Walter, Cell therapy using microencapsulated 293 cells transfected with a gene construct expressing CYP2B1, an ifosfamide converting enzyme, instilled intra-arterially in patients with advanced-stage pancreatic carcinoma: a phase I/II study, J. Mol. Med. Berl. Ger. 77 (1999) 393–398.

[106] M. Löhr, A. Hoffmeyer, J. Kröger, M. Freund, J. Hain, A. Holle, P. Karle, W.T. Knöfel, S. Liebe, P. Müller, H. Nizze, M. Renner, R.M. Saller, T. Wagner, K. Hauenstein, W.H. Günzburg, B. Salmons, Microencapsulated cell-mediated treatment of inoperable pancreatic carcinoma, Lancet Lond. Engl. 357 (2001) 1591–1592.

[107] M. Löhr, J.-C. Kröger, A. Hoffmeyer, M. Freund, J. Hain, A. Holle, W. Knoefel, S. Liebe, H. Nizze, M. Renner, R. Saller, P. Müller, T. Wagner, K. Hauenstein, B. Salmons, W. Günzburg, Safety, feasibility and clinical benefit of localized chemotherapy using microencapsulated cells for inoperable pancreatic carcinoma in a phase I/II trial Research Article, Cancer Ther. 1 (2003) 121–131.

[108] B. Salmons, M. Löhr, W.H. Günzburg, Treatment of inoperable pancreatic carcinoma using a cell-based local chemotherapy: results of a phase I/II clinical trial, J. Gastroenterol. 38 Suppl 15 (2003) 78–84.

[109] S. Vériter, J. Mergen, R.-M. Goebbels, N. Aouassar, C. Grégoire, B. Jordan, P. Levêque, B. Gallez, P. Gianello, D. Dufrane, In vivo selection of biocompatible alginates for islet encapsulation and subcutaneous transplantation, Tissue Eng. Part A. 16 (2010) 1503–1513. doi:10.1089/ten.TEA.2009.0286.

[110] P.O. Carlsson, F. Palm, A. Andersson, P. Liss, Markedly decreased oxygen tension in transplanted rat pancreatic islets irrespective of the implantation site, Diabetes. 50 (2001) 489–495.

[111] K.E. Dionne, C.K. Colton, M.L. Yarmush, Effect of hypoxia on insulin secretion by isolated rat and canine islets of Langerhans, Diabetes. 42 (1993) 12–21.

[112] Y. Sato, H. Endo, H. Okuyama, T. Takeda, H. Iwahashi, A. Imagawa, K. Yamagata, I. Shimomura, M. Inoue, Cellular Hypoxia of Pancreatic β-Cells Due to High Levels of Oxygen Consumption for Insulin Secretion in Vitro, J. Biol. Chem. 286 (2011) 12524–12532. doi:10.1074/jbc.M110.194738.

[113] K. Bloch, E. Papismedov, K. Yavriyants, M. Vorobeychik, S. Beer, P. Vardi, Photosynthetic oxygen generator for bioartificial pancreas, Tissue Eng. 12 (2006) 337–344. doi:10.1089/ten.2006.12.337.

[114] C.E. Nyitray, R. Chang, G. Faleo, K.D. Lance, D.A. Bernards, Q. Tang, T.A. Desai, Polycaprolactone Thin-Film Micro- and Nanoporous Cell-Encapsulation Devices, ACS Nano. 9 (2015) 5675–5682. doi:10.1021/acsnano.5b00679.

[115] J.H. Brauker, V.E. Carr-Brendel, L.A. Martinson, J. Crudele, W.D. Johnston, R.C. Johnson, Neovascularization of synthetic membranes directed by membrane microarchitecture, J. Biomed. Mater. Res. 29 (1995) 1517–1524. doi:10.1002/jbm.820291208.

[116] M. Mitsuo, K. Inoue, I. Nakai, T. Oda, Y. Gu, S. Shinohara, M. Kogire, T. Fujisato, S. Maetani, Y. Ikada, Efficacy of mesh reinforced polyvinylalcohol tube as a novel device for bioartificial pancreas: a functional study of rat islets in vivo, Transplant. Proc. 24 (1992) 2939–2940.

[117] K.K. Papas, E.S. Avgoustiniatos, T.M. Suszynski, Effect of oxygen supply on the size of implantable islet-containing encapsulation devices, Panminerva Med. 58 (2016) 72–77.

[118] T.M. Suszynski, E.S. Avgoustiniatos, K.K. Papas, Intraportal Islet Oxygenation, J. Diabetes Sci. Technol. 8 (2014) 575–580. doi:10.1177/1932296814525827.

[119] A.H. Zisch, M.P. Lutolf, M. Ehrbar, G.P. Raeber, S.C. Rizzi, N. Davies, H. Schmökel, D. Bezuidenhout, V. Djonov, P. Zilla, J.A. Hubbell, Cell-demanded release of VEGF from synthetic, biointeractive cell ingrowth matrices for vascularized tissue growth, FASEB J. Off. Publ. Fed. Am. Soc. Exp. Biol. 17 (2003) 2260–2262. doi:10.1096/fj.02-1041fje.

[120] A. Kerby, E.S. Jones, P.M. Jones, A.J. King, Co-transplantation of islets with mesenchymal stem cells in microcapsules demonstrates graft outcome can be improved in an isolated-graft model of islet transplantation in mice, Cytotherapy. 15 (2013) 192–200. doi:10.1016/j.jcyt.2012.10.018.

[121] M. Ehrbar, V.G. Djonov, C. Schnell, S.A. Tschanz, G. Martiny-Baron, U. Schenk, J. Wood, P.H. Burri, J.A. Hubbell, A.H. Zisch, Cell-demanded liberation of VEGF121 from fibrin implants induces local and controlled blood vessel growth, Circ. Res. 94 (2004) 1124–1132. doi:10.1161/01.RES.0000126411.29641.08.

[122] B.L. Strand, L. Ryan, P.I. Veld, B. Kulseng, A.M. Rokstad, G. Skjåk-Bræk, T. Espevik, Poly-L-Lysine Induces Fibrosis on Alginate Microcapsules via the Induction of Cytokines, Cell Transplant. 10 (2001) 263–275. doi:10.3727/000000001783986800.

[123] J.J. Schmidt, J. Rowley, H.J. Kong, Hydrogels used for cell-based drug delivery, J. Biomed. Mater. Res. A. 87 (2008) 1113–1122. doi:10.1002/jbm.a.32287.

[124] Microcapsules and Nanoparticles in Medicine and Pharmacy - CRC Press Book, (n.d.). https://www.crcpress.com/Microcapsules-and-Nanoparticles-in-Medicine-and-Pharmacy/Donbrow/p/book/9780849369865 (accessed January 10, 2018).

[125] M. Qi, Transplantation of Encapsulated Pancreatic Islets as a Treatment for Patients with Type 1 Diabetes Mellitus, Adv. Med. (2014). doi:10.1155/2014/429710.

[126] B. Blum, N. Benvenisty, The tumorigenicity of human embryonic stem cells, Adv. Cancer Res. 100 (2008) 133–158. doi:10.1016/S0065-230X(08)00005-5.

[127] B.P. Barnett, D.L. Kraitchman, C. Lauzon, C.A. Magee, P. Walczak, W.D. Gilson, A. Arepally, J.W.M. Bulte, Radiopaque Alginate Microcapsules for X-ray Visualization and Immunoprotection of Cellular Therapeutics, Mol. Pharm. 3 (2006) 531–538. doi:10.1021/mp060056l.

[128] H. Iwata, T. Takagi, H. Amemiya, H. Shimizu, K. Yamashita, K. Kobayashi, T. Akutsu, Agarose for a bioartificial pancreas, J. Biomed. Mater. Res. 26 (1992) 967–977. doi:10.1002/jbm.820260711.

[129] T. Kobayashi, Y. Aomatsu, H. Iwata, T. Kin, H. Kanehiro, M. Hisanaga, S. Ko, M. Nagao, Y. Nakajima, Indefinite islet protection from autoimmune destruction in nonobese diabetic mice by agarose microencapsulation without immunosuppression, Transplantation. 75 (2003) 619–625. doi:10.1097/01.TP.0000053749.36365.7E.

[130] P. Soon-Shiong, R.E. Heintz, N. Merideth, Q.X. Yao, Z. Yao, T. Zheng, M. Murphy, M.K. Moloney, M. Schmehl, M. Harris, Insulin independence in a type 1 diabetic patient after encapsulated islet transplantation, Lancet Lond. Engl. 343 (1994) 950–951.

[131] R.B. Elliott, L. Escobar, P.L.J. Tan, M. Muzina, S. Zwain, C. Buchanan, Live encapsulated porcine islets from a type 1 diabetic patient 9.5 yr after xenotransplantation, Xenotransplantation. 14 (2007) 157–161. doi:10.1111/j.1399-3089.2007.00384.x.

[132] H. Zhu, L. Lu, X. Liu, L. Yu, Y. Lyu, B. Wang, Treatment of diabetes with encapsulated pig islets: an update on current developments, J. Zhejiang Univ. Sci. B. 16 (2015) 329–343. doi:10.1631/jzus.B1400310.

[133] H.-T. Zhu, W.-L. Wang, L. Yu, B. Wang, Pig-Islet Xenotransplantation: Recent Progress and Current Perspectives, Front. Surg. 1 (2014). doi:10.3389/fsurg.2014.00007.

[134] T. Wang, J. Adcock, W. Kühtreiber, D. Qiang, K.J. Salleng, I. Trenary, P. Williams, Successful Allotransplantation of Encapsulated Islets in Pancreatectomized Canines for Diabetic Management Without the Use of Immunosuppression, Transplantation. 85 (2008) 331. doi:10.1097/TP.0b013e3181629c25.

[135] Encapsulife, (n.d.). http://www.encapsulife.org/technologies/publications/ (accessed January 11, 2018).

[136] D. Jacobs-Tulleneers-Thevissen, M. Chintinne, Z. Ling, P. Gillard, L. Schoonjans, G. Delvaux, B.L. Strand, F. Gorus, B. Keymeulen, D. Pipeleers, Beta Cell Therapy Consortium EU-FP7, Sustained function of alginate-encapsulated human islet cell implants in the peritoneal cavity of mice leading to a pilot study in a type 1 diabetic patient, Diabetologia. 56 (2013) 1605–1614. doi:10.1007/s00125-013-2906-0.

[137] D. Pipeleers, B. Keymeulen, Boost for Alginate Encapsulation in Beta Cell Transplantation, Trends Endocrinol. Metab. 27 (2016) 247–248. doi:10.1016/j.tem.2016.03.010.

[138] P. Montanucci, S. Terenzi, C. Santi, I. Pennoni, V. Bini, T. Pescara, G. Basta, R. Calafiore, Insights in Behavior of Variably Formulated Alginate-Based Microcapsules for Cell Transplantation, BioMed Res. Int. 2015 (2015). doi:10.1155/2015/965804.

[139] R. Calafiore, G. Basta, G. Luca, A. Lemmi, M.P. Montanucci, G. Calabrese, L. Racanicchi, F. Mancuso, P. Brunetti, Microencapsulated pancreatic islet allografts into nonimmunosuppressed patients with type 1 diabetes: first two cases, Diabetes Care. 29 (2006) 137–138.

[140] V. Manzoli, C. Villa, A.L. Bayer, L.C. Morales, R.D. Molano, Y. Torrente, C. Ricordi, J.A. Hubbell, A.A. Tomei, Immunoisolation of murine islet allografts in vascularized sites through conformal coating with polyethylene glycol, Am. J. Transplant. (n.d.) n/a-n/a. doi:10.1111/ajt.14547.

[141] C. Villa, V. Manzoli, M.M. Abreu, C.A. Verheyen, M. Seskin, M. Najjar, R.D. Molano, Y. Torrente, C. Ricordi, A.A. Tomei, Effects of Composition of Alginate-Polyethylene Glycol Microcapsules and Transplant Site on Encapsulated Islet Graft Outcomes in Mice, Transplantation. 101 (2017) 1025–1035. doi:10.1097/TP.0000000000001454.

[142] A.L. Hillberg, K. Kathirgamanathan, J.B.B. Lam, L.Y. Law, O. Garkavenko, R.B. Elliott, Improving alginate-poly-L-ornithine-alginate capsule biocompatibility through genipin crosslinking, J. Biomed. Mater. Res. B Appl. Biomater. 101 (2013) 258–268. doi:10.1002/jbm.b.32835.

[143] R.B. Elliott, L. Escobar, R. Calafiore, G. Basta, O. Garkavenko, A. Vasconcellos, C. Bambra, Transplantation of micro- and

macroencapsulated piglet islets into mice and monkeys, Transplant. Proc. 37 (2005) 466–469. doi:10.1016/j.transproceed.2004.12.198.

[144] Open-label Investigation of the Safety and Efficacy of DIABECELL in Patients With Type 1 Diabetes Mellitus - Full Text View - ClinicalTrials.gov, (n.d.). https://clinicaltrials.gov/ct2/show/NCT01736228 (accessed January 10, 2018).

[145] CXCL12 as Innovative Immune Isolating Chemokine for Microencapsulated Allo and Xeno-Transplantation in NHPs., ATC Abstr. (n.d.). http://atcmeetingabstracts.com/abstract/cxcl12-as-innovative-immune-isolating-chemokine-for-microencapsulated-allo-and-xeno-transplantation-in-nhps/ (accessed January 11, 2018).

[146] Vicapsys – VICAPSYN encapsulation, (n.d.). http://vicapsys.com/#approach (accessed January 24, 2018).

[147] D.W. Scharp, P. Marchetti, Encapsulated islets for diabetes therapy: history, current progress, and critical issues requiring solution, Adv. Drug Deliv. Rev. 67–68 (2014) 35–73. doi:10.1016/j.addr.2013.07.018.

[148] G. Orive, E. Santos, D. Poncelet, R.M. Hernández, J.L. Pedraz, L.U. Wahlberg, P. De Vos, D. Emerich, Cell encapsulation: technical and clinical advances, Trends Pharmacol. Sci. 36 (2015) 537–546. doi:10.1016/j.tips.2015.05.003.

[149] H. Komatsu, C. Cook, C.-H. Wang, L. Medrano, H. Lin, F. Kandeel, Y.-C. Tai, Y. Mullen, Oxygen environment and islet size are the primary limiting factors of isolated pancreatic islet survival, PLOS ONE. 12 (2017) e0183780. doi:10.1371/journal.pone.0183780.

[150] Human islet mass, morphology, and survival after cryopreservation using the Edmonton protocol: Islets: Vol 5, No 5, (n.d.). http://www.tandfonline.com/doi/full/10.4161/isl.26304 (accessed January 10, 2018).

[151] J.S. Bromberg, B. Kaplan, P.F. Halloran, R.P. Robertson, The Islet Transplant Experiment: Time for a Reassessment, Am. J. Transplant. 7 (2007) 2217–2218. doi:10.1111/j.1600-6143.2007.01957.x.

[152] N.V. Krishnamurthy, B. Gimi, Encapsulated cell grafts to treat cellular deficiencies and dysfunction, Crit. Rev. Biomed. Eng. 39 (2011) 473–491.

[153] N. Sakata, S. Sumi, G. Yoshimatsu, M. Goto, S. Egawa, M. Unno, Encapsulated islets transplantation: Past, present and future, World J. Gastrointest. Pathophysiol. 3 (2012) 19–26. doi:10.4291/wjgp.v3.i1.19.

[154] W. Kühtreiber, R.P. Lanza, W.L. Chick, Cell Encapsulation Technology and Therapeutics, Springer Science & Business Media, 2013.

[155] V. Vaithilingam, B.E. Tuch, Islet Transplantation and Encapsulation: An Update on Recent Developments, Rev. Diabet. Stud. RDS. 8 (2011) 51–67. doi:10.1900/RDS.2011.8.51.

[156] Principles of Tissue Engineering - 3rd Edition, (n.d.). https://www.elsevier.com/books/principles-of-tissue-engineering/lanza/978-0-12-370615-7 (accessed January 11, 2018).

[157] Collagenase Immobilized on Cellulose Acetate Membranes - Advances in Chemistry (ACS Publications), (n.d.). http://pubs.acs.org/doi/abs/10.1021/ba-1982-0199.ch030 (accessed January 24, 2018).

[158] C.G. Thanos, J.L. Gaglia, F.W. Pagliuca, Considerations for Successful Encapsulated β-Cell Therapy, in: Cell Ther., Springer, 2017: pp. 19–52.

[159] Silicon nanofilter with absolute pore size and high mechanical strength, (n.d.). https://www.spiedigitallibrary.org/conference-proceedings-of-spie/2593/1/Silicon-nanofilter-with-absolute-pore-size-and-high-mechanical-strength/10.1117/12.228643.short?SSO=1 (accessed January 24, 2018).

[160] A. Pimpinelli, M. Ferrari, A. Grattoni, Scaling and crossovers in molecular transport in nano-fluidic systems, Appl. Phys. Lett. 103 (2013) 113104. doi:10.1063/1.4819156.

[161] A. Grattoni, D. Fine, E. Zabre, A. Ziemys, J. Gill, Y. Mackeyev, M.A. Cheney, D.C. Danila, S. Hosali, L.J. Wilson, F. Hussain, M. Ferrari, Gated and Near-Surface Diffusion of Charged Fullerenes in Nanochannels, ACS Nano. 5 (2011) 9382–9391. doi:10.1021/nn2037863.

[162] G. Bruno, T. Geninatti, R.L. Hood, D. Fine, G. Scorrano, J. Schmulen, S. Hosali, M. Ferrari, A. Grattoni, Leveraging electrokinetics for the active control of dendritic fullerene-1 release across a nanochannel membrane, Nanoscale. 7 (2015) 5240–5248. doi:10.1039/c4nr06209d.

[163] A. Ziemys, A. Grattoni, D. Fine, F. Hussain, M. Ferrari, Confinement Effects on Monosaccharide Transport in Nanochannels, J. Phys. Chem. B. 114 (2010) 11117–11126. doi:10.1021/jp103519d.

[164] A. Grattoni, D. Fine, A. Ziemys, J. Gill, E. Zabre, R. Goodall, M. Ferrari, Nanochannel systems for personalized therapy and laboratory diagnostics, Curr. Pharm. Biotechnol. 11 (2010) 343–365.

[165] T.A. Desai, W.H. Chu, J.K. Tu, G.M. Beattie, A. Hayek, M. Ferrari, Microfabricated immunoisolating biocapsules, Biotechnol. Bioeng. 57 (1998) 118–120.

[166] W.H. Chu, T. Huen, J.K. Tu, M. Ferrari, Silicon-micromachined direct-pore filters for ultrafiltration, in: International Society for Optics and Photonics, 1997: pp. 111–123. doi:10.1117/12.269961.

[167] T.A. Desai, T. West, M. Cohen, T. Boiarski, A. Rampersaud, Nanoporous microsystems for islet cell replacement, Adv. Drug Deliv. Rev. 56 (2004) 1661–1673. doi:10.1016/j.addr.2003.11.006.

[168] T.A. Desai, D.J. Hansford, W.H. Chu, T. Huen, M. Ferrari, Investigating Islet Immunoisolation Parameters Using Microfabricated Membranes, MRS Online Proc. Libr. Arch. 530 (1998). doi:10.1557/PROC-530-7.

[169] Implantation of microfabricated immunoisolating biocapsules, (n.d.). https://www.spiedigitallibrary.org/conference-proceedings-of-spie/3258/0000/Implantation-of-microfabricated-immunoisolating-biocapsules/10.1117/12.304387.short (accessed January 24, 2018).

[170] K.E. La Flamme, K.C. Popat, L. Leoni, E. Markiewicz, T.J. La Tempa, B.B. Roman, C.A. Grimes, T.A. Desai, Biocompatibility of nanoporous alumina membranes for immunoisolation, Biomaterials. 28 (2007) 2638–2645. doi:10.1016/j.biomaterials.2007.02.010.

[171] G.H. Algire, J.M. Weaver, R.T. Prehn, Studies on Tissue Homotransplantation in Mice, Using Diffusion-Chamber Methods, Ann. N. Y. Acad. Sci. 64 (1957) 1009–1013. doi:10.1111/j.1749-6632.1957.tb52492.x.

[172] A. Mendelsohn, T. Desai, Inorganic Nanoporous Membranes for Immunoisolated Cell-Based Drug Delivery, Adv. Exp. Med. Biol. 670 (2010) 104–125.

[173] Tissue Response to Implants, in: Biomaterials, Springer, New York, NY, 2007: pp. 265–290. doi:10.1007/978-0-387-37880-0_10.

[174] J. Schweicher, C. Nyitray, T.A. Desai, Membranes to achieve immunoprotection of transplanted islets, Front. Biosci. Landmark Ed. 19 (2014) 49–76.

[175] J. Brauker, G.H. Frost, V. Dwarki, T. Nijjar, R. Chin, V. Carr-Brendel, C. Jasunas, D. Hodgett, W. Stone, L.K. Cohen, R.C. Johnson, Sustained Expression of High Levels of Human Factor IX from Human Cells Implanted within an Immunoisolation Device into Athymic Rodents, Hum. Gene Ther. 9 (1998) 879–888. doi:10.1089/hum.1998.9.6-879.

[176] T. Neufeld, B. Ludwig, U. Barkai, G.C. Weir, C.K. Colton, Y. Evron, M. Balyura, K. Yavriyants, B. Zimermann, D. Azarov, S. Maimon, N. Shabtay, T. Rozenshtein, D. Lorber, A. Steffen, U. Willenz, K. Bloch, P. Vardi, R. Taube, P. de Vos, E.C. Lewis, S.R. Bornstein, A. Rotem, The Efficacy of an Immunoisolating Membrane System for Islet Xenotransplantation in Minipigs, PLoS ONE. 8 (2013). doi:10.1371/journal.pone.0070150.

[177] K. Suzuki, S. Bonner-Weir, N. Trivedi, K.H. Yoon, J. Hollister-Lock, C.K. Colton, G.C. Weir, Function and survival of macroencapsulated syngeneic islets transplanted into streptozocin-diabetic mice, Transplantation. 66 (1998) 21–28.

[178] An Open Label, Pilot Investigation, to Assess the Safety and Efficacy of Transplantation of Macro-encapsulated Human Islets Within the Bioartificial Pancreas Beta-Air in Patients With Type 1 Diabetes Mellitus - Full Text View - ClinicalTrials.gov, (n.d.). https://clinicaltrials.gov/ct2/show/NCT02064309 (accessed January 10, 2018).

[179] R. Storrs, R. Dorian, S.R. King, J. Lakey, H. Rilo, Preclinical development of the Islet Sheet, Ann. N. Y. Acad. Sci. 944 (2001) 252–266.

[180] Function and Viability of Human Islets Encapsulated in Alginate Sheets: In Vitro and in Vivo Culture - ScienceDirect, (n.d.). http://www.sciencedirect.com/science/article/pii/S0041134511014114 (accessed January 10, 2018).

[181] B. Ludwig, A. Reichel, A. Steffen, B. Zimerman, A.V. Schally, N.L. Block, C.K. Colton, S. Ludwig, S. Kersting, E. Bonifacio, M. Solimena, Z.

Gendler, A. Rotem, U. Barkai, S.R. Bornstein, Transplantation of human islets without immunosuppression, Proc. Natl. Acad. Sci. 110 (2013) 19054–19058. doi:10.1073/pnas.1317561110.

[182] J. Yingling, ViaCyte Announces First Patients Implanted in Cohort 2 with Potentially Efficacious Dose of PEC-Direct Islet Cell Replacement Therapy, Viacyte Inc. (n.d.). http://viacyte.com/archives/press-releases/cohort2-and-biotech-showcase (accessed January 24, 2018).

[183] A.R. Pepper, R. Pawlick, B. Gala-Lopez, A. MacGillivary, D.M. Mazzuca, D.J.G. White, P.M. Toleikis, A.M.J. Shapiro, Diabetes Is Reversed in a Murine Model by Marginal Mass Syngeneic Islet Transplantation Using a Subcutaneous Cell Pouch Device, Transplantation. 99 (2015) 2294–2300. doi:10.1097/TP.0000000000000864.

[184] A novel technique for the transplantation of pancreatic islets within a vascularized device into the greater omentum to achieve insulin independence. - PubMed - NCBI, (n.d.). https://www.ncbi.nlm.nih.gov/pubmed/21683938 (accessed January 25, 2018).

[185] Sernova Corp - Press Room, (n.d.). http://www.sernova.com/press/ (accessed January 24, 2018).

[186] About Defymed, advanced therapies inspired for you, Defymed. (n.d.). https://www.defymed.com/about-us/ (accessed January 10, 2018).

[187] Cell Replacement Strategies Aimed at Reconstitution of the β-Cell Compartment in Type 1 Diabetes | Diabetes, (n.d.). http://diabetes.diabetesjournals.org/content/63/5/1433 (accessed January 24, 2018).

[188] D. Dufrane, P. Gianello, Macro- or microencapsulation of pig islets to cure type 1 diabetes, World J. Gastroenterol. WJG. 18 (2012) 6885–6893. doi:10.3748/wjg.v18.i47.6885.

[189] D. Dufrane, P.R.R. Gianello, J.E. Melvik, Alginate coated, collagen matrix cellular device, preparative methods, and uses thereof, WO2007144389 A3, 2008. http://google.ch/patents/WO2007144389A3 (accessed January 10, 2018).

[190] D. Dufrane, R.-M. Goebbels, P. Gianello, Alginate macroencapsulation of pig islets allows correction of streptozotocin-induced diabetes in primates

up to 6 months without immunosuppression, Transplantation. 90 (2010) 1054–1062. doi:10.1097/TP.0b013e3181f6e267.

[191] D. Dufrane, M. Mourad, E. Goffin, N. Aouassar, P. Gianello, B. Vandeleene, A Simple and Safe Clinical Procedure for Human Encapsulated Islet Transplantation in the Subcutaneous Tissue for Diabetes Treatment., in: TRANSPLANTATION, LIPPINCOTT WILLIAMS & WILKINS 530 WALNUT ST, PHILADELPHIA, PA 19106-3621 USA, 2013: pp. S43–S43.

[192] Safety and Efficacy Study of Encapsulated Human Islets Allotransplantation to Treat Type 1 Diabetes - Full Text View - ClinicalTrials.gov, (n.d.). https://clinicaltrials.gov/ct2/show/NCT00790257 (accessed January 10, 2018).

[193] S. Vériter, P. Gianello, Y. Igarashi, G. Beaurin, A. Ghyselinck, N. Aouassar, B. Jordan, B. Gallez, D. Dufrane, Improvement of subcutaneous bioartificial pancreas vascularization and function by coencapsulation of pig islets and mesenchymal stem cells in primates, Cell Transplant. 23 (2014) 1349–1364. doi:10.3727/096368913X663550.

[194] The Immune System: Islet Cell Encapsulation, (n.d.). https://www.diabetesresearch.org/islet-cell-encapsulation (accessed January 10, 2018).

[195] D.M. Berman, R.D. Molano, C. Fotino, U. Ulissi, J. Gimeno, A.J. Mendez, N.M. Kenyon, N.S. Kenyon, D.M. Andrews, C. Ricordi, A. Pileggi, Bioengineering the Endocrine Pancreas: Intraomental Islet Transplantation Within a Biologic Resorbable Scaffold, Diabetes. 65 (2016) 1350–1361. doi:10.2337/db15-1525.

[196] Allogeneic Islet Cells Transplanted Onto the Omentum - Full Text View - ClinicalTrials.gov, (n.d.). https://clinicaltrials.gov/ct2/show/NCT02213003 (accessed January 10, 2018).

[197] D.A. Baidal, C. Ricordi, D.M. Berman, A. Alvarez, N. Padilla, G. Ciancio, E. Linetsky, A. Pileggi, R. Alejandro, Bioengineering of an Intraabdominal Endocrine Pancreas, N. Engl. J. Med. 376 (2017) 1887–1889. doi:10.1056/NEJMc1613959.

[198] Platform & Pipeline, (n.d.). http://www.neurotechusa.com/platform---pipeline.html (accessed January 10, 2018).

[199] D.F. Emerich, C.G. Thanos, NT-501: an ophthalmic implant of polymer-encapsulated ciliary neurotrophic factor-producing cells, Curr. Opin. Mol. Ther. 10 (2008) 506–515.

[200] K. Kauper, C. McGovern, S. Sherman, P. Heatherton, R. Rapoza, P. Stabila, B. Dean, A. Lee, S. Borges, B. Bouchard, W. Tao, Two-year intraocular delivery of ciliary neurotrophic factor by encapsulated cell technology implants in patients with chronic retinal degenerative diseases, Invest. Ophthalmol. Vis. Sci. 53 (2012) 7484–7491. doi:10.1167/iovs.12-9970.

[201] D.G. BIRCH, R.G. WELEBER, J.L. DUNCAN, G.J. JAFFE, W. TAO, Randomized Trial of Ciliary Neurotrophic Factor Delivered by Encapsulated Cell Intraocular Implants for Retinitis Pigmentosa, Am. J. Ophthalmol. 156 (2013) 283-292.e1. doi:10.1016/j.ajo.2013.03.021.

[202] K. Zhang, J.J. Hopkins, J.S. Heier, D.G. Birch, L.S. Halperin, T.A. Albini, D.M. Brown, G.J. Jaffe, W. Tao, G.A. Williams, Ciliary neurotrophic factor delivered by encapsulated cell intraocular implants for treatment of geographic atrophy in age-related macular degeneration, Proc. Natl. Acad. Sci. U. S. A. 108 (2011) 6241–6245. doi:10.1073/pnas.1018987108.

[203] F.S.Y. Wong, K.K. Tsang, A.C.Y. Lo, Delivery of therapeutics to posterior eye segment: cell-encapsulating systems, Neural Regen. Res. 12 (2017) 576–577. doi:10.4103/1673-5374.205093.

[204] D. Dalkara, O. Goureau, K. Marazova, J.-A. Sahel, Let There Be Light: Gene and Cell Therapy for Blindness, Hum. Gene Ther. 27 (2016) 134–147. doi:10.1089/hum.2015.147.

[205] Extension Study of NT-501 Ciliary Neurotrophic Factor (CNTF) Implant for Macular Telangiectasia (MacTel) - Full Text View - ClinicalTrials.gov, (n.d.). https://clinicaltrials.gov/ct2/show/NCT03071965 (accessed January 10, 2018).

[206] Generation of Combination PDGF / VEGF-antagonist ECT devices | IOVS | ARVO Journals, (n.d.). http://iovs.arvojournals.org/article.aspx?articleid=2148056 (accessed January 10, 2018).

[207] L. Zhou, M. Miranda-Saksena, N.K. Saksena, Viruses and neurodegeneration, Virol. J. 10 (2013) 172. doi:10.1186/1743-422X-10-172.

[208] R.G. Thorne, W.H. Frey, Delivery of neurotrophic factors to the central nervous system: pharmacokinetic considerations, Clin. Pharmacokinet. 40 (2001) 907–946. doi:10.2165/00003088-200140120-00003.

[209] A.M. Weissmiller, C. Wu, Current advances in using neurotrophic factors to treat neurodegenerative disorders, Transl. Neurodegener. 1 (2012) 14. doi:10.1186/2047-9158-1-14.

[210] A. Aleynik, K.M. Gernavage, Y.S. Mourad, L.S. Sherman, K. Liu, Y.A. Gubenko, P. Rameshwar, Stem cell delivery of therapies for brain disorders, Clin. Transl. Med. 3 (2014) 24. doi:10.1186/2001-1326-3-24.

[211] A. Lathuilière, N. Mach, B.L. Schneider, Encapsulated Cellular Implants for Recombinant Protein Delivery and Therapeutic Modulation of the Immune System, Int. J. Mol. Sci. 16 (2015) 10578–10600. doi:10.3390/ijms160510578.

[212] F.S.Y. Wong, B.P. Chan, A.C.Y. Lo, Carriers in Cell-Based Therapies for Neurological Disorders, Int. J. Mol. Sci. 15 (2014) 10669–10723. doi:10.3390/ijms150610669.

[213] F.T. Gentile, E.J. Doherty, D.H. Rein, M.S. Shoichet, S.R. Winn, Polymer science for macroencapsulation of cells for central nervous system transplantation, React. Polym. 25 (1995) 207–227. doi:10.1016/0923-1137(94)00097-O.

[214] Y. Miyoshi, I. Date, T. Ono, T. Imaoka, S. Asari, T. Ohmoto, H. Iwata, [Encapsulated dopamine-secreting cells transplanted into the brain: a possible therapy for Parkinson's disease], No Shinkei Geka. 24 (1996) 35–39.

[215] A. Fisher, M. Memo, F. Stocchi, I. Hanin, Advances in Alzheimer's and Parkinson's Disease: Insights, Progress, and Perspectives, Springer Science & Business Media, 2007.

[216] H. Yoshida, I. Date, T. Shingo, K. Fujiwara, K. Kobayashi, Y. Miyoshi, T. Ohmoto, Stereotactic transplantation of a dopamine-producing capsule into the striatum for treatment of Parkinson disease: a preclinical primate study, J. Neurosurg. 98 (2003) 874–881. doi:10.3171/jns.2003.98.4.0874.

[217] M.J. Bourque, L.E. Trudeau, GDNF enhances the synaptic efficacy of dopaminergic neurons in culture, Eur. J. Neurosci. 12 (2000) 3172–3180.

[218] F. Yang, L. Feng, F. Zheng, S.W. Johnson, J. Du, L. Shen, C. Wu, B. Lu, GDNF acutely modulates excitability and A-type K^+ channels in midbrain dopaminergic neurons, Nat. Neurosci. 4 (2001) 1071. doi:10.1038/nn734.

[219] J.L. Tseng, E.E. Baetge, A.D. Zurn, P. Aebischer, GDNF reduces drug-induced rotational behavior after medial forebrain bundle transection by a mechanism not involving striatal dopamine, J. Neurosci. Off. J. Soc. Neurosci. 17 (1997) 325–333.

[220] N.S. Templeton, Gene and Cell Therapy: Therapeutic Mechanisms and Strategies, Third Edition, CRC Press, 2008.

[221] C.D. Davis, P.R. Sanberg, Cell Therapy, Stem Cells and Brain Repair, Springer Science & Business Media, 2007.

[222] P. Carmillo, L. Dagø, E.S. Day, D.S. Worley, A. Rossomando, L. Walus, O. Orozco, C. Buckley, S. Miller, A. Tse, R.L. Cate, C. Rosenblad, D.W.Y. Sah, M. Grønborg, A. Whitty, Glial Cell Line-Derived Neurotrophic Factor (GDNF) Receptor α-1 (GFRα1) Is Highly Selective for GDNF versus Artemin, Biochemistry (Mosc.). 44 (2005) 2545–2554. doi:10.1021/bi049247p.

[223] K.K. Jain, K.K. Jain, A Special Report on Gene Therapy, John Wiley & Sons, 2000.

[224] O. Lindvall, L.U. Wahlberg, Encapsulated cell biodelivery of GDNF: A novel clinical strategy for neuroprotection and neuroregeneration in Parkinson's disease?, Exp. Neurol. 209 (2008) 82–88. doi:10.1016/j.expneurol.2007.08.019.

[225] L. Wahlberg, Partnering Program, (n.d.). https://www.michaeljfox.org/files/accelerate/participants/NSGene.pdf.

[226] D.F. Emerich, G. Orive, C. Thanos, J. Tornoe, L.U. Wahlberg, Encapsulated cell therapy for neurodegenerative diseases: From promise to product, Adv. Drug Deliv. Rev. 67–68 (2014) 131–141. doi:10.1016/j.addr.2013.07.008.

[227] J.L. Cummings, R.S. Isaacson, F.A. Schmitt, D.M. Velting, A practical algorithm for managing Alzheimer's disease: what, when, and why?, Ann. Clin. Transl. Neurol. 2 (2015) 307–323. doi:10.1002/acn3.166.

[228] S.R. Winn, M.D. Lindner, A. Lee, G. Haggett, J.M. Francis, D.F. Emerich, Polymer-Encapsulated Genetically Modified Cells Continue to Secrete Human Nerve Growth Factor for over One Year in Rat Ventricles: Behavioral and Anatomical Consequences, Exp. Neurol. 140 (1996) 126–138. doi:10.1006/exnr.1996.0123.

[229] D.F. Emerich, S.R. Winn, J. Harper, J.P. Hammang, E.E. Baetge, J.H. Kordower, Implants of polymer-encapsulated human NGF-secreting cells in the nonhuman primate: rescue and sprouting of degenerating cholinergic basal forebrain neurons, J. Comp. Neurol. 349 (1994) 148–164. doi:10.1002/cne.903490110.

[230] T.E. Golde, L.S. Schneider, E.H. Koo, Anti-Aβ therapeutics in Alzheimer's disease: The Need for a Paradigm Shift, Neuron. 69 (2011) 203–213. doi:10.1016/j.neuron.2011.01.002.

[231] C.H. van Dyck, Anti-Amyloid-β Monoclonal Antibodies for Alzheimer's Disease: Pitfalls and Promise, Biol. Psychiatry. 83 (2018) 311–319. doi:10.1016/j.biopsych.2017.08.010.

[232] Encapsulated Cell Biodelivery of Nerve Growth Factor to Alzheimer´s Disease Patients - Full Text View - ClinicalTrials.gov, (n.d.). https://clinicaltrials.gov/ct2/show/NCT01163825 (accessed January 26, 2018).

[233] L.U. Wahlberg, G. Lind, P.M. Almqvist, P. Kusk, J. Tornøe, B. Juliusson, M. Söderman, E. Selldén, Å. Seiger, M. Eriksdotter-Jönhagen, B. Linderoth, Targeted delivery of nerve growth factor via encapsulated cell biodelivery in Alzheimer disease: a technology platform for restorative neurosurgery, J. Neurosurg. 117 (2012) 340–347. doi:10.3171/2012.2.JNS11714.

[234] H. Eyjolfsdottir, M. Eriksdotter, B. Linderoth, G. Lind, B. Juliusson, P. Kusk, O. Almkvist, N. Andreasen, K. Blennow, D. Ferreira, E. Westman, I. Nennesmo, A. Karami, T. Darreh-Shori, A. Kadir, A. Nordberg, E. Sundström, L.-O. Wahlund, A. Wall, M. Wiberg, B. Winblad, Å. Seiger, L. Wahlberg, P. Almqvist, Targeted delivery of nerve growth factor to the cholinergic basal forebrain of Alzheimer's disease patients: application of a second-generation encapsulated cell biodelivery device, Alzheimers Res. Ther. 8 (2016). doi:10.1186/s13195-016-0195-9.

[235] D.B. Rodrigues, R. Chammas, N.V. Malavasi, P.L.N. da Costa, R.M. Chura-Chambi, K.N. Balduino, L. Morganti, Anti-tumor therapy with macroencapsulated endostatin producer cells, BMC Biotechnol. 10 (2010) 19. doi:10.1186/1472-6750-10-19.

[236] J. Michaels, M. Dobryansky, R.D. Galiano, K.A. Bhatt, R. Ashinoff, D.J. Ceradini, G.C. Gurtner, Topical vascular endothelial growth factor reverses delayed wound healing secondary to angiogenesis inhibitor administration, Wound Repair Regen. Off. Publ. Wound Heal. Soc. Eur. Tissue Repair Soc. 13 (2005) 506–512. doi:10.1111/j.1067-1927.2005.00071.x.

[237] W. Bloch, K. Huggel, T. Sasaki, R. Grose, P. Bugnon, K. Addicks, R. Timpl, S. Werner, The angiogenesis inhibitor endostatin impairs blood vessel maturation during wound healing, FASEB J. Off. Publ. Fed. Am. Soc. Exp. Biol. 14 (2000) 2373–2376. doi:10.1096/fj.00-0490fje.

[238] N. Mach, Vaccination With Immuno-Isolated Cells Producing An Immunomodulator, US20140341982 A1, 2014. http://www.google.com/patents/US20140341982 (accessed January 11, 2018).

[239] J. Nemunaitis, D. Sterman, D. Jablons, J.W. Smith, B. Fox, P. Maples, S. Hamilton, F. Borellini, A. Lin, S. Morali, K. Hege, Granulocyte–Macrophage Colony-Stimulating Factor Gene-Modified Autologous Tumor Vaccines in Non–Small-Cell Lung Cancer, JNCI J. Natl. Cancer Inst. 96 (2004) 326–331. doi:10.1093/jnci/djh028.

[240] N. Mach, D. Migliorini, R. Vernet, M.-C. Belkouch, P. Luy, V. Ancrenaz, C. Py, J. Grogg, P. Harboe-Schmidt, N. Bouche, 5PDCell-based immunotherapy combining encapsulation cell technology and irradiated autologous tumor cells: A novel technology platform that is both safe and feasible. Results from first in man trial, Ann. Oncol. 26 (2015) viii2–viii2. doi:10.1093/annonc/mdv513.05.

[241] F. Schwenter, S. Zarei, P. Luy, V. Padrun, N. Bouche, J.S. Lee, R.C. Mulligan, P. Morel, N. Mach, Cell encapsulation technology as a novel strategy for human anti-tumor immunotherapy, Cancer Gene Ther. 18 (2011) 553. doi:10.1038/cgt.2011.22.

[242] N. Mach, R. Vernet, M.-C. Belkouch, P. Luy, V. Ancrenaz, P. Teta, N. Blazek, N. Grandjean, J. Wasem, J. Grogg, T. Perez, D. Migliorini, MVX-

ONCO-1 phase 1 final results of the first personalized cell-based immunotherapy using cell encapsulation technology, Ann. Oncol. 27 (2016). doi:10.1093/annonc/mdw378.12.

[243] K. Järbrink, G. Ni, H. Sönnergren, A. Schmidtchen, C. Pang, R. Bajpai, J. Car, Prevalence and incidence of chronic wounds and related complications: a protocol for a systematic review, Syst. Rev. 5 (2016). doi:10.1186/s13643-016-0329-y.

[244] M.S. Hu, T. Leavitt, S. Malhotra, D. Duscher, M.S. Pollhammer, G.G. Walmsley, Z.N. Maan, A.T.M. Cheung, M. Schmidt, G.M. Huemer, M.T. Longaker, H.P. Lorenz, Stem Cell-Based Therapeutics to Improve Wound Healing, Plast. Surg. Int. (2015). doi:10.1155/2015/383581.

[245] S. Zhong, Y. Zhang, C. Lim, Tissue scaffolds for skin wound healing and dermal reconstruction, Wiley Interdiscip. Rev. Nanomed. Nanobiotechnol. 2 (2010) 510–525.

[246] N.J. Turner, S.F. Badylak, The use of biologic scaffolds in the treatment of chronic nonhealing wounds, Adv. Wound Care. 4 (2015) 490–500.

[247] L.E. Dickinson, S. Gerecht, Engineered biopolymeric scaffolds for chronic wound healing, Front. Physiol. 7 (2016).

[248] K.C. Rustad, V.W. Wong, M. Sorkin, J.P. Glotzbach, M.R. Major, J. Rajadas, M.T. Longaker, G.C. Gurtner, Enhancement of mesenchymal stem cell angiogenic capacity and stemness by a biomimetic hydrogel scaffold, Biomaterials. 33 (2012) 80–90. doi:10.1016/j.biomaterials.2011.09.041.

[249] D. Duscher, J. Barrera, V.W. Wong, Z.N. Maan, A.J. Whittam, M. Januszyk, G.C. Gurtner, Stem Cells in Wound Healing: The Future of Regenerative Medicine? A Mini-Review, Gerontology. 62 (2016) 216–225. doi:10.1159/000381877.

[250] L. Zaulyanov, R.S. Kirsner, A review of a bi-layered living cell treatment (Apligraf ®) in the treatment of venous leg ulcers and diabetic foot ulcers, Clin. Interv. Aging. 2 (2007) 93–98.

[251] J.D. Raguse, H.J. Gath, A metabolically active dermal replacement (Dermagraft) for vestibuloplasty, J. Oral Rehabil. 32 (2005) 337–340. doi:10.1111/j.1365-2842.2004.01430.x.

[252] Dermagraft(R) for the Treatment of Patients With Diabetic Foot Ulcers - Full Text View - ClinicalTrials.gov, (n.d.).

https://clinicaltrials.gov/ct2/show/NCT01181440 (accessed January 10, 2018).

[253] C.J. Pino, A.S. Yevzlin, J. Tumlin, H.D. Humes, Cell-based strategies for the treatment of kidney dysfunction: a review, Blood Purif. 34 (2012) 117–123.

[254] A.J. Collins, R.N. Foley, D.T. Gilbertson, S.-C. Chen, The state of chronic kidney disease, ESRD, and morbidity and mortality in the first year of dialysis, Clin. J. Am. Soc. Nephrol. CJASN. 4 Suppl 1 (2009) S5-11. doi:10.2215/CJN.05980809.

[255] E. Rosines, K. Johkura, X. Zhang, H.J. Schmidt, M. DeCambre, K.T. Bush, S.K. Nigam, Constructing Kidney-like Tissues from Cells Based on Programs for Organ Development: Toward a Method of In Vitro Tissue Engineering of the Kidney, Tissue Eng. Part A. 16 (2010) 2441–2455. doi:10.1089/ten.tea.2009.0548.

[256] J.H. Song, H.D. Humes, The Bioartificial Kidney in the Treatment of Acute Kidney Injury, Curr. Drug Targets. 10 (2009) 1227–1234.

[257] H.D. Humes, W.F. Weitzel, R.H. Bartlett, F.C. Swaniker, E.P. Paganini, J.R. Luderer, J. Sobota, Initial clinical results of the bioartificial kidney containing human cells in ICU patients with acute renal failure, Kidney Int. 66 (2004) 1578–1588. doi:10.1111/j.1523-1755.2004.00923.x.

[258] H.D. Humes, W.H. Fissell, W.F. Weitzel, D.A. Buffington, A.J. Westover, S.M. MacKay, J.M. Gutierrez, Metabolic replacement of kidney function in uremic animals with a bioartificial kidney containing human cells, Am. J. Kidney Dis. Off. J. Natl. Kidney Found. 39 (2002) 1078–1087. doi:10.1053/ajkd.2002.32792.

[259] H.D. Humes, D.A. Buffington, L. Lou, S. Abrishami, M. Wang, J. Xia, W.H. Fissell, Cell therapy with a tissue-engineered kidney reduces the multiple-organ consequences of septic shock, Crit. Care Med. 31 (2003) 2421–2428. doi:10.1097/01.CCM.0000089644.70597.C1.

[260] I.T. S, K.C. M, R. Mohamed, Dialysis: History, Development And Promise, World Scientific, 2012.

[261] J. Tumlin, R. Wali, W. Williams, P. Murray, A.J. Tolwani, A.K. Vinnikova, H.M. Szerlip, J. Ye, E.P. Paganini, L. Dworkin, K.W. Finkel, M.A. Kraus, H.D. Humes, Efficacy and Safety of Renal Tubule Cell Therapy for Acute

Renal Failure, J. Am. Soc. Nephrol. JASN. 19 (2008) 1034–1040. doi:10.1681/ASN.2007080895.

[262] C.J. Pino, A.S. Yevzlin, K. Lee, A.J. Westover, P.L. Smith, D.A. Buffington, H.D. Humes, Cell-based approaches for the treatment of systemic inflammation, Nephrol. Dial. Transplant. 28 (2013) 296–302. doi:10.1093/ndt/gfs503.

[263] D.A. Buffington, C.J. Pino, L. Chen, A.J. Westover, G. Hageman, H.D. Humes, Bioartificial Renal Epithelial Cell System (BRECS): A Compact, Cryopreservable Extracorporeal Renal Replacement Device, Cell Med. 4 (2012) 33–43. doi:10.3727/215517912X653328.

[264] J.A. Tumlin, L. Chawla, A.J. Tolwani, R. Mehta, J. Dillon, K.W. Finkel, J.R. DaSilva, B.C. Astor, A.S. Yevzlin, H.D. Humes, The Effect of the Selective Cytopheretic Device on Acute Kidney Injury Outcomes in the Intensive Care Unit: A Multicenter Pilot Study, Semin. Dial. 26 (2013) 616–623. doi:10.1111/sdi.12032.

[265] Efficacy Study of a Selective Cytopheretic Device (SCD) in Patients With Acute Kidney Injury - Full Text View - ClinicalTrials.gov, (n.d.). https://clinicaltrials.gov/ct2/show/NCT01400893 (accessed January 28, 2018).

[266] J.A. Tumlin, C.M. Galphin, A.J. Tolwani, M.R. Chan, A. Vijayan, K. Finkel, B. Szamosfalvi, D. Dev, J.R. DaSilva, B.C. Astor, A.S. Yevzlin, H.D. Humes, SCD Investigator Group, A Multi-Center, Randomized, Controlled, Pivotal Study to Assess the Safety and Efficacy of a Selective Cytopheretic Device in Patients with Acute Kidney Injury, PloS One. 10 (2015) e0132482. doi:10.1371/journal.pone.0132482.

[267] A Study of Cell Therapy for Subjects With Acute Kidney Injury Who Are Receiving Continuous Renal Replacement Therapy - Full Text View - ClinicalTrials.gov, (n.d.). https://clinicaltrials.gov/ct2/show/NCT03015623 (accessed January 10, 2018).

[268] J.M. Milwid, T. Ichimura, M. Li, Y. Jiao, J. Lee, J.S. Yarmush, B. Parekkadan, A.W. Tilles, J.V. Bonventre, M.L. Yarmush, Secreted Factors from Bone Marrow Stromal Cells Upregulate IL-10 and Reverse Acute Kidney Injury, Stem Cells Int. 2012 (2012). doi:10.1155/2012/392050.

[269] S. Kim, W.H. Fissell, H.D. Humes, S. Roy, Current Strategies and Challenges in Engineering a Bioartificial Kidney, Front. Biosci. Elite Ed. 7 (2015) 215–228.

[270] W.H. Fissell, S. Roy, The implantable artificial kidney, Semin. Dial. 22 (2009) 665–670. doi:10.1111/j.1525-139X.2009.00662.x.

[271] S. Roy, K. Goldman, R. Marchant, A. Zydney, D. Brown, A. Fleischman, A. Conlisk, T. Desai, S. Duffy, H. Humes, W. Fissell, Implanted renal replacement for end-stage renal disease, Panminerva Med. 53 (2011) 155–166.

[272] Writing Group Members, D. Mozaffarian, E.J. Benjamin, A.S. Go, D.K. Arnett, M.J. Blaha, M. Cushman, S.R. Das, S. de Ferranti, J.-P. Després, H.J. Fullerton, V.J. Howard, M.D. Huffman, C.R. Isasi, M.C. Jiménez, S.E. Judd, B.M. Kissela, J.H. Lichtman, L.D. Lisabeth, S. Liu, R.H. Mackey, D.J. Magid, D.K. McGuire, E.R. Mohler, C.S. Moy, P. Muntner, M.E. Mussolino, K. Nasir, R.W. Neumar, G. Nichol, L. Palaniappan, D.K. Pandey, M.J. Reeves, C.J. Rodriguez, W. Rosamond, P.D. Sorlie, J. Stein, A. Towfighi, T.N. Turan, S.S. Virani, D. Woo, R.W. Yeh, M.B. Turner, American Heart Association Statistics Committee, Stroke Statistics Subcommittee, Heart Disease and Stroke Statistics-2016 Update: A Report From the American Heart Association, Circulation. 133 (2016) e38-360. doi:10.1161/CIR.0000000000000350.

[273] N.H. Goradel, F.G.- Hour, B. Negahdari, Z.V. Malekshahi, M. Hashemzehi, A. Masoudifar, H. Mirzaei, Stem Cell Therapy: A New Therapeutic Option for Cardiovascular Diseases, J. Cell. Biochem. (2017). doi:10.1002/jcb.26169.

[274] Heart regeneration. - PubMed - NCBI, (n.d.). https://www.ncbi.nlm.nih.gov/pubmed/21593865 (accessed January 24, 2018).

[275] Nongenetic method for purifying stem cell–derived cardiomyocytes | Nature Methods, (n.d.). https://www.nature.com/articles/nmeth.1403 (accessed January 24, 2018).

[276] J. Rehman, D. Traktuev, J. Li, S. Merfeld-Clauss, C.J. Temm-Grove, J.E. Bovenkerk, C.L. Pell, B.H. Johnstone, R.V. Considine, K.L. March, Secretion of angiogenic and antiapoptotic factors by human adipose stromal

cells, Circulation. 109 (2004) 1292–1298. doi:10.1161/01.CIR.0000121425.42966.F1.

[277] S. Aggarwal, M.F. Pittenger, Human mesenchymal stem cells modulate allogeneic immune cell responses, Blood. 105 (2005) 1815–1822. doi:10.1182/blood-2004-04-1559.

[278] M.F. Berry, A.J. Engler, Y.J. Woo, T.J. Pirolli, L.T. Bish, V. Jayasankar, K.J. Morine, T.J. Gardner, D.E. Discher, H.L. Sweeney, Mesenchymal stem cell injection after myocardial infarction improves myocardial compliance, Am. J. Physiol. Heart Circ. Physiol. 290 (2006) H2196-2203. doi:10.1152/ajpheart.01017.2005.

[279] M. Nian, P. Lee, N. Khaper, P. Liu, Inflammatory cytokines and postmyocardial infarction remodeling, Circ. Res. 94 (2004) 1543–1553. doi:10.1161/01.RES.0000130526.20854.fa.

[280] R.D. Levit, N. Landázuri, E.A. Phelps, M.E. Brown, A.J. García, M.E. Davis, G. Joseph, R. Long, S.A. Safley, J.D. Suever, A.N. Lyle, C.J. Weber, W.R. Taylor, Cellular encapsulation enhances cardiac repair, J. Am. Heart Assoc. 2 (2013) e000367. doi:10.1161/JAHA.113.000367.

[281] J. Tang, X. Cui, T.G. Caranasos, M.T. Hensley, A.C. Vandergriff, Y. Hartanto, D. Shen, H. Zhang, J. Zhang, K. Cheng, Heart Repair Using Nanogel-Encapsulated Human Cardiac Stem Cells in Mice and Pigs with Myocardial Infarction, ACS Nano. 11 (2017) 9738–9749. doi:10.1021/acsnano.7b01008.

[282] N.-H. Chi, M.-C. Yang, T.-W. Chung, J.-Y. Chen, N.-K. Chou, S.-S. Wang, Cardiac repair achieved by bone marrow mesenchymal stem cells/silk fibroin/hyaluronic acid patches in a rat of myocardial infarction model, Biomaterials. 33 (2012) 5541–5551. doi:10.1016/j.biomaterials.2012.04.030.

[283] B.E. Strauer, M. Brehm, T. Zeus, M. Köstering, A. Hernandez, R.V. Sorg, G. Kögler, P. Wernet, Repair of infarcted myocardium by autologous intracoronary mononuclear bone marrow cell transplantation in humans, Circulation. 106 (2002) 1913–1918.

[284] T. Siminiak, R. Kalawski, D. Fiszer, O. Jerzykowska, J. Rzeźniczak, N. Rozwadowska, M. Kurpisz, Autologous skeletal myoblast transplantation for the treatment of postinfarction myocardial injury: phase I clinical study

with 12 months of follow-up, Am. Heart J. 148 (2004) 531–537. doi:10.1016/j.ahj.2004.03.043.

[285] N. Dib, R.E. Michler, F.D. Pagani, S. Wright, D.J. Kereiakes, R. Lengerich, P. Binkley, D. Buchele, I. Anand, C. Swingen, M.F. Di Carli, J.D. Thomas, W.A. Jaber, S.R. Opie, A. Campbell, P. McCarthy, M. Yeager, V. Dilsizian, B.P. Griffith, R. Korn, S.K. Kreuger, M. Ghazoul, W.R. MacLellan, G. Fonarow, H.J. Eisen, J. Dinsmore, E. Diethrich, Safety and feasibility of autologous myoblast transplantation in patients with ischemic cardiomyopathy: four-year follow-up, Circulation. 112 (2005) 1748–1755. doi:10.1161/CIRCULATIONAHA.105.547810.

[286] C.E. Veltman, O.I.I. Soliman, M.L. Geleijnse, W.B. Vletter, P.C. Smits, F.J. ten Cate, L.J. Jordaens, A.H.H.M. Balk, P.W. Serruys, E. Boersma, R.T. van Domburg, W.J. van der Giessen, Four-year follow-up of treatment with intramyocardial skeletal myoblasts injection in patients with ischaemic cardiomyopathy, Eur. Heart J. 29 (2008) 1386–1396. doi:10.1093/eurheartj/ehn171.

[287] T.J. Povsic, C.M. O'Connor, T. Henry, A. Taussig, D.J. Kereiakes, F.D. Fortuin, A. Niederman, R. Schatz, R. Spencer, D. Owens, M. Banks, D. Joseph, R. Roberts, J.H. Alexander, W. Sherman, A double-blind, randomized, controlled, multicenter study to assess the safety and cardiovascular effects of skeletal myoblast implantation by catheter delivery in patients with chronic heart failure after myocardial infarction, Am. Heart J. 162 (2011) 654-662.e1. doi:10.1016/j.ahj.2011.07.020.

[288] A. Pepper, B. Gala-Lopez, R. Pawlick, A. Shapiro, A Prevascularized Subcutaneous 'Device-Less'' Site for Islet Transplantation.: Abstract# C1557,' Transplantation. 98 (2014) 331.

[289] Prevascularized Tissue-Engineered Construct Serves as an Alternative Site for Pancreatic Islet Transplantation, A, ATC Abstr. (n.d.). http://atcmeetingabstracts.com/abstract/prevascularized-tissue-engineered-construct-serves-as-an-alternative-site-for-pancreatic-islet-transplantation-a/ (accessed January 24, 2018).

[290] J.M. Morais, F. Papadimitrakopoulos, D.J. Burgess, Biomaterials/Tissue Interactions: Possible Solutions to Overcome Foreign Body Response, AAPS J. 12 (2010) 188–196. doi:10.1208/s12248-010-9175-3.

[291] J.B. Park, Biomaterials Science and Engineering, Springer Science & Business Media, 2012.

[292] M.H. de Vaal, J. Neville, J. Scherman, P. Zilla, M. Litow, T. Franz, The in vivo assessment of mechanical loadings on pectoral pacemaker implants, J. Biomech. 43 (2010) 1717–1722. doi:10.1016/j.jbiomech.2010.02.028.

[293] H. Zeinalabedini, Y.O. Yildiz, P. Zhang, K. Laux, M. Kirca, A.C. To, Homogenization of additive manufactured polymeric foams with spherical cells, Addit. Manuf. 12 (2016) 274–281.

[294] O.A. Shergold, N.A. Fleck, D. Radford, The uniaxial stress versus strain response of pig skin and silicone rubber at low and high strain rates, Int. J. Impact Eng. 32 (2006) 1384–1402.

[295] R.B. Groves, S. Coulman, J.C. Birchall, S.L. Evans, Quantifying the mechanical properties of human skin to optimise future microneedle device design, Comput. Methods Biomech. Biomed. Engin. 15 (2012) 73–82.

[296] T. Tervoort, E. Klompen, L. Govaert, A multi-mode approach to finite, three-dimensional, nonlinear viscoelastic behavior of polymer glasses, J. Rheol. 40 (1996) 779–797.

[297] J. Zhang, H. Jiang, G. Kang, C. Jiang, F. Lu, A new form of equivalent stress for combined axial–torsional loading considering the tension–compression asymmetry of polymeric materials, RSC Adv. 5 (2015) 72780–72784.

[298] N.A. Weir, F.J. Buchanan, J.F. Orr, G.R. Dickson, Degradation of poly-L-lactide. Part 1: in vitro and in vivo physiological temperature degradation, Proc. Inst. Mech. Eng. [H]. 218 (2004) 307–319. doi:10.1243/0954411041932782.

[299] Degradation of poly-L-lactide. Part 2: increased temperature accelerated degradation. - PubMed - NCBI, (n.d.). https://www.ncbi.nlm.nih.gov/pubmed/15532997 (accessed February 9, 2018).

[300] G. Kang, Y. Liu, J. Ding, Q. Gao, Uniaxial ratcheting and fatigue failure of tempered 42CrMo steel: damage evolution and damage-coupled visco-plastic constitutive model, Int. J. Plast. 25 (2009) 838–860.

[301] Z. Xia, X. Shen, F. Ellyin, Cyclic deformation behavior of an epoxy polymer. Part II: Predictions of viscoelastic constitutive models, Polym. Eng. Sci. 45 (2005) 103–113.

[302] S. Holopainen, T. Barriere, G. Cheng, R. Kouhia, Continuum approach for modeling fatigue in amorphous glassy polymers. Applications to the investigation of damage-ratcheting interaction in polycarbonate, Int. J. Plast. 91 (2017) 109–133.

[303] A. Chrysochoos, B. Berthel, F. Latourte, S. Pagano, B. Wattrisse, B. Weber, Local energy approach to steel fatigue, Strain. 44 (2008) 327–334.

[304] F. Curà, R. Sesana, Mechanical and thermal parameters for high-cycle fatigue characterization in commercial steels, Fatigue Fract. Eng. Mater. Struct. 37 (2014) 883–896.

[305] A. Levy, K. Kopplin, A. Gefen, Simulations of skin and subcutaneous tissue loading in the buttocks while regaining weight-bearing after a push-up in wheelchair users, J. Mech. Behav. Biomed. Mater. 28 (2013) 436–447.

[306] S.E. Zeltmann, N. Gupta, N.G. Tsoutsos, M. Maniatakos, J. Rajendran, R. Karri, Manufacturing and security challenges in 3D printing, Jom. 68 (2016) 1872–1881.

[307] S. Beretta, S. Romano, A comparison of fatigue strength sensitivity to defects for materials manufactured by AM or traditional processes, Int. J. Fatigue. 94 (2017) 178–191.

[308] C. Fu, Y. Guo, 3-dimensional finite element modeling of selective laser melting ti-6al-4v alloy, in: Solid Free. Fabr. Symp. 2014 Proc., 2014: pp. 1129–1144.

[309] G. Campoli, M. Borleffs, S.A. Yavari, R. Wauthle, H. Weinans, A.A. Zadpoor, Mechanical properties of open-cell metallic biomaterials manufactured using additive manufacturing, Mater. Des. 49 (2013) 957–965.

[310] C. Celia, S. Ferrati, S. Bansal, A.L. van de Ven, B. Ruozi, E. Zabre, S. Hosali, D. Paolino, M.G. Sarpietro, D. Fine, M. Fresta, M. Ferrari, A. Grattoni, Sustained zero-order release of intact ultra-stable drug-loaded liposomes from an implantable nanochannel delivery system, Adv. Healthc. Mater. 3 (2014) 230–238. doi:10.1002/adhm.201300188.

[311] S.E. Kahn, M.E. Cooper, S. Del Prato, Pathophysiology and treatment of type 2 diabetes: perspectives on the past, present, and future, Lancet Lond. Engl. 383 (2014) 1068–1083. doi:10.1016/S0140-6736(13)62154-6.

[312] B. Johannesson, L. Sui, D.O. Freytes, R.J. Creusot, D. Egli, Toward beta cell replacement for diabetes, EMBO J. 34 (2015) 841–855. doi:10.15252/embj.201490685.

[313] A.O. Gaber, D.W. Fraga, C.S. Callicutt, I.C. Gerling, O.M. Sabek, M.Y. Kotb, Improved in vivo pancreatic islet function after prolonged in vitro islet culture, Transplantation. 72 (2001) 1730–1736.

[314] M.M. Gabr, M.M. Zakaria, A.F. Refaie, A.M. Ismail, M.A. Abou-El-Mahasen, S.A. Ashamallah, S.M. Khater, S.M. El-Halawani, R.Y. Ibrahim, G.S. Uin, M. Kloc, R.Y. Calne, M.A. Ghoneim, Insulin-producing cells from adult human bone marrow mesenchymal stem cells control streptozotocin-induced diabetes in nude mice, Cell Transplant. 22 (2013) 133–145. doi:10.3727/096368912X647162.

[315] Y. Xia, F. Boey, S.S. Venkatraman, Surface modification of poly(L-lactic acid) with biomolecules to promote endothelialization, Biointerphases. 5 (2010) FA32-40. doi:10.1116/1.3467508.

[316] V.K. Thakur, A.S. Singha, Surface Modification of Biopolymers, John Wiley & Sons, 2015.

[317] L. Bacakova, E. Filova, M. Parizek, T. Ruml, V. Svorcik, Modulation of cell adhesion, proliferation and differentiation on materials designed for body implants, Biotechnol. Adv. 29 (2011) 739–767. doi:10.1016/j.biotechadv.2011.06.004.

[318] E. Lammert, G. Gu, M. McLaughlin, D. Brown, R. Brekken, L.C. Murtaugh, H.P. Gerber, N. Ferrara, D.A. Melton, Role of VEGF-A in vascularization of pancreatic islets, Curr. Biol. CB. 13 (2003) 1070–1074.

[319] T. Van Belle, M. von Herrath, Immunosuppression in islet transplantation, J. Clin. Invest. 118 (2008) 1625–1628. doi:10.1172/JCI35639.

[320] S.H. Golden, K.A. Robinson, I. Saldanha, B. Anton, P.W. Ladenson, Prevalence and Incidence of Endocrine and Metabolic Disorders in the United States: A Comprehensive Review, J. Clin. Endocrinol. Metab. 94 (2009) 1853–1878. doi:10.1210/jc.2008-2291.

[321] S.H. Golden, A. Brown, J.A. Cauley, M.H. Chin, T.L. Gary-Webb, C. Kim, J.A. Sosa, A.E. Sumner, B. Anton, Health disparities in endocrine disorders: biological, clinical, and nonclinical factors--an Endocrine Society scientific statement, J. Clin. Endocrinol. Metab. 97 (2012) E1579-1639. doi:10.1210/jc.2012-2043.

[322] E.C. Osterberg, A.M. Bernie, R. Ramasamy, Risks of testosterone replacement therapy in men, Indian J. Urol. IJU J. Urol. Soc. India. 30 (2014) 2–7. doi:10.4103/0970-1591.124197.

[323] P.A.M. Everts, J.T.A. Knape, G. Weibrich, J.P.A.M. Schönberger, J. Hoffmann, E.P. Overdevest, H.A.M. Box, A. van Zundert, Platelet-Rich Plasma and Platelet Gel: A Review, J. Extra. Corpor. Technol. 38 (2006) 174–187.

[324] N.A. Lokman, A.S.F. Elder, C. Ricciardelli, M.K. Oehler, Chick Chorioallantoic Membrane (CAM) Assay as an In Vivo Model to Study the Effect of Newly Identified Molecules on Ovarian Cancer Invasion and Metastasis, Int. J. Mol. Sci. 13 (2012) 9959–9970. doi:10.3390/ijms13089959.

[325] J. Stagner, B. Ahren, F. Sundler, K. White, Reconstructing the pancreas: restoration of normoglycemia, exocrine function, and islet innervation by islet transplantation to the pancreas, Transplant. Proc. 40 (2008) 452–454. doi:10.1016/j.transproceed.2008.01.031.

[326] M.R. Rickels, Recovery of Endocrine Function After Islet and Pancreas Transplantation, Curr. Diab. Rep. 12 (2012) 587–596. doi:10.1007/s11892-012-0294-3.

[327] E. Maillard, M.T. Juszczak, A. Langlois, C. Kleiss, M.C. Sencier, W. Bietiger, M. Sanchez-Dominguez, M.P. Krafft, P.R.V. Johnson, M. Pinget, S. Sigrist, Perfluorocarbon emulsions prevent hypoxia of pancreatic β-cells, Cell Transplant. 21 (2012) 657–669. doi:10.3727/096368911X593136.

[328] M. Cappa, M. Caruso, G. Saggese, M.C. Salerno, G. Tonini, GH therapy in transition age: state of the art and future perspectives, Minerva Endocrinol. 40 (2015) 23–35.

[329] A. Chico, D. Tundidor, L. Jordana, I. Saigi, M.A. Maria, R. Corcoy, A. de Leiva, Changes in Insulin Requirements From the Onset of Continuous Subcutaneous Insulin Infusion (CSII) Until Optimization of Glycemic

Control, J. Diabetes Sci. Technol. 8 (2014) 371–377. doi:10.1177/1932296813520205.

[330] J. Clarkson, A.E. Herbison, Hypothalamic control of the male neonatal testosterone surge, Phil Trans R Soc B. 371 (2016) 20150115. doi:10.1098/rstb.2015.0115.

[331] H. Alipour, A. Raz, S. Zakeri, N. Dinparast Djadid, Therapeutic applications of collagenase (metalloproteases): A review, Asian Pac. J. Trop. Biomed. 6 (2016) 975–981. doi:10.1016/j.apjtb.2016.07.017.

[332] A.R. Pepper, B. Gala-Lopez, R. Pawlick, S. Merani, T. Kin, A.M.J. Shapiro, A prevascularized subcutaneous device-less site for islet and cellular transplantation, Nat. Biotechnol. 33 (2015) 518. doi:10.1038/nbt.3211.

[333] B. Buder, M. Alexander, R. Krishnan, D.W. Chapman, J.R. Lakey, Encapsulated Islet Transplantation: Strategies and Clinical Trials, Immune Netw. 13 (2013) 235–239. doi:10.4110/in.2013.13.6.235.

Appendix A: Article Reprinting Permissions

1. **Cell Encapsulation: Overcoming Barriers in Cell Transplantation in Diabetes and Beyond *(Advanced Drug Delivery Review)***

2. **Transcutaneously refillable, 3D-printed biopolymeric encapsulation system for the transplantation of endocrine cells *(Biomaterials)***

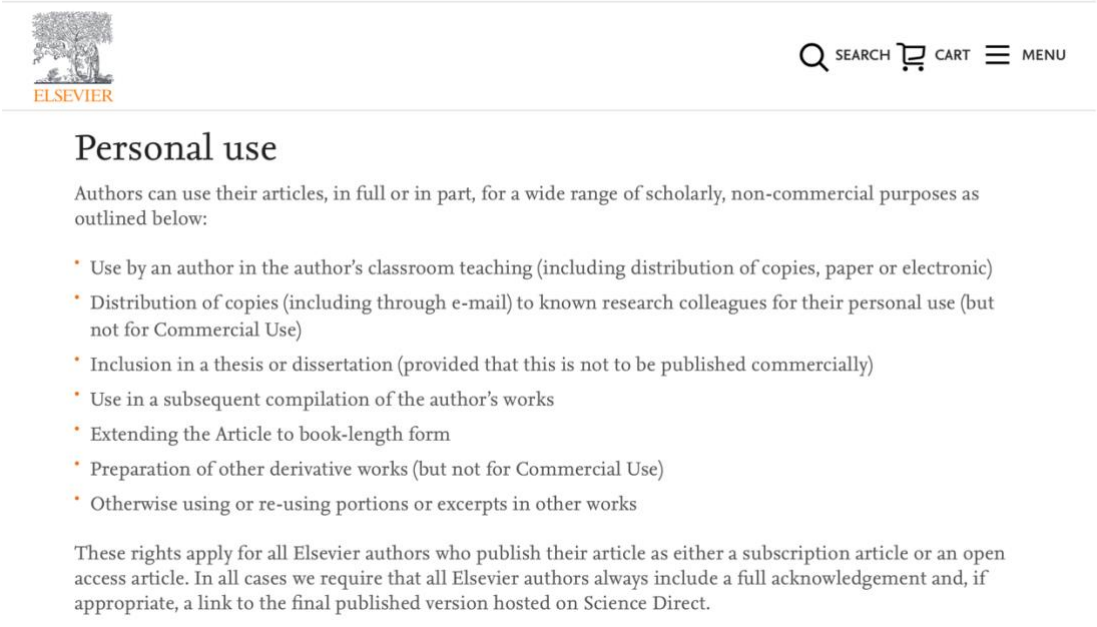

ELSEVIER

SEARCH CART MENU

Personal use

Authors can use their articles, in full or in part, for a wide range of scholarly, non-commercial purposes as outlined below:

- Use by an author in the author's classroom teaching (including distribution of copies, paper or electronic)
- Distribution of copies (including through e-mail) to known research colleagues for their personal use (but not for Commercial Use)
- Inclusion in a thesis or dissertation (provided that this is not to be published commercially)
- Use in a subsequent compilation of the author's works
- Extending the Article to book-length form
- Preparation of other derivative works (but not for Commercial Use)
- Otherwise using or re-using portions or excerpts in other works

These rights apply for all Elsevier authors who publish their article as either a subscription article or an open access article. In all cases we require that all Elsevier authors always include a full acknowledgement and, if appropriate, a link to the final published version hosted on Science Direct.

3. Three-dimensional printed polymeric system to encapsulate human mesenchymal stem cells differentiated into islet-like insulin-producing aggregatres for diabetes treatment

4. 3D Printed Vascularized Device for Subcutaneous Transplantation of Human Islets

Order Completed

Thank you for your order.

This Agreement between Marco Farina ("You") and John Wiley and Sons ("John Wiley and Sons") consists of your license details and the terms and conditions provided by John Wiley and Sons and Copyright Clearance Center.

Your confirmation email will contain your order number for future reference.

printable details

License Number	4318390707354
License date	Mar 29, 2018
Licensed Content Publisher	John Wiley and Sons
Licensed Content Publication	Biotechnology Journal
Licensed Content Title	3D Printed Vascularized Device for Subcutaneous Transplantation of Human Islets
Licensed Content Author	Marco Farina, Andrea Ballerini, Daniel W. Fraga, et al
Licensed Content Date	Aug 23, 2017
Licensed Content Volume	12
Licensed Content Issue	9
Licensed Content Pages	5
Type of use	Dissertation/Thesis
Requestor type	Author of this Wiley article
Format	Print and electronic
Portion	Full article
Will you be translating?	No
Title of your thesis / dissertation	Implantable medical devices for drug and cell release
Expected completion date	May 2018
Expected size (number of pages)	160
Attachment	
Requestor Location	Marco Farina 6670 bertner avenue HOUSTON, TX 77030 United States Attn: Marco Farina
Publisher Tax ID	EU826007151

5. Mechanical characterization and numerical simulation of a subcutaneous implantable 3D printed cell encapsulation system